DOCTORAL THESIS

Development of chemical derivatization methods for cis-diol-containing metabolite detection by using liquid chromatography-mass spectrometry

Li, Shangfu

Date of Award:
2016

HONG KONG BAPTIST UNIVERSITY

Doctor of Philosophy

THESIS ACCEPTANCE

DATE: September 5, 2016

STUDENT'S NAME: LI Shangfu

THESIS TITLE: Development of Chemical Derivatization Methods for *Cis*-diol-containing Metabolite Detection by Using Liquid Chromatography-mass Spectrometry

This is to certify that the above student's thesis has been examined by the following panel members and has received full approval for acceptance in partial fulfillment of the requirements for the degree of Doctor of Philosophy.

Chairman:	Prof. Zhu Fu Rong Professor, Department of Physics, HKBU (Designated by Dean of Faculty of Science)
Internal Members:	Dr. Ma Edmond Dik Lung Associate Professor, Department of Chemistry, HKBU (Designated by Head of Department of Chemistry)
	Dr. Li Hung Wing Associate Professor, Department of Chemistry, HKBU
External Members:	Prof. Li Liang Professor Department of Chemistry University of Alberta Canada
	Dr. Yao Zhongping Associate Professor Department of Applied Biology & Chemical Technology The Hong Kong Polytechnic University
Proxy:	Dr. Shiu Kwok Keung Associate Professor, Department of Chemistry, HKBU (as proxy for Prof. Li Liang)
In-attendance:	Prof. Cai Zongwei Chair Professor in Chemistry, Department of Chemistry, HKBU

Issued by Graduate School, HKBU

Development of Chemical Derivatization Methods for *Cis*-diol-containing Metabolite Detection by Using Liquid Chromatography-Mass Spectrometry

LI Shangfu

A thesis submitted in partial fulfillment of the requirements

for the degree of

Doctor of Philosophy

Principle Supervisor: Prof. CAI Zongwei

Hong Kong Baptist University

September 2016

DECLARATION

I hereby declare that this thesis represents my own work which has been done after registration for the degree of PhD at Hong Kong Baptist University, and has not been previously included in a thesis or dissertation submitted to this or any other institution for a degree, diploma or other qualifications.

Signature: Li Shangfu

Date: 09/05/2016

ABSTRACT

Cis-diol-containing metabolites have attracted increasing attention in recent years. These metabolites widely exist in the body fluids and tissues. They play important roles in the structure, function and metabolic activity of cells. Some of them are related to cell proliferation and metabolic processes. And they have been used to denote a state of disease as potential biomarkers. Several methods have been developed for the analysis of *cis*-diol-containing metabolites. However, these methods faced a challenge to separate and detect isomers of these compounds, particularly for compounds with low abundance and high polarity. Therefore, novel methods were necessary to improve the separation and detection sensitivity of this kind of metabolites.

With this aim, chemical derivatization methods were developed for *cis*-diol-containing metabolite detection by using liquid chromatography-mass spectrometry in this project. These methods were optimized and validated to achieve the optimal reaction conditions. And they were applied to study real-world biological systems, including the changes of modified nucleosides in hepatocellular carcinoma (HCC) nude mice and toxic effects of bisphenol A (BPA) exposure.

Firstly, the derivatization reaction of *cis*-diol compounds with acetone were optimized. Factors that affected reaction efficiency were investigated by reacting guanosine (G) with acetone. The optimal reaction conditions were validated by detecting four acetonides of urinary nucleosides by using LC-MS/MS. The results

showed that the approach had good linearity, accuracy and precision. The recoveries were ranged from 92.9% to 103.5%. It indicated that the assay was reproducible. The robust method should be potentially useful for the analysis of modified nucleosides and other *cis*-diol-containing metabolites in biological samples.

The validated derivatization method was applied to determine urinary nucleosides by LC-MS. This method not only improved the retention of nucleosides on reversed-phase column, but also reduced the matrix effect from urine samples and enhanced detection sensitivity of mass spectrometry. Isotope labeling method with acetone-d_6 and multivariate statistical analysis enabled the positive identification of 56 nucleosides, including 52 modified nucleosides. The obtained results indicated that the derivatization method was practical, fast and effective for the identification of urinary nucleosides. It was successfully applied to study the changes of urinary nucleosides in nude mice bearing HCC. Some significantly changed nucleosides were identified as potential biomarkers.

Subsequently, this approach was modified by employing parallel reaction monitoring (PRM) method which was based on high resolution MS to detect urinary nucleosides in rats exposed to BPA. Comparing to the data acquired by triple quadrupole MS with neutral loss scanning, higher specificity and sensitivity were achieved by using PRM scanning mode. Therefore, more nucleosides were identified by using the method in urine samples (from 56 up to 66). The changes of the detected nucleosides were studied in the rats exposed to BPA. Various trends of

modified nucleosides were observed with different dose BPA exposure. Specifically, the high-dose exposure group was the most strongly affected. The biomarker of RNA oxidation, 8-hydroxyguanosine (8-oxoG), showed significant change in this group. It proved that BPA exposure could induce RNA damage when the dose of BPA was beyond a certain amount.

Except for nucleosides, other *cis*-diol-containing metabolites, such as carbohydrates, were also studied by using the derivatization method. Acetone and acetone-d_6 were applied to label the *cis*-diol metabolites. Based on the chemical isotope labeling, *cis*-diol metabolites were easily recognized from urine samples. Influence of BPA exposure on these metabolites was investigated by comparing different doses of BPA administration on rats. Analytes showed noticeable difference were highlighted. Pathway analysis indicated that galactose metabolism, nucleoside and its analogues metabolism were disturbed.

The derivatization method was extended to quantify nucleotides in plasma samples. According to the specific physical-chemical properties of nucleotides, the method was improved to fit the requirement of analysis by using 1,1-Dimethoxycyclohexane (DMCH) as derivatization agent and formic acid (FA) as catalyst. Tip micro-columns packed with TiO_2 were used for selective adsorption of nucleotides in the plasma. Then in-situ derivatization were carried out to change the polarity of targeted compounds. LC-MS analysis of the derivatization products were employed without using ion-pairing reagents. This method exhibited a high

selectivity for the extraction of nucleotides. After derivatization, retention of nucleotides on reversed-phase C_{18} column was improved. Complete separation of nucleotides with the same base was achieved. The peak shape was symmetrical and the tailing was eliminated by using high pH mobile phase. The method settled the problems of nucleotide detection, which were poor retention, trailing, in-source fragmentation and contamination of ion-pairing reagents. The quantitative method was successfully applied to determine the content of nucleotides in plasma samples of rats exposed to BPA. It was simple and fast, as well as good selectivity and stability. It could be extended to detection of other phosphorylated metabolites with similar structure.

To our best knowledge, it was the first time to employ derivatization methods to detect *cis*-diol-containing metabolites. The methods decreased the matrix effects of complex biological samples, and also decreased the polarity of *cis*-diol-containing metabolites. The changes of properties not only improved the chromatographic separation, but also enhanced the MS intensities. The methods overcame the problems of *cis*-diol-containing metabolite detection on reversed-phase column. They were successfully applied to study the changes of *cis*-diol-containing metabolites of HCC and toxic effects of BPA exposure. The method might be extended to determine other *cis*-diol-containing metabolites in urine samples as well as in cells, tissues and plasma samples. It might be valuable for the understanding of the roles of *cis*-diol-containing metabolites in in cell metabolism.

ACKNOWLEDGEMENTS

Foremost, I would like to express my heartfelt thanks to my principal supervisor, Prof. CAI Zongwei, for the opportunity that he gave me to study in Hong Kong, and for his invaluable advice and suggestions on my work. I am deeply grateful of his support from all sides in my PhD study. I would also thank Dr. CHUNG Arthur C K, Dr. HONG Yanjun and my co-supervisor Dr. LEUNG Kelvin S.Y for their sincere help and encouragement.

I am also deeply indebted to Prof. JIANG Yuyang and Prof. LIU Hongxia, who are from the Key Lab of Chemical Biology, Graduate School at Shenzhen, Tsinghua University, for allowing me to use instruments in their lab and providing the mice urine samples of hepatocellular carcinoma.

I am indebted to Dr. WANG Tiejie and my wife, Dr. JIN Yibao, in Shenzhen Institute for Drug Control, for supporting the animal experiments in the project of bisphenol A exposure and its toxic effects studies.

Special thanks should go to Mr. CHIK David T.W., Mr. NG John S. L. and Ms. MO Silvia T. for providing LC-MS technical support during the experiments.

My sincere thanks must go to all other former and present members of Prof. Cai's group for their instantaneous help and support: Dr. LIN Shuhai, Dr. WU Hanzhi, Dr. SHEN Yang, Dr. TANG Zhi, Dr. LIN Zian, Dr. ZHAO Chao, Dr. ZHAO Hongzhi, Dr. WANG Shujuan, Dr. WU Qian, Dr. ZHAO Yun, Dr. LIU Rui, Mr. XIN Xiong, Ms. ZHANG Manwen, Ms. XIANG Li, Mr. LUAN Hemi, Ms. LI Xiaona,

Ms. ZHANG Fan, Ms. JI Fenfeng, Ms. FANG Jing, Mr. WEI Juntong, MS. YANG Chunxue, Mr. YANG Zhiyi, for their support and helpful discussion.

I also appreciate the financial supports from the Research Grants Council of the Hong Kong Special Administrative Region, China (No. 12301915) and the National Natural Science Foundation of China (No. NSFC21437002). I am particularly grateful to the Hong Kong PhD Fellowship Scheme from Hong Kong Research Grant Council, as well as Mr. Kwok Yat Wai and Madam Kwok Chung Bo Fun Graduate School Development Fund.

Finally, and very importantly, I should like to express my gratitude to my family for their understanding, support and encouragement to my study.

Table of Contents

List of Tables

List of Figures

List of Abbreviations

5-FU	5-Fluorouracil
5MedCyd	5-Methyl-2'-deoxycytidine
8-oxoG	8-Hydroxyguanosine
A	Adenosine
ACN	Acetonitrile
ADP	Adenosine 5’-diphosphate
ADP-$^{15}N_5$	Adenosine-$^{15}N_5$ 5’-diphosphate
AFP	Alpha-fetoprotein
AIDS	Acquired immunodeficiency diseases
AMC	Against 5-methylcytidine
AMP	Adenosine 5’-monophosphate
ANOVA	Analysis of Variance
AR	Androgen receptors
ATP	Adenosine-5'-triphosphate
BPA	Bisphenol A
BPAH	Rats treated with high-dose BPA
BPAL	Rats treated with low-dose BPA
BPAM	Rats treated with middle-dose BPA
C	Cytidine
CDP	Cytidine 5’-diphosphocholine

CEA	Carcinoembryonic antigen
CE-MS	Capillary electrophoresis-mass spectrometry
CMP	Cytidine 5’-monophosphate
CNL	Constant neutral loss
CRC	Colorectal cancer
Cre	Creatinine
CSA	Camphorsulfonic acid
CTP	Cytidine 5’-triphosphate
DMEM	Dulbecco's modified eagle medium
DNA	Deoxyribonucleic acid
DOPA	3,4-Dihydroxyphenylalanine
EDC	Endocrine disrupting chemical
ELISA	Enzyme-linked immunosorbent assay
ER	Estrogen receptor
ERE	Estrogen response element
ESI	Electrospray ionization
FAIMS	Field asymmetric waveform ion mobility spectrometry
FBS	Fetal bovine serum
G	Guanosine
GC	Gas chromatography

GDP	Guanosine 5’-diphosphate
GMP	Guanosine 5’-monophosphate
GTP	Guanosine 5’-triphosphate
H_2SO_4	Sulfuric acid
HCC	Hepatocellular carcinoma
HCCFU	HCC mice treated with 5-FU
$HClO_4$	Perchloric acid
HPLC	High-performance liquid chromatography
HRMS	High resolution mass spectrometry
IL-6	Interleukin-6
IS	Internal standard
LC-MS	Liquid chromatography-mass spectrometry
LC–MS/MS	LC coupled with tandem mass spectrometry
LD50	Half lethal dose
LH	Luteinizing hormone
LOD	Limit of detection
LOQ	Limit of quantification
LSD	Least significant difference
m/z	Mass to charge ratio
m^1G	1-Methylguanosine
m^2G	N^2-methylguanosine

m^7G	7-Methylguanosine
MeOH	Methanol
MRM	Multiple reaction monitoring
Npt	Neopterine
OPLS-DA	Orthogonal partial least square discriminant analysis
PBS	Phosphate buffer saline
PCA	Principal component analysis
PPTS	Pyridinium p-toluenesulfonate
PRM	Parallel reaction monitoring
Pseu	Pseudouridine
p-TsOH	*p*-Toluenesulfonic acid
QC	Quality control
QCD	QC samples reacted with acetone-d_6
QCH	QC samples reacted with acetone
RACB	Reproductive assessment by continuous breeding
RE	Relative error
RNA	Ribonucleic acid
ROS	Reactive oxygen species
RPLC	Reversed-phase liquid chromatography
rRNA	Transfer RNA
rRNA	Ribosomal RNA

RSD	Relative standard deviation
RT	Retention time
SAX	Strong anion exchange
SCID	Severe combined immunodeficiency diseases
snRNA	Small nuclear RNA
SPE	Solid-phase extraction
SPF	Specific pathogen free
TFA	Trifluoroacetic acid
TIC	Total ion chromatogram
tRNA	Transfer RNA
U	Uridine
UDP	Uridine 5’-diphosphoglucuronic acid
UHPLC	Ultra-high performance liquid chromatography
UMP	Uridine 5’-monophosphate
UPLC	Ultra high performance liquid chromatography
UTP	Uridine 5’-triphosphate
WAX	Weak anion exchange
ZIC-HILIC	Zwitterionic hydrophilic interaction chromatography

Chapter 1 Introduction

1.1 General introduction of *cis*-diol-containing metabolites

A diol is a chemical compound containing two hydroxyl groups (−OH groups), such as *cis*-diol, 1,3-diol and *trans*-diol. The three kinds of compounds have similar structures, but different functions. The most obvious examples are nucleosides and Deoxynucleosides. The former contains *cis*-diol groups, which are building blocks of RNA. The latter contains 1,3-diol groups, which are building blocks of DNA. Another example is cytidine and its isomer, cytarabine. Cytidine is an endogenous normal nucleoside with a *cis*-diol group. It is an essential metabolite for cell growing. However, cytarabine has a *trans*-diol group. Its structure is similar enough to cytidine, but different enough that it kills the cell[1]. It is a chemotherapy agent used mainly in the treatment of cancers, such as acute myeloid leukemia (AML) and non-Hodgkin lymphoma[2]. It means that slight modification of the molecule configuration between cytarabine and cytidine altered the compound properties significantly. Therefore, distinction of *cis*-diol, 1,3-diol and *trans*-diol compounds is important to understand their respective functions.

Cis-diol-containing metabolites are a kind of unique compounds, including glycoproteins, glycopeptides, RNA, nucleotides, nucleosides, carbohydrates and its conjugates, and so on. In addition, catecholamine compounds, as well as certain antibiotics such as vancomycin also belong to the *cis*-diol biological molecules. Because *cis*-diol compounds involved in many ways on growth, metabolism and

proliferation of cells[3]. They play important roles in cellular work, but their detection still faces some challenges, so, the project focused on this kind of metabolites. The studies of them may have great significance to comprehend their function in genomics, transcriptomics, and proteomics and metabolomics[4].

1.2 Brief introduction of carbohydrates

Carbohydrates are one of the most important specie of *cis*-diol-containing compounds. Carbohydrates are used as organism structure composition and energy source.[5] They are also important intermediate metabolites in cell metabolism as well as cell recognition and signal transduction molecules[6]. Carbohydrates involved in lots of biological reactions in the body independently[7]. And in many cases, it can be endowed with new functions by forming conjugated complex with other molecules. Typical conjugated complex, including glycoproteins, proteoglycan and glycolipids, are important biological molecules[8]. With the development of systems biology, carbohydrates become more and more important due to its potential applications as biological function molecules and disease biomarkers. For instance, amino acid composition of peptides in tumor cells may be identical to that of normal cells, but with different modification of glycosylation or deglycosylation, the structure and function of the proteins may be completely different[9]. Therefore, they may be used as biomarkers for clinical diagnosis. Now, a variety of glycoproteins have been identified as biomarkers of cancers, such as alpha-fetoprotein (AFP), carcinoembryonic antigen (CEA), tumor specific antigen, prostate specific antigen,

and so on[10].

Glycolipids are another kind of important *cis*-diol biological molecules. They refer to sugar connected with lipid compounds through hemiacetal hydroxyl bonds. Glycolipids can be divided into glycosphingolipids, glyceroglycolipids and steroid derivative glycolipids, etc[11]. All glycolipids are amphiphilic. Some of them are the components of the cell membrane, and they are closely related to the cell physiological conditions[12]. The ceramide and sugar chain of glycosphingolipids, for example, showed certain cell specificity in individuals, organizations, and even each part within the same organization[13]. For the same kind of cells, the composition of glycosphingolipids may be different in different cell growth stage[14]. Because of the specificity of glycosphingolipids, these compounds are often referred to as biomarkers in cell surface[15]. Glycosphingolipids are important components of cell surface antigen. They show obvious changes when the normal cells are cancerous[16]. Some surface antigens isolated from cancer cells have been proved to be glycosphingolipids[17]. Glycosphingolipids on the cell surface are extracellular receptors and physiological active substances and they participate in many cell recognition and information transfer processes[18].

Besides glycoproteins and glycolipids, other *cis*-diol-containing small molecules, for example, glycosides, also have important biological functions[19]. Glycosides contain two parts, which are sugar residues (sugar losing hemiacetal hydroxyl) and ligands. The function and nature of glycosides depend on the properties of ligands.

In plant, glycosides are widely distributed in roots, stems, leaves, flowers and fruits[20]. In animals, the most important kinds of glycosides are nucleotides and nucleosides.

1.3 Brief introduction of ribonucleotides

Nucleotides are important molecules which are building-blocks of nucleic acids (RNA or DNA). These special molecules are involved in many physical activities in living organisms. They take park in enzyme reactions in the body to produce energy and to serve as cell signaling molecules[21]. Moreover, these metabolites are driving forces for cell growth, playing important regulatory functions on cell differentiation and proliferation[22].

A nucleotide is composed of three parts. The first part of the molecules is a nitrogenous base which can be a purine or a pyrimidine. The base attaches to a five-carbon sugar (ribose or deoxyribose) via a beta-glycosidic linkage to form a nucleoside. The nucleoside in turn pluses one (or two, or three) phosphate group(s) to yield a nucleotide. Depending on the number of phosphate groups, nucleotides are distinguished into nucleoside monophosphate, nucleoside diphosphate and nucleoside triphosphate. And based on the type of pentose sugar, nucleotides could also be divided into deoxyribonucleotide or ribonucleotide. In the case of ribonucleotide, the sugar is a ribose. While in deoxyribonucleotide, the sugar is a deoxyribose. A ribonucleotide is a precursor to form a critical part of RNA. Ribonucleotides are reduced by ribonucleotide reductase to remove oxygen to

generate deoxyribonucleotides, which are precursors of DNA.

Ribonucleotides are also key factors in other cellular functions. These special monomers are utilized in both cell regulation and cell signaling[23]. Nucleoside triphosphates (ATP, GTP, CTP and UTP) function as a main source of energy within the cell, playing a central role in cell metabolism[24]. They can both hold and release energy via the phosphate groups when necessary. The energy was released by removing one phosphate group to yield nucleoside diphosphates (ADP, GDP, CDP and UDP), and the removal of a further phosphate group forms nucleoside monophosphates (AMP, GMP, CMP and UMP). Nucleoside diphosphates could be interconvertible via the energy currency to form nucleoside triphosphates. The conversion back and forth between the two kinds of metabolites are critical for maintaining energy levels in cells[25]. Ribonucleotides can be converted to cyclic nucleoside monophosphate (cAMP and cGMP) to participate in cell signaling in organisms as well[26]. In addition, ribonucleotides are also served as integral cofactors to assist the process of enzymatic reactions (e.g. coenzyme A, FAD, NAD, and NADP+)[27]. Quantification of these metabolites are required for oxidative stress evaluation, microorganisms' distinction, cell status study, human cerebrospinal fluid determination, cardiovascular system monitoring, food investigation, erythrocytes analysis, and so on[28].

Because of the great importance of nucleotides in the fields of biochemistry, determination of these metabolites provides valuable information for understanding

cellular physical activities. However, there are many challenges for the detection of nucleotides. Firstly, various sample constituents, especially in biological samples, serious matrix interferences greatly suppress the signals of targeted compounds. Secondly, due to the presence of extremely polar phosphate and *cis*-diol groups, nucleotides are poorly retained on reversed-phase columns. In addition, instability of phosphorylated compounds leads to a high level of in-source fragmentation for all the nucleotides. For example, ionization of adenosine-5'-triphosphate (ATP) produced considerable amounts of adenosine-5'-diphosphate (ADP) and adenosine-5'-monophosphate (AMP) fragment ions, even using the softest ionization technique, that is, electrospray ionization (ESI)[29]. To deal with these problems, efficient sample pre-treatment, completely chromatographic separation and high sensitive, high selective detections technologies are necessary for LC-MS analysis[30]. For sample preparation, solid-phase extraction (SPE) was the most popular technology in recent years[31]. Compared to organic solvents precipitates, the selectivity of SPE was much better. But due to the protein binding of nucleotides, the procedures suffered from the problem of low recoveries. For example, by using ion-pair reversed phase SPE, the recovery was only 43% at low concentrations[32]. Strong Anion Exchange (SAX) SPE was also applied for nucleotides extraction, but the high concentrations of salt in the solution required further desalination steps before the samples were injected to LC-MS. It might also lead to further losses of recoveries[33]. Increase of recoveries could be achieved by using combination

technologies. Combined phenol-chloroform LLE and ion-pair reverse phase SPE, relatively high recoveries across a wide dynamic range (72–85%) were observed[34]. However, the limitation of the method was that it was laborious and time-consuming to perform multiple extraction and sample transfer steps. To overcome the problem, a one-step method was developed by employing weak anion exchange (WAX) SPE[35]. The recoveries of the method were good to meet the needs, except that the cost for per sample was fairly high. Therefore, a rapid, high efficient method for sample pre-treatment is still a major bottleneck for extracting nucleotides with good reproducibility and recovery.

A variety of techniques have been used to chromatograph nucleotides. In the earlier studies, traditional reversed-phase liquid chromatography (RPLC) with UV detection were frequently applied for nucleotides detection by adding phosphate buffer to the mobile phases[36]. Additionally, strong anion exchange (SAX) columns were also used for nucleotides separation by utilizing high concentrations of non-volatile salt buffer[37]. However, these modifiers were not compatible with mass spectrometry and the sensitivity fell far short of what was required[38]. During the last ten years, LC coupled with tandem mass spectrometry (LC–MS/MS) has proven to be a highly sensitive technique with specificity and structural characterization capability[39]. Many related works employed the technique to analyze nucleotides in complex biological matrices[40]. Volatile ion-pairing agents were often used as mobile phase modifiers[41]. Although the methods achieved good

separation for nucleotides and decreased salt precipitation in ion source, persistent residues of these agents could never be cleared away completely from the column, even with extensive column flushing. Residual trace levels of the ion-pair agent might greatly change the retention and reproducibility of a column[42]. It also caused contamination of the mass spectrometer, resulting in significant signal suppression and requiring frequent cleanings of ionization source[43]. Therefore, a suitable LC-MS method is eager for sensitive and selective detection of nucleotides under acceptable chromatographic condition with low concentration and volatile buffer salts, but without using ion-pairing agents.

1.4 Brief introduction of ribonucleosides

Ribonucleic acid (RNA) plays a very important role in the process of cell growth. It copies the genetic information from deoxyribonucleic acid (DNA) and translates the information into proteins. After completing their assigned tasks, RNA is catabolized to free nucleosides. The main composition of the metabolites is normal nucleosides, i.e., adenosine (A), uridine (U), guanosine (G) and cytidine (C). Modified nucleosides are also the end products of RNA metabolism. Transfer RNA (tRNA) is a main source of modified nucleosides[44]. A total of 93 different modified nucleosides have been reported in RNA, with the largest number and greatest structural diversity in tRNA, 79; and 28 in ribosomal RNA (rRNA), 12 in messenger RNA (mRNA), 11 in small nuclear RNA (snRNA) and 3 in other small RNAs[45]. The four normal nucleosides are reused to construct new RNA. However,

the modified nucleosides are excreted from the cell to the urine, due to the lack of salvage enzymes for these substrates[40, 46].

All the modified nucleosides are derived by modifying the basic structure of the four major nucleosides, i.e., A, U, G, and C, at specific sites in the RNA chain. The most common type of modification is methylation of either the nucleobases, the sugar hydroxyls, or, in some cases, both portions of the nucleoside. After performing these post-transcriptional modifications, the modified RNAs are released from the precursor RNA molecules by site-specific nucleases[47]. Although some specific structures can only be found in certain types of RNA, most modifications are general and can be detected in different types of RNA from different organisms. Therefore, nucleosides in urine, which are derived from the degradation of RNA, are not only from human mammalian cells, but also from other organisms such as bacteria, fungi, and viruses[48].

1.4.1 Levels of modified nucleosides in urine

Modified nucleosides in urine as end products directly reflect the degradation rate of RNA. The conversion of RNA has a quantitative relationship with protein turnover rate in infants and adults[49]. Fast excretion of modified nucleosides, which may be related to the high speed of cell proliferation[50], was observed in babies with 6-10 times higher than that in adults. In healthy adults, excretion of modified nucleosides is relatively stable. It is not influenced by sex and age[51]. In addition, diets show little effect on the levels of urinary modified nucleosides[52]. However,

some physical illnesses, such as inflammation, immune diseases, cancers, especially urological diseases, have a great influence on the levels of these metabolites[53]. Therefore, the levels of nucleosides can be used to monitor status of bodies. Moreover, urine samples are easy to collect and it is non-invasive to patients. So, it is suitable for disease research, especially for discoveries of potential candidates for use as "biological markers" of cancers.

1.4.2 Relationship between urinary modified nucleosides and tumor

Tumor is an abnormal mass of tissue as a result of abnormal growth or division of cells. Early symptoms and physical signs of tumor are not special[54]. The early diagnosis rate of tumor is yet not high, although some markers have been found for auxiliary examinations. Generally, when the symptoms are in evidence, the carcinoma has been advanced and it is too late for treatment[55]. It is a great significance to develop an effective method for early diagnosis of tumor. It is instant requirement to search biomarkers and novel therapeutic targets for early diagnostic to improve the treatment of these diseases. Traditional tumor markers are genes and proteins. The levels of these markers are very low. Sometimes they are hard to detect and cannot meet the demands for early diagnosis[56]. Modified nucleosides is the component of RNA. Because the RNA metabolism is very fast in cancers, the concentrations of modified nucleosides are significantly higher in cancer patients than in healthy controls. Therefore, modified nucleosides can server as potential tumor markers for early diagnosis[57, 58].

1.4.3 Studies of urinary nucleosides as tumor markers

The levels of urinary nucleosides have been shown to be a signal of the disease status, indicating the patient's response to therapy, and correlating with the progression of disease[59]. Some papers have discussed the feasibility of urinary nucleosides as biomarkers for cancer diagnosis. For example, an inhibition ELISA system using a monoclonal antibody (AMC) was established to determine urinary levels of 5-methyl-2'-deoxycytidine (5MedCyd) in healthy individuals and cancer patients. Various types of cancer were tested. The levels of 5-methyl-2'-deoxycytidine were higher in leukemia patients than in healthy individuals. The results showed that urinary 5MedCyd might be applicable as a biologic marker for leukemia[60]. Another report also mentioned that evaluation of the urinary 5-methyl-2'-deoxycytidine level as a biological marker for leukemic patients was possible[61]. A good correlation was found between the clinical stage in high-grade lymphoma and healthy controls by comparing pseudouridine levels[62].

Many urinary nucleosides have been determined as potential markers of breast cancer. One study found that, compared to the breast cancer patients in surgical ward, patients hospitalized in the medical excreted significantly higher levels of 1-methylinosine and 1-methyladenosine. In addition, the two compounds could be used to suggest an unfavorable prognostic by reflecting more advanced disease[63]. Four modified nucleosides, i.e., 5-hydroxymethyl-2'-deoxyuridine, 8-hydroxy-2'-deoxyguanosine, 1-methyladenosine, and N^2,N^2-dimethylguanosine, were detected

significantly higher levels in pre-operative patients than in both normal controls and post-operative patients. It stated that these nucleosides could be used to evaluate the effects on medical treatment before and after tumor removal[64]. Urinary nucleoside levels measured in female breast cancer patients (n = 36) showed that levels of cytidine, 3-methylcytidine and inosine were significantly higher in patients than in normal controls ($p < 0.01$)[65]. Besides, quite a few reports confirmed that significant changes of urinary modified nucleoside levels have a close relationship with breast cancer[66-69].

Fourteen urinary nucleosides were determined in the samples of 62 healthy persons and 52 consecutive patients who suffered from colorectal cancer (CRC). The levels of 11 out of 14 of the determined nucleosides in urine were much higher in the CRC group than in normal controls. Two modified nucleosides, 1-methylguanosine (m^1G) and pseudouridine (Pseu), showed good sensitivity-specificity to diagnose CRC[70]. A study of urinary metabolic profiling of 34 healthy volunteers, 34 benign colorectal tumor and 50 colorectal carcinoma patients showed that nucleotide biosynthesis was significantly disordered in CRC patients[71].

The levels of modified nucleosides also showed significant changes in urine samples of other cancer patients, such as urogenital cancer[72, 73], hepatocellular carcinoma[74, 75], head and neck cancer[76, 77], uterine cervical cancer[78], lung cancer[79], and so on. In addition, elevated levels of modified nucleosides were detected in the urine of patients suffered from immunodeficiency diseases, for example, acquired

immunodeficiency diseases (AIDS)[80, 81] and severe combined immunodeficiency diseases (SCID)[82].

1.4.4 Analysis of urinary nucleosides

HPLC methods, which were developed by Gherke et al.[83, 84], were the most common methods used for the analysis of urinary nucleosides. The sensitivity and resolution of HPLC were better than paper-, thin-layer-, and open tubular column chromatography methods which were used prior to the development of HPLC methods. Most of modern HPLC methods are based on the research of Gherke and co-workers and used to separate mixtures of urinary nucleosides. A reversed-phase high-performance liquid chromatography (RP-HPLC) method with photodiode-array detection was used to quantitatively analyze urinary normal and modified nucleosides in 55 persons with malignant tumors of various types[84]. Following the extraction of urinary nucleosides with affinity chromatography on a phenylboronic acid column, a reversed-phase high-performance liquid chromatography method was applied for a complete separation of sixteen urinary ribonucleosides[85]. An ion-pair HPLC coupled with a fluorescence and a UV detector has been developed for the simultaneous determination of neopterine (Npt), pseudouridine (Psu) and creatinine (Cre) in urine[86]. Compared to HPLC, Ultra High Performance Liquid Chromatography (UPLC) is a much faster, more precise and higher resolution tool for separation. A method based on UPLC was applied to quantify eight modified

nucleosides in urine during 4 min with good linearity, accuracy and low LOQ values[87].

Gas chromatography (GC) has some advantages and limitations compared to HPLC. Limited references have been reported for the analysis of urinary nucleosides by GC[88, 89]. The resolution of GC is higher than other chromatographic techniques, but limited to the bad volatility of nucleosides, application of GC technique for nucleosides determination is still rare even after chemical derivatization. Urinary excretion of the modified nucleoside/base was analyzed with a methodology involving HPLC prepurification followed by GC with isotope dilution mass spectrometric detection[90]. A similar method was employed to determine oxidatively damaged DNA biomarkers in head and neck cancer patients, who were involved in the therapeutic effect or the ionizing radiation and in the side effects. The results showed that only urinary excretion of the modified nucleosides significantly increased[91].

Enzyme-linked immunosorbent assay (ELISA) is a test that uses antibodies and color change to identify a substance. The technique allows to analyze urine samples directly. It was easy and quick to quantify targeted urinary nucleosides of individual samples[92, 93]. Therefore, the methods could be applied to simultaneously analyze a large number of clinical samples. An inhibition ELISA system was developed by using a monoclonal antibody against 5-methylcytidine (AMC). It was employed to determine urinary levels of 5-methyl-2'-deoxycytidine in healthy individuals and

leukemia patients. Elevated levels of 5-methyl-2'-deoxycytidine were detected and the compound might be applicable as a biologic marker for leukemia[60]. Another inhibition ELISA was used to measure urinary levels of pseudouridine and 1-methyladenosine in leukemia and lymphoma patients. Significantly elevated levels of these nucleosides were detected. It means that the two metabolites in urine might be clinically useful as complementary markers to monitor disease status of leukemia and lymphoma patients[94]. Although ELISA is rapid enough to analyze hundreds of samples a day, the lack of specificity, which is caused by cross-reaction with other urinary components, reduces the accuracy of the quantitative result[95]. Therefore, results with a different type of assay are required to perform confirmatory testing.

Capillary electrophoresis was applied to analyze modified nucleosides in urine for the first time in 1997. The concentrations of modified nucleosides were tested in urine samples from 25 patients with 14 different types of cancer disease. The study found that the levels of pseu, inosine, N^4-acetyleytidine, N^1-methyl-anosine and N^2-methyl-anosine in patients with cancer were significantly higher than healthy controls[96]. Results of artificial neural network classification for urinary nucleosides analysis by capillary electrophoresis, were used for the clinical diagnosis of tumors. The recognition rate for the training set reached to 100%. Above 85% of the members in the predicting set were correctly classified[97]. Similarly, the combination of capillary electrophoresis and wavelet neural network was proved to be an effective and efficient tool for the clinical diagnosis of breast cancer[98].

Capillary electrophoresis coupled with electrochemical detector could detect the concentration of urinary 8-hydroxydeoxyguanosine as a biomarker for oxidative DNA damage[99]. Reversed electroosmotic flow was another kind of method that was applied for screening of inherited disorders of purine and pyrimidine metabolism by capillary electrophoresis[100].

Mass spectrometry has played a major role in the confirmation and/or assignment of structure to nucleosides isolated from human urine. More and more articles described the application of mass spectrometry methods for the analysis of urinary nucleosides[101-104]. For example, MALDI-TOF and high field asymmetric waveform ion mobility spectrometry (FAIMS) were used to directly identify modified nucleosides in urine[105, 106]. However, due to the complex composition of urine, direct analysis suffered from serious matrix effects. Therefore, chromatography and mass spectrometry were often combined together to reduce the interference of matrix. One example was that high performance liquid chromatography coupled with electrospray ionization tandem mass spectrometry (LC-MS/MS) was used to measure urinary nucleosides in female breast cancer patients (n = 36) to evaluate the diagnostic value of nucleosides as potential tumor markers[65]. LC-MS/MS method employing constant neutral loss (CNL) scanning for the loss of the ribose moiety (132 u) was also used to detect ribonucleosides in human urine[107]. C_{18} columns were widely used for LC separation. But some modified nucleosides are very polar. The retention of these compounds on C_{18} columns are quite poor.

Therefore, some novel columns were applied for isolate of nucleosides, such as hydrophilic interaction chromatography (HILIC)[108, 109] and zwitterionic hydrophilic interaction chromatography (ZIC-HILIC)[110]. For example, a HILIC/ESI-MS method was employed to detect RNA modifications by using a HILIC column. Chromatography with an ACN-rich solvent facilitated desolvation and ionization of modified nucleosides. Moreover, strong retention of uridine derivatives was another advantage of HILIC/ESI-MS over RPC/ESI-MS. The method could detect 34 nucleosides in urine samples. It was a valuable alternative for profiling modified nucleosides[111]. Although HILIC provided a practical alternative for nucleosides detection, its separation for some isomers were still unsatisfactory. And in some cases, there are some strong interaction between the hydroxyl groups of *cis*-diol containing compounds and the free residue of the stationary phase, which caused broad peak shapes and low sensibility[109, 112].

Another common technique is capillary electrophoresis-mass spectrometry (CE-MS). Capillary electrophoresis is especially applicable for separation of polar substance[113]. A method based on capillary electrophoresis-mass spectrometry coupled with synthetic urine as a surrogate matrix was developed for direct determination of urinary modified nucleosides. Results of 9 nucleosides demonstrated that the methodology offered a valid and reliable alternative for the determination of urinary nucleosides at naturally occurring levels in healthy individuals[114]. A sample treatment assay based on solid-phase extraction (SPE) with

polymeric sorbents has been developed for the simultaneous isolation and pre-concentration of nucleosides and nucleobases from urine prior to analyses by CE-ESI-MS. Not only *cis*-diols, but also non-*cis*-diol compounds were detected with the methodology[115].

Table 1.1 Comparison of analytical methods for analyzing urinary nucleosides.

Methods	Advantage	Limitation
HPLC-UV	Compatible with phosphate buffer or ion-paring agents	Low sensitivity and long operation time
UPLC-UV	Higher resolution than HPLC, good separation with phosphate buffer or ion-pairing agents as mobile phase	Unsatisfactory sensitivity for some low abundance nucleosides
GC-MS	Higher resolution than other chromatographic techniques	Not very suitable for nucleosides determination because of the bad volatility of nucleosides
ELISA	Rapid enough to analyze hundreds of samples a day	Lack of specificity, due to cross-reaction with other components, low accuracy for quantitative analysis

MALDI-MS	Fast and direct detection method	Suffered from serious matrix effects and difficult to distinguish isomers
RPLC-MS	Robust and well-developed methods	Poor retention for some very polar nucleosides without using ion-paring agents
LC-HILIC-MS	Better retention for polar nucleosides than RPLC, better intensity due to high organic mobile phase, unnecessary for ion-pairing agents	Unsatisfactory separation for some isomers. In some cases, peak shapes were broad due to strong interaction between the stationary phase and the cis-diol of nucleosides
CE-MS	High resolution for separation, and appropriate for the detection of polar compounds	Unsatisfactory stability and reproducibility

Although many techniques have been applied for urinary nucleoside determination, each analysis method described above still has advantages and limitations relative to the other techniques (Table 1.1). No one method can server as a “method of

choice" to identify and quantify all the urinary nucleosides simultaneously. Therefore, the result would be more objective and overall with combination of several techniques.

1.5 Brief introduction of bisphenol A

Recently, the effects of endocrine disrupting chemicals (EDC) on human health and enviremation have gradually caused extensive concern. Bisphenol A (BPA) is a classical endocrine disrupting chemical[116]. It is commonly used to produce epoxy resin, polycarbonate, polysulfone resin, and so on[117]. The products are applied to make a variety of common consumer goods, such as water bottles, household electronics, beverage cans, thermal paper for sales receipts, medical and dental devices[118]. Frequently contacting with these goods greatly increases the chance of BPA exposure.

BPA is a low toxic chemical. The half lethal dose (LD_{50}) of rats through the mouth was 3250 mg kg^{-1}. Inhalation exposure LD_{50} was 0.02%. And the oral LD_{50} in mice was 2400 mg kg^{-1} [119, 120]. In the daily production and life, BPA can enter human body through the skin and respiratory tract. BPA are moderate irritation to skin, respiratory tract, enteron and cornea. It was reported that the maximum daily intake of BPA was 1 μg kg^{-1} for a man or woman[121].

Under certain environmental pollution conditions, BPA exposure interferes with a variety of biological endocrine function. It may result in a decline in all sorts of biological reproductive functions[122], genital tumors[123], lowered immunity[124]. It

could also cause various reproductive abnormalities[125], disrupt the normal human body endocrine function[126], affect wildlife safety[127], and threating to human health[128]. Therefore, BPA has been blacklisted with several EU countries, restricting the use of the related products on some baby items[129]. In order to make better use of the compound, to study the toxicological effects and its mechanism of action of BPA have the vital significance.

1.5.1 Toxicological effects of BPA

BPA can affect the endocrine system, estrogen receptor (ER) mediated pathway, antagonism androgen receptors (AR) mediated pathways and enzymes within the organization to disrupt the body's normal functions.

BPA had effects on the endocrine system. BPA could combine with E2 to compete with sex hormone-binding protein in plasma. It resulted in displacement of endogenous hormones, increasing the plasma concentrations of free T and E2[130]. BPA could also take effect on the nervous tissue. It disrupted the synthesis, secretion and release of pituitary hormone in the physiological targeted organs via the hypothalamus-hypophysis-gonadal axis[131]. It was reported that BPA could be derived for a number of halogenated aromatic hydrocarbon metabolites, which suppressed the sulfuric acid salinization of E2 by estrogen sulfo transferase, resulting in a dramatic increase of E2 concentration in some tissues[132]. Kester M H found that pregnant SD rats infected with BPA significantly reduced the plasma levels of luteinizing hormone (LH) in offspring of rats, which stimulated the

formation of female corpus luteum and secretion of male testosterone synthesis[133]. BPA could combine to the anterior lobe and posterior lobe with ER in F344 rats, to increase the regulatory factor activity of posterior lobe cells PRL and to promote anterior lobe cells proliferation by estrogen response element (ERE) regulating prolactin (PRL) transcription[134].

BPA had effects on male morphological characters. BPA has damage effects on the male reproductive system and fertility. Different BPA dose exposure could lead to different reproductive toxicity. Some studies have found that the influence of low dose of BPA on the testicular weight was greater than high dose[122]. An example was that adult rats exposed to 750 ppm [50 mg $(kg \cdot d)^{-1}$] of BPA through the mouth did not show adverse reproductive effects. But when the doses decreased to 50 μg d^{-1}, sperm activity rate was lower and deformity rate increased[135].

BPA has potential embryo toxicity and genetic toxicity. Animals reproductive assessment by continuous breeding (RACB) confirmed that BPA showed effects on reproductive function of F1 generation, leading to significantly reducing of epididymis and seminal vesicle weight[136]. And rats exposed to 139 mg $(kg \cdot d)^{-1}$ BPA caused morphological changes of testicular tissue and concentrations decrease of the plasma free testosterone[137].

BPA had effects on genetic material. It was reported that after treated human embryo liver cells with BPA, the comet test showed that BPA had DNA oxidative damage effect ($p < 0.05$) even in very low dose (10 μmol L^{-1})[138]. And as the dose increased,

the DNA damage effect also increased. A variety of enzymes involved in DNA damage repair were activated. The effect was slowed down when the cells were treated with vitamin C[139].

BPA had effects on immune system. BPA can affect non-specific immune defense system of host. Female BALB/c mice (four weeks) were subcutaneously injected with 5 mg (kg Bw)$^{-1}$ BPA for five days consecutively. The results showed that not only the numbers of mice spleen T cells, B cells and macrophages decreased significantly, but also the migration and accumulation of lymphocytes and macrophages were inhibited in the infected area[140]. BPA exposure also reduced the serum levels of interleukin-6 (IL-6) and the activity of neutrophils, which led to weakening of the body nonspecific immune defenses[141].

1.5.2 Metabolomic studies on BPA exposure

It has been reported that BPA exhibited hormone-like properties. It may alter hormone regulation even in very low-dose exposure[142]. The adverse effects of BPA exposure were shown to cause female precocious puberty[143], sperm count falling[144], prostatic hyperplasia[145], and other diseases. Data showed that BPA had a certain embryo toxicity and teratogenicity, posing a threat to fetuses and young children[146, 147]. Disrupting hormone metabolism by BPA increased risks of ovarian cancer, prostate cancer, leukemia and other cancers in animal models[148].

Besides, some studies have linked the nearly ubiquitous environmental contaminant exposure to metabolic disorders. Skin mucus-based metabolomics of the BPA

exposed fathead minnow showed a statistically significant bias with regard to sex by analyzing 72 of the detected metabolites[149]. The phenomenon of gender differences also occurred in marine ecotoxicology such as male and female mussel, which presented different sensitive to BPA exposures[150]. In rats, BPA induced DNA methylation damage and broad protein degradation, and elevated the levels of deleterious metabolites in choline pathway[151]. In another paper, the authors found that BPA altered testicular n-6 fatty acid composition and decreased antioxidant enzyme levels[152]. The relationship of bisphenol A and human health has been well reviewed by Johanna R. Rochester in 2013[153].

The toxic effects of BPA have been reported to contribute to amino acids, organic acids and neuro-transmitters, as well as *cis*-diol-containing metabolites such like galacturonic acid, cytidine monophosphate, 7,8-dihydrobiopterin, and so on[154, 155]. However, only several *cis*-diol compounds were mentioned in just a few articles. There were no papers describing the effects of BPA on the profiling of *cis*-diol metabolites. That may be because these metabolites were not readily detected due to their low abundance, high polarity and serious matrix interferences in biological samples. These characteristics made them poor separation on reverse phase column, serious ionic interference and low sensitivity of mass spectrometric detection. These factors have posed a grave challenge to the determination of *cis*-diol metabolites.

BPA, the environmental estrogen compound, is widespread in the ecological environment. Because of the long period of incubation and frequent high-level contact, it had become a kind of environmental pollutants harm to people. It has come to be a hot research area in the environmental research field. The influence of BPA differed in biological species, exposure dose and contact models[156]. The mechanism, sphere, proceed and effects of this compound were variety and still not very clear[157]. Especially, few studies were reported its effects on the key endogenous metabolites, such as nucleosides, nucleotides, sugars and other active small molecular metabolites. Therefore, it is necessary to perform some research on this aspect to further understand the environmental impact and new mechanism of BPA exposure. The findings could have substantial implications for establishing effective prevention system to against toxic effects of BPA. This may be an important topic related to environmental protection and peoples' health.

1.6 Objectives

Due to the great importance of *cis*-diol-containing metabolites, determination of these compounds provides valuable information for understanding their function in cellular physical activities. However, there are many challenges for the detection of these metabolites. Firstly, because of complex sample components, especially in biological samples, serious matrix interferences greatly suppress the signals of targeted compounds. Secondly, due to the presence of polar *cis*-diol groups, these compounds are poorly retained on reversed-phase columns. In addition, some of the

compounds are at low concentrations, meaning that selective separation and enrichment are necessary. Although different strategies have been proposed to settle these problems, there remain some bottlenecks to determine these compounds, such as low recoveries, laborious and time-consuming, high cost, modification of the instrument, and so on. These situations limit the applicability of these methods. Therefore, to deal with these problems, efficient sample pre-treatment, completely chromatographic separation and high sensitive, high selective detections technologies are necessary for analysis of *cis*-diol-containing metabolites.

Compounds containing *cis*-diol groups can react with acetone or dimethyl ketal to form acetonides (isopropylidene ketal). The polarity of acetonides is much smaller than the substrates. Therefore, this reaction has been used as a derivatization method for the analysis of carbohydrates by GC[158]. Nucleosides containing *cis*-diol groups can also react with acetone to form isopropylidene-nucleosides. The reaction has a wide range of applications to protect group of *cis*-diol for synthesis of nucleoside derivatives in organic synthesis[159]. However, there has not yet been reported that the reaction was applied for the identification and quantification of nucleosides or nucleotides by LC-MS. Therefore, in this work, a derivatization method based on the reaction would be established. Following the optimization and validation of the method, identification of nucleosides, nucleotides or carbohydrates were performed by using LC-MS. The aim of the work was to establish a practical,

fast and effective method for identification of *cis*-diol-containing metabolites, and to apply these methods to study real-world biological samples.

Chapter 2 Development and validation of a chemical derivatization method for *cis*-diol-containing metabolite detection by using liquid chromatography-mass spectrometry

2.1 Introduction

Ketal formed by reacting *cis*-diol compounds with acetone is known as acetonide or isopropylidene ketal. To form acetonide is one of the most common protecting approach for *cis*-diol compounds in organic chemistry. The most economical and convenient synthesis method to generate acetonide is through the reaction of anhydrous acetone and *cis*-diol compounds. Catalysts are necessary for the reactions. The most commonly used catalysts include protic acids, such as sulfuric acid (H_2SO_4)[160], perchloric acid ($HClO_4$)[161], *p*-toluenesulfonic acid (PTSA or *p*-TsOH)[162], camphorsulfonic acid (CSA)[163] and pyridinium *p*-toluenesulfonate (PPTS)[164], as well as Lewis acids, for example, $FeCl_3$[165], $SnCl_2$[166], $CuSO_4$[167], and $ZnCl_2$[168]. The reaction products can be dissolved in acetone, so no extra solvents are needed.

The reaction of using acetone to protect *cis*-diol has a wide range of applications in organic synthesis. It has been widely used in the carbohydrate chemistry to selectively mask different hydroxyl groups[169, 170]. It was used to prepare 2,2-disubstituted and 2-monosubstituted 1,3-benzodioxoles[171]. The reaction could achieve quantitative yield in protecting the catechol residue of 3,4-dihydroxyphenylalanine (DOPA) derivative as an acetonide[172]. For example,

suspended 6 g uridine in 359 mL of dry acetone and used 1.5 mL conc. H_2SO_4 as catalyst. After reacting for 2 h at room temperature, a white solid was obtained. The reaction yield was 86%[173]. The reaction was also used to protect the *cis*-diol groups of nucleosides before they were modified to other compounds[159, 174].

The reaction of acetone and *cis*-diol belongs to nucleophilic addition reaction. A possible reaction mechanism is that acetone reacts with one hydroxyl of *cis*-diol to give hemiketal, and then the hemiketal reacts with another hydroxyl of *cis*-diol to form ketal. The overall reaction is that a molecule of acetone reacts with a molecule of *cis*-diol to generate a molecule of ketal and to lose a molecule of water. The reaction process is shown in Figure 2.1. First, carbonyl is combined with hydrogen ion of the catalyst to form oxonium ion (α) to increase the electrophile of carbon atom of the carbonyl. After the addition reaction of α with one hydroxyl of *cis*-diol compound, the hydrogen ion is lost from the intermediate to form an unstable hemiketal β. The hydrogen ion combines with β to form oxonium ion again. Intermediate γ, the product of oxonium ion losing water, takes nucleophilic addition reaction with another hydroxyl of the *cis*-diol compound. And then the hydrogen ion is removed. Finally, the product of acetone reacted with *cis*-diol, which is called acetonide or ketal, is generated δ.

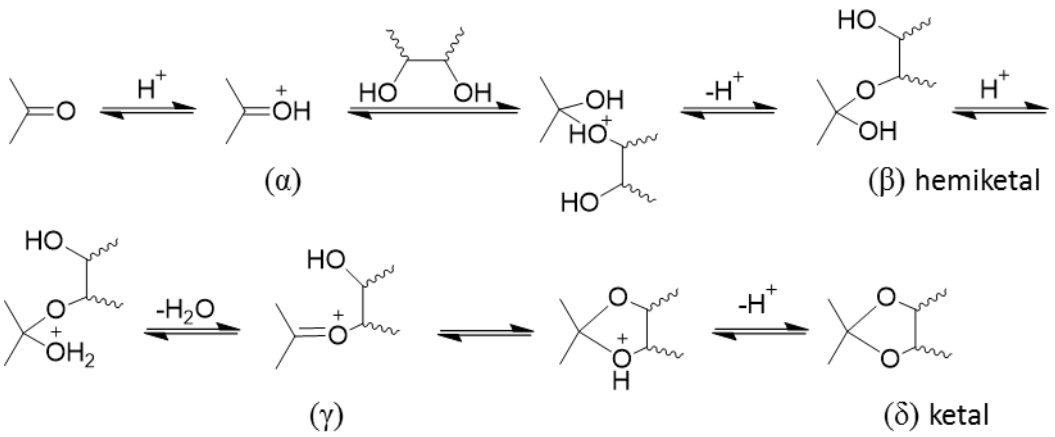

Figure 2.1 Reaction mechanism of *cis*-diol compounds with acetone to form ketal.

The reactions are reversible. Hemiketal is unstable in an acidic or alkaline solution. Ketal is also unstable in a strong acidic solution, but it is stable to alkalis and oxidants. Therefore, it is necessary to ensure the reaction system is at the presence of acidic catalyst and water-free. However, the reaction of acetone with the *cis*-diol could form water, which makes the reversible reaction move backward. Thus, it needs to minimize the content of water in the system during the reaction, in order to drive the equilibrium reaction forward and increase the yield of the acetonide. Based on the reaction mechanism, it can be speculated that the yield of reaction is affected by various factors, including kinds of catalyst, concentration of the catalyst, ratio of reactants, reaction temperature and reaction time. In this chapter, therefore, optimization was carried out to determine how these factors influenced the reaction yield. The arm was to find out the optimal reaction conditions for the derivatization of *cis*-diol-containing metabolites.

2.2 Material and methods

2.2.1 Chemicals

Nucleosides were purchased from Sigma-Aldrich (St. Louis, MO, USA), including guanosine (≥ 98%, G), adenosine (≥ 99%, A), cytidine (≥ 99%, C) and uridine (≥ 99%, U). Acids which were used as catalysts included concentrated sulfuric acid (98% H_2SO_4, Aladdin Industrial Inc, Shanghai, China), *p*-Toluenesulfonic acid monohydrate (*p*-TsOH, Aladdin Industrial Inc, Shanghai, China), and 70% perchloric acid ($HClO_4$, Sigma-Aldrich). HPLC grade methanol was obtained from Merck (Dermstadt, Germany). Water was purified by using a Milli-Q system (Millipore, Milford, MA). Formic acid (HPLC grade) was also purchased from Sigma-Aldrich.

2.2.2 Optimization of derivatization conditions

According to previous reports, three different catalysts, i.e., 98% H_2SO_4, *p*-TsOH and 70% $HClO_4$, were chosen to compare their effects on the reaction. The reaction was hold for 2 h at 0 ^oC. Then saturated K_2CO_3 solution was added to neutralize the acids. The precipitate was removed by centrifugation. Supernatant was dried with nitrogen flow. The obtained residue was dissolved with methanol/water (1:1, V/V), and diluted to 100 μg mL^{-1}. The products were detected by using UPLC-PDA at 260 nm.

To compare the effects of concentration of the catalyst on the reaction efficiency, 70% $HClO_4$ was added to the reaction system at the concentration of 0.01%, 0.25%,

0.50%, 1.00%, 2.50% and 5.00% (percentage compared to acetone volume), respectively. The amount of acetone was 200 μL. The reaction temperature was 0 ^{o}C. The reaction time was 2 h. The treatment of reaction products was the same as mentioned above.

In order to compare the influence of different temperature on the reaction efficiency, the reaction underwent at four temperatures, i.e., 20, 4, 0 and -20 ^{o}C. In the reaction system, 70% $HClO_4$ was used as catalyst at the concentration of 1.00%. The amount of acetone was 200 μL. The reaction time was 2 h. The treatment of reaction products was the same as mentioned above.

Different mole ratios of G and acetone, including 1:195, 1:390, 1:585, 1:780, 1:975, 1:1170 and 1:1365 were compared to determine the influence of reactant ratio on the reaction efficiency. The concentration of catalyst (70% $HClO_4$) was 1.00%. The reaction time was 2 h. The reaction temperature was -20 ^{o}C. The treatment of reaction products was the same as mentioned above.

To determine the reaction time, the ratio of acetone and G was set at 1:585 in the reaction system. 1.00% of catalyst (70% $HClO_4$) was added. The reaction temperature was -20 ^{o}C. 50 μL reaction mixture was sampled at the following point-in-time: 1 min, 2 min, 5 min, 10 min, 15 min, 30 min, 60 min, 120 min, 180 min, 240 min, 360 min and 480 min. The treatment of reaction products was the same as mentioned above.

The applicability of the reaction conditions was determined by extending the reaction to other nucleosides. Four nucleosides, A (1.23 mg), G (1.18 mg), U (1.15 mg) and C (1.33 mg), were mixed together. 734 μL acetone and 7.34 μL 70% $HClO_4$, were added. The reaction was held for 30 min at -20 ºC. The processing of reaction products was the same as mentioned above.

2.2.3 Sample preparation

To validate the method, real human urine samples were used to perform derivatization. 100 μL urine sample was dried with vacuum freeze drying technology. Acetone (600 μL) containing internal standard (IS 50 ng mL^{-1}) was added to the residue in combination with 6 μL $HClO_4$ (70%). The mixture was vigorous vortex for 30 s and set aside at -20 ºC for 30 min. And then, the acid was neutralized with 12 μL saturated K_2CO_3 solution. The suspension was centrifuged at 12,000 × *g* for 10 min at 4 ◦C to remove the precipitation. The supernatant was dried with a stream of nitrogen. The residue was reconstituted with 100 μL methanol/water (5:95, v/v). The solution was centrifuged at 12,000 × *g* for 10 min at 4 ◦C and the supernatant was used for LC-MS/MS analysis (Figure 2.2).

As a control, methanol/water (3:1, 600 μL) containing internal standard (IS 50 ng mL^{-1}) was added to the residue of vacuum freeze-dried urine (100 μL). After vigorous vortex for 30 s, the mixture was set aside for 30 min at -20 ºC. And then it was centrifuged at 12,000 × *g* for 10 min at 4 ◦C to remove the precipitation. The supernatant was dried with a stream of nitrogen. The residue was reconstituted with

100 μL methanol/water (5:95, v/v). The solution was centrifuged at 12,000 × *g* for 10 min at 4 ◦C and the supernatant was used for LC-MS/MS analysis.

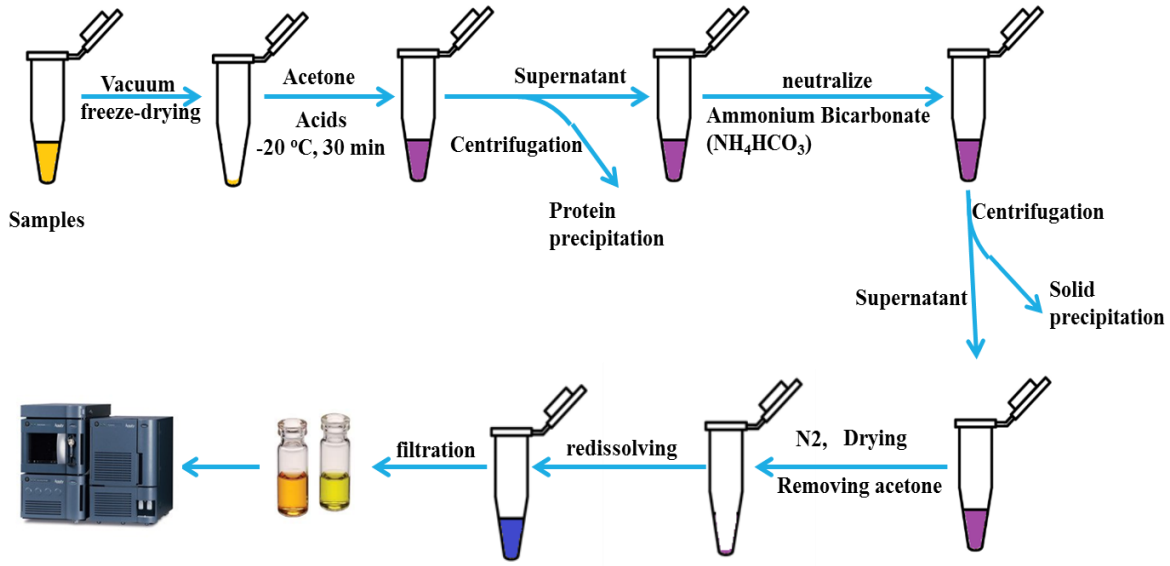

Figure 2.2 Flow chart of sample preparation.

2.2.4 Ultra-performance liquid chromatography

An Acquity™ Ultra-performance liquid chromatography (UPLC) system coupled to PDA or TQ detector (Waters Corporation, MA, USA) was used to perform the analysis. A Waters Acquity™ BEH phenyl column (100 mm × 2.1 mm, 1.7 μm) was employed for chromatographic separation. The mobile phases were water containing 0.05% formic acid (A) and methanol (B). Linearity gradient elution began at 5% B, then increased to 20% within 2 min, then to 35% within 8 min, then to 95% within 4 min and held for 1 min, then returned to 5%. Total running time was 20 min. The flow rate was 0.30 mL min^{-1}. The column temperature was set at

35 ◦C for all analyses. Injection volume was 10 µL. For optimization, PDA detector was set at 260 nm. For method validation, a Triple Quadrupole Detector was used.

2.2.5 Mass spectrometry

A Triple Quadrupole Detector (Waters, Manchester, UK) equipped with an ESI source was employed to determine the derivative nucleosides in urine. Data was acquired in the positive ionized mode and multiple reaction monitoring (MRM) scanning mode. Capillary voltage was 3.00 kV. Ion source temperature was 110 ◦C and desolvation gas temperature was 450 ◦C. Desolvation gas flow was 1000 L h^{-1}. Cone gas flow was 150 L h^{-1}. Dwell time was 0.1 s. The ion transitions for MRM was in Table 2.1.

Table 2.1 Ion transitions for MRM scan of nucleoside derivatives in urine.

Name	Abbreviation	Formula	Cone (V)	Collision Energy	Parent ion	Daughter ions
Adenosine + Acetone	A + Ace	$C_{13}H_{17}N_5O_4$	25	15	308	136
Guanosine + Acetone	G + Ace	$C_{13}H_{17}N_5O_5$	20	9	324	152
Uridine + Acetone	U + Ace	$C_{12}H_{16}N_2O_6$	20	7	285	113
Cytidine +	C + Ace	$C_{12}H_{17}N_3O_5$	20	9	284	112

Acetone						
Guanosine + Acetone-d_6	G + Ace-d_6	$C_{13}H_{11}D_6N_5O_5$	20	9	330	152

2.2.6 Preparation of standard solutions and QC samples

The 10 mg mL^{-1} stock solutions of A, G, U and C were prepared in deionized water. All stock solutions were kept at -20 ^oC until they were used. The stock solutions were diluted to the concentration range of 0.5-2500 ng mL^{-1} (0.5, 5, 10, 50, 100, 500, 1000 and 2500 ng mL^{-1}) with PBS (pH 7.4) containing 0.5% bovine serum albumin (BSA) as matrix to form working solutions. The working solutions were derivate with acetone as described in *Sample preparation*. Working solutions at three concentration levels (5.00, 50.0 and 500 ng mL^{-1}) were used as quality control (QC) samples.

2.2.7 Validation of the method

Calibration of the method was performed by analyzing the derivate working solutions in at least triplicate runs. Calibration curves were established by plotting the peak-area ratios of the target compound/IS versus concentrations of the working solutions. A linear least-squares regression was used to evaluate the linearity of the assay. The limit of detection (LOD) and limit of quantification (LOQ) of this method were defined as the concentration where the signal-to-noise ratio of one peak was 3 and 10, respectively. They were experimentally measured by diluting

the working solution to appropriate concentration

Accuracy and precision of the assay were determined with QC samples at levels of 5.00, 50.0 and 500 ng mL^{-1} in five replicate runs. The assay accuracy was expressed as relative error (RE%). The precision was evaluated by using relative standard deviation (RSD). Extraction recoveries of the four nucleosides in urine were evaluated by adding three levels of A, G, U and C to 100 μL urine samples (n = 5). Stability of four nucleoside derivatives was evaluated by analyzing the QC samples at three concentrations (5.00, 50.0 and 500 ng mL^{-1}) in five replicate runs. The intra-day stability was performed by using the QC samples with a four-hour interval in the same day. And inter-day stability was determined after the QC samples were stored at -20 ºC for 72 h.

2.2.8 Data analysis

All statistical analysis was performed by using OriginPro 9.0 (OriginLab, MA). Average, standard deviation and relative standard deviation were calculated for the parallel experiments. The figures were plotted by using OriginPro software. The reaction efficiency was evaluated by comparing the peak area percentage of products in the sum of the area of guanosine and products.

2.3 Results and discussion

2.3.1 Selection of catalyst

Catalysts are necessary to convert *cis*-diol compounds into acetonides. Commonly used catalysts are proton acids and Lewis acids. Lewis acids contain metal ions, and

the residual of the ions has bad effects on mass spectrometry. Therefore, Lewis acids were not used in this experiment. Commonly used proton acids include 98% H_2SO_4, *p*-TsOH and 70% $HClO_4$[175-177]. All the three kinds of catalysts could catalyze the reaction of *cis*-diol compounds with acetone. But when 98% H_2SO_4 or *p*-TsOH was used, reactants would form caking. And it needed a long time and violently rocking to make the caking be dissolved completely[178]. But when the catalyst was 70% $HClO_4$, reactants could be completely dissolved in a half minutes. The reaction finished fast by using this acid. Therefore, 70% $HClO_4$ was chosen as catalysts in the experiment.

2.3.2 Effects of concentration of the catalyst on the reaction efficiency

To evaluate the effect of catalyst concentration on the reaction efficiency, different concentration of 70% $HClO_4$ (0.01%, 0.25%, 0.50%, 1.00%, 2.50% and 5.00%, respectively) was added to the reaction system of G and acetone. The results were shown in Figure 2.3. When the catalyst was at low concentration (0.10%), the percentage of the product was about 86%. When the volume ratios of $HClO_4$ and acetone were 0.25%, 0.50% and 1.00%, the percentages were more than 97%. It means that as the content of catalyst rose, the percentage of the product increased. The highest point appeared at 1.00%. However, the percentages dipped down to 95.70% and 92.15% when the ratios rose to 2.50% and 5.00%. This was due to the amount of water following the catalyst into the reaction system was too large to

inhibit the reaction to the positive direction, resulting in the decrease of reaction yield.

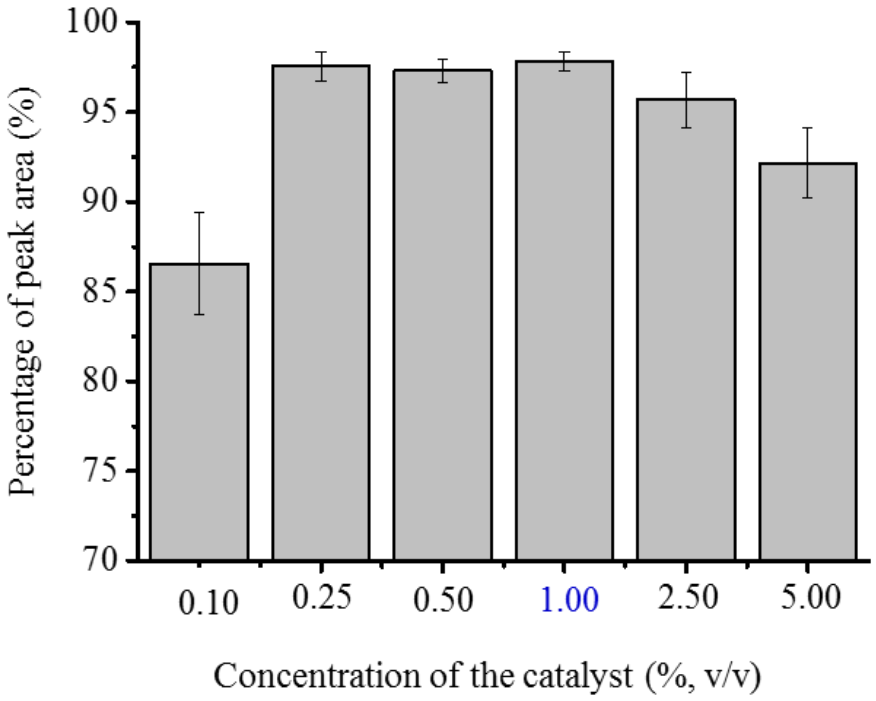

Figure 2.3 Effects of concentrations of catalyst on the peak area percentage of products.

2.3.3 Effects of reaction temperature on the reaction efficiency

In order to evaluate the influence of temperature on the reaction efficiency, G was used to react with acetone at temperature that could easily reach in the lab, i.e., 20, 4, 0 and -20 ^{o}C, respectively. The peak area percentages of products at the different temperature showed that the content of G in the reaction system fell off as the temperature decreased (Figure 2.4). Oppositely, the production yields increased. The percentage was only 86.2% at 20 ^{o}C, but it rose to 98.5% when the temperature

was down to -20 °C. This suggests that low temperature was favorable for the reaction. In addition, biological samples stored at low temperature could protect them from degradation. This was a very important factor that had to consider for biological sample analysis. Therefore, the temperature chosen for the derivatization was -20 °C.

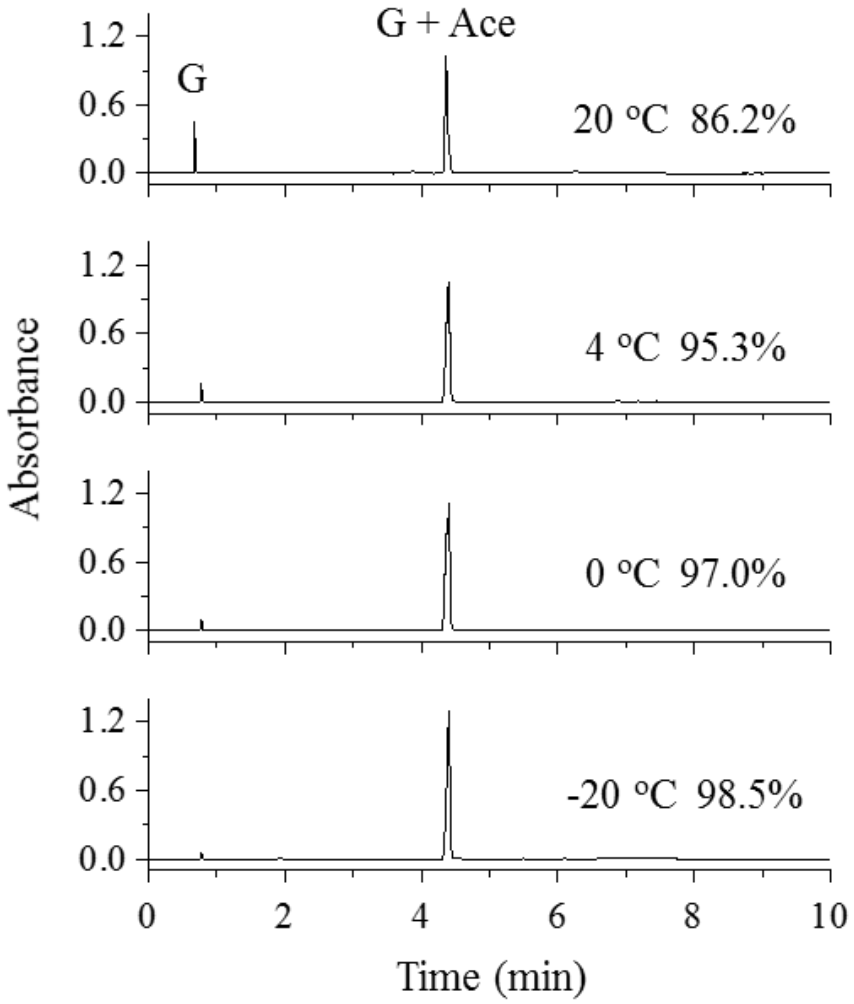

Figure 2.4 Effects of temperature on the reaction efficiency.

2.3.4 Effects of reaction time on the reaction efficiency

As mentioned above, when 70% $HClO_4$ was used as catalyst, the reactants could quickly dissolve in acetone. Results of sampling at different reaction time proved that the reaction speed was really fast (Figure 2.5). About 97% of reactants had transformed into products in the first one minute. With the extension of time, the production rate showed a slight increase, but the change was not obvious. It means that the reaction was relatively easy to reach the balance under these conditions. Because there were many kinds of *cis*-diol compounds in biological samples, in order to ensure that all the compounds were completely reacted with acetone, the reaction time was set for 30 min.

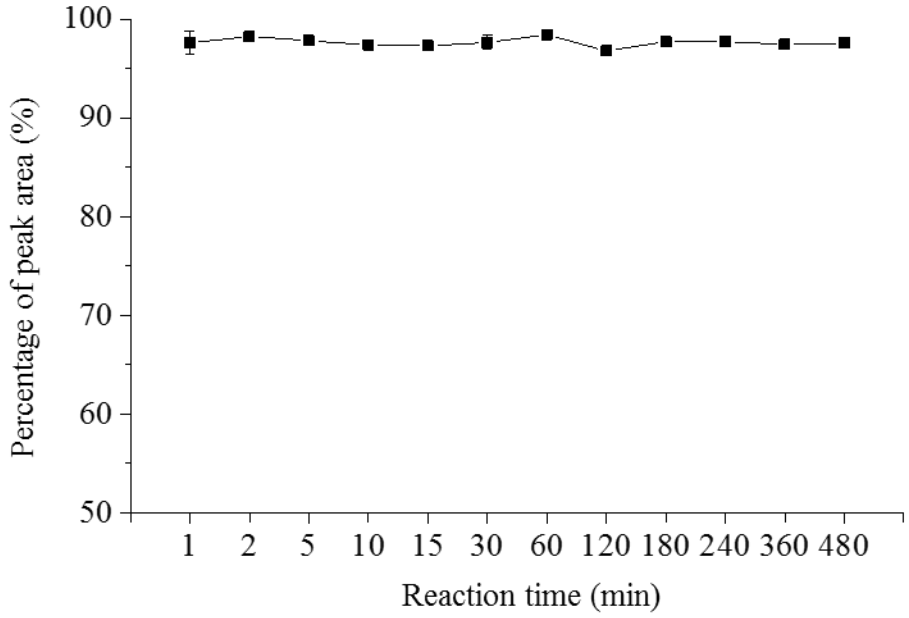

Figure 2.5 Effects of reaction time on the reaction efficiency.

2.3.5 Effects of reactant ratio on the reaction efficiency

Acetone was both reactant and solvent in the reaction. The change of its volume had obvious effect on reaction efficiency. When the ratio of G and acetone was 1:195, the peak area percentage of products was only 91.75% (Table 2.2). When the ratio is equal to or greater than 1:390, the percentages were more than 98%, even to 99%. The experimental phenomena were related to the concentration of water in the reaction system. When the dosage of acetone was small, the concentration of water in the catalyst and generated by the reaction was large. It forced the equilibrium reaction to move to the left, resulting in the decrease of peak area percentage. When the volume of acetone was large enough, the influence of water was small. Its impact on the production rate was very weak. According to the results, when the ratio of G and acetone was 1:585, the reaction could give the highest percentage (99.05%). However, the content of *cis*-diol compounds in real samples was unknown and the matrix of biological samples was complex, which were likely to be influential to the reaction. Therefore, the amount of acetone used in the real samples was still needed further experimental confirmation.

Table 2.2 Effects of reactant ratio on the reaction efficiency.

Mole ratio of Reactant	Peak area percentage of product (%)			Mean ± SD (%)
	Trial 1	Trial 2	Trial 3	
1:195	91.75	91.13	93.15	92.01 ± 0.84
1:390	99.00	98.60	98.82	98.81 ± 0.16
1:585	99.01	98.96	99.17	99.05 ± 0.09
1:780	98.48	97.08	97.19	97.58 ± 0.64
1:975	98.55	98.64	97.37	98.19 ± 0.58
1:1170	98.74	98.60	97.94	98.43 ± 0.35
1:1365	98.02	99.11	98.57	98.57 ± 0.44

2.3.6 Applicability of the derivatization method to other nucleosides

The reaction conditions for G and acetone had been optimized. More than 95% of G could be converted into acetonide when the ratio of G and acetone was 1:585, with 1.00% of $HClO_4$ (70%) as catalyst and reacting for 30 min at -20 ^oC (Figure 2.6). This results showed that such reaction conditions were appropriate for G. However, due to a wide variety of modified nucleosides in biological samples, applicability of the derivatization method to other nucleoside was still needed to be confirmed. Because all the modified nucleosides were based on A, G, U and C, thus, the four nucleotides would be used to examine whether the derivatization method was practical. Chromatograms of products showed that all the 4 nucleosides could

react with acetone (Figure 2.7). All the peak area percentages were higher than 95%. It means that the derivatization method was applicable to other nucleosides.

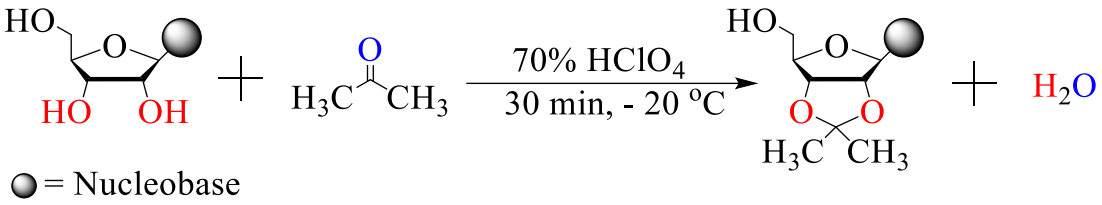

Figure 2.6 The optimized reaction conditions for nucleosides and acetone.

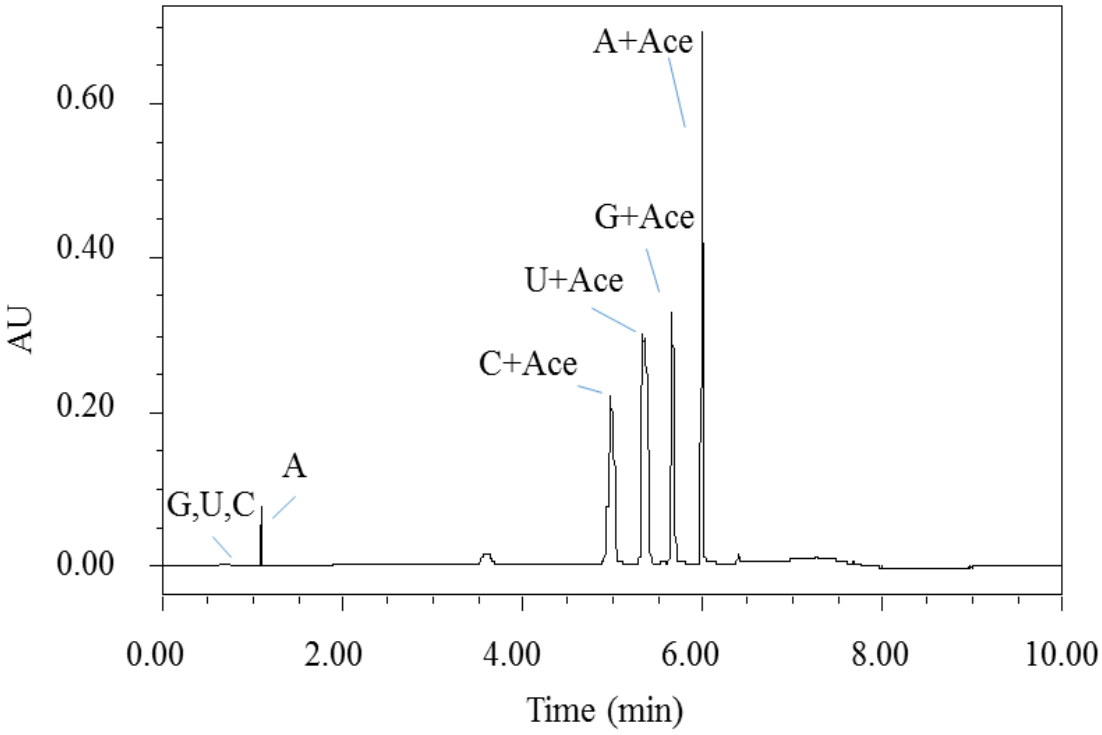

Figure 2.7 Chromatograms of products of A, G, U and C reacted with acetone. Ace: acetone.

2.3.7 Optimization of derivatization reaction conditions with urine samples

In the process of optimization of derivatization reaction conditions, it was found that the amount of acetone had important influence on reaction results. Though the ratio of acetone and standard have been determined, the ratio of acetone and urine samples was still necessary to be further confirmed. Following the approach described above, 100 μL urine sample was reacted with 300, 400, 500, 600, 700 and 800 μL acetone, respectively. The reaction products were analyzed by using LC-MS/MS. By comparing the peak area of acetonides of A, G, U and C, it was found that the content of the four compounds was the highest with the ratio of 1:6 (Figure 2.8). It implied that nucleosides in urine could adequately react with acetone under the proportion. Therefore, in the subsequent experiments, the ratio of urine and acetone was set as 1:6.

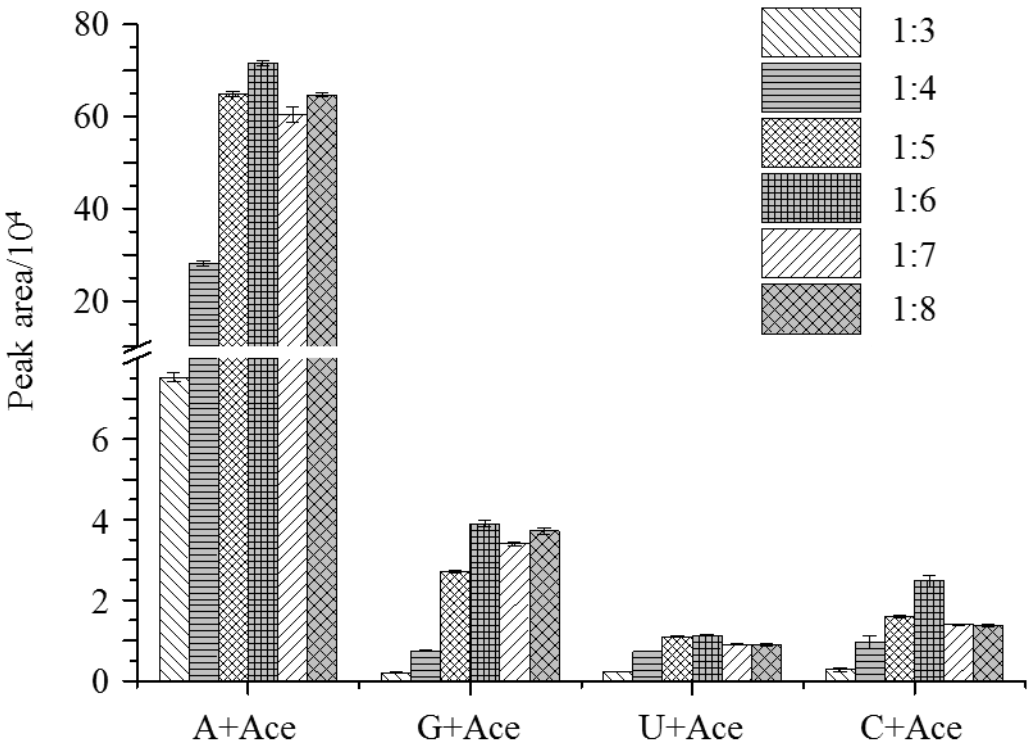

Figure 2.8 Effects of ratio of urine and acetone on the peak area of acetonides of A, G, U and C. A+Ace: acetonides of adenosine; G+Ace: acetonides of guanosine; U+Ace: acetonides of uridine; C+Ace: acetonides of cytidine.

2.3.8 Specificity

A good chromatographic separation was the basis of accurate identification and quantification. Urine samples contained more than 3,000 compounds, which included many isomers. The complex components made the separation very important for the determination of specific compounds in urine. Figure 2.9 showed the chromatograms of four nucleosides (A, G, U and C) and their acetonides with direct analysis (Figure 2.9A) and derivatization (Figure 2.9B). Results showed that peak separation in Figure 2.9B was much better than that in Figure 2.9A. For

example, only one peak was detected with the ion transition 244>112 (compound C) when urine samples were analyzed directly. The retention time of the peak was 1.04 min. It was very close to the dead time and the matrix effects were very serious. These factors may impact the accuracy and reliability of the results. After reacted with acetone, the ion transition of the compound became 284>112. Four peaks were detected with the ion transition and all peaks were baseline separation. The retention time increased to 3-5 min which alleviated the matrix effects. It means that better separation was achieved with the derivatization method for sample preparation. The results showed that direct analysis could not accurately determine the content of the four nucleosides. But the derivatization method could overcome the problem.

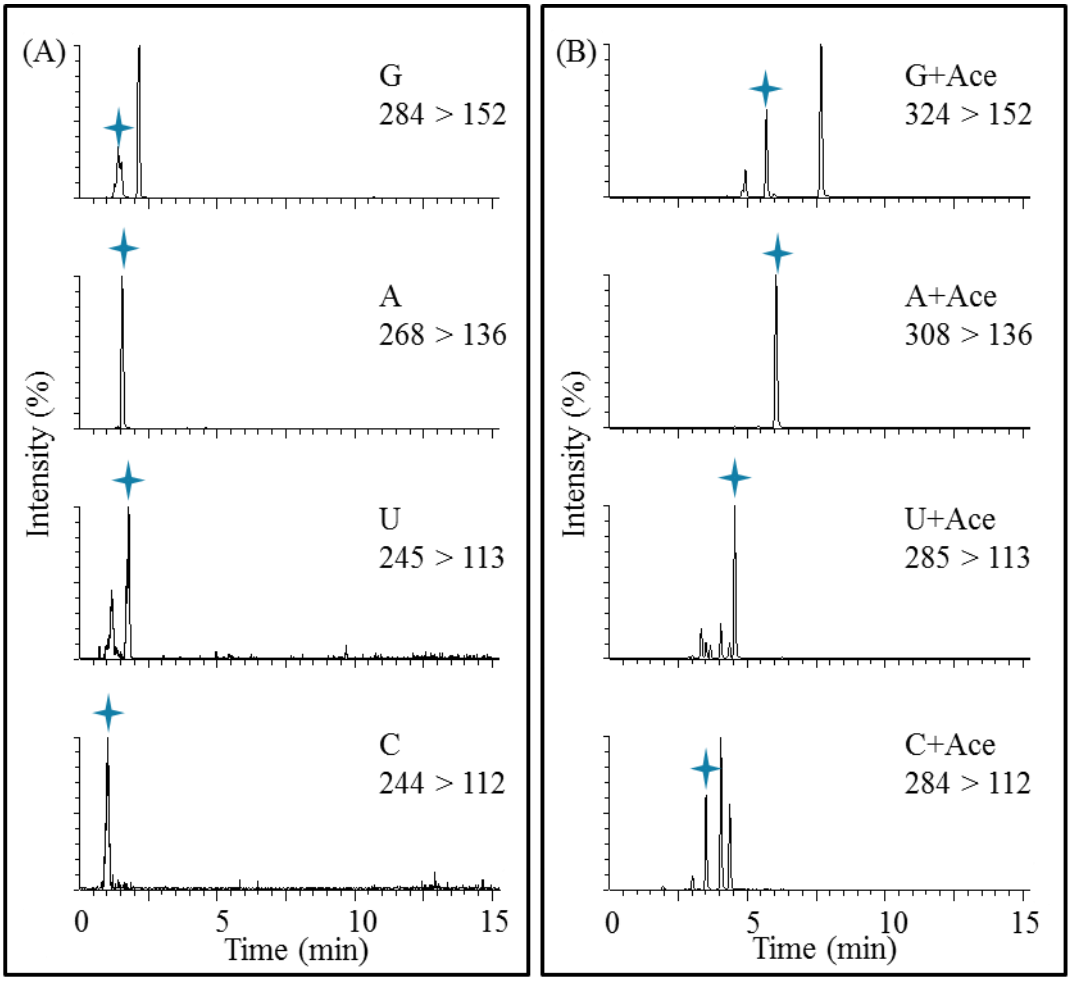

Figure 2.9 Extracted ion chromatograms of nucleosides (A) and their acetonides (B) in urine samples.

2.3.9 Validation of the derivatization method

Further, the method was validated through quantitative analysis of four normal nucleosides. In the linearity study, the calibration curves of four acetonides were linear in the range of 1.00-1000 ng mL^{-1}. All the correlation coefficients for the analyte were greater than 0.9997 (Table 2.2), which indicated good linearity. The LOD of this method ranged from 0.026 to 0.16 ng mL^{-1} and LOQ from 0.089 to

0.55 ng mL^{-1}. The results demonstrated that the method was sensitive enough for nucleoside detection in urine samples. The accuracy and precision results of intra-day and inter-day analyses were listed in Table 2.3. The accuracy was in the range of -4.7% to 2.1%. The precision was less than 2.2% for intra-day and 2.9% for inter-day analysis. The recoveries of the four acetonides were ranged from 92.9% to 103.5%. The results indicated that the assay was reproducible and the products of urine reacted with acetone were very stable during the analysis. It demonstrated that the method was robust and could be employed to determine other nucleosides in urine samples.

Table 2.3 Linearity, LOQ, LOD and recovery of the derivatization method.

Compound	Correlation coefficient (r^2)	LOQ (ng mL^{-1})	LOD (ng mL^{-1})	Recovery		
				c_1[a] (ng mL^{-1})	Mean (%)	RSD (%)
A + Ace	0.9998	0.12	0.034	120.0	96.6	6.3
				150.0	94.6	3.7
				180.0	97.5	6.5
G + Ace	0.9998	0.089	0.026	24.00	97.3	4.7
				30.00	92.9	3.5
				36.00	95.4	3.4

U + Ace	0.9997	0.55	0.16	40.00	97.5	4.7
				50.00	97.3	6.2
				60.00	94.7	4.5
C + Ace	0.9997	0.13	0.037	48.00	101.5	3.1
				60.00	97.2	1.9
				72.00	103.5	2.8

[a] c_3: Final concentration of adding standards for recovery evaluation.

Table 2.4 Stability of the derivatization method.

Compound	Intra-day			Inter-day		
	c_1[a] (ng mL^{-1})	RE[b] (%)	RSD[c] (%)	c_2[a] (ng mL^{-1})	RE (%)	RSD (%)
A + Ace	5.000	-1.1	2.1	5.000	1.7	2.9
	50.00	1.2	1.1	50.00	-2.9	1.2
	500.0	-1.6	1.2	500.0	-3.2	2.7
G + Ace	5.000	-1.9	2.2	5.000	-2.5	2.0
	50.00	0.20	1.6	50.00	2.1	1.5
	500.0	-2.5	2.1	500.0	-3.0	2.1
U + Ace	5.000	0.17	1.8	5.000	1.0	1.2

	50.00	-1.1	2.0	50.00	-0.8	1.7
	500.0	-3.9	1.1	500.0	-0.8	1.8
C + Ace	5.000	-2.7	2.1	5.000	-3.2	1.6
	50.00	-1.0	2.0	50.00	-2.7	1.4
	500.0	-3.8	1.3	500.0	-4.7	1.3

[a] c_1 and c_2: Concentration of QC samples for accuracy and precision evaluation.

[b] RE: relative error. RE (%) = (O - T)/T x 100. O, observed value; T, true value.

[c] RSD: relative standard deviation.

2.4 Chapter summary

In this chapter, the factors that affected the derivatization reaction, including catalyst, reaction temperature, reaction time and ratios of reactants, were investigated. The optimal reaction conditions were that the mole ratio of G and acetone should be 1:585, with 1.00% of $HClO_4$ (70%) as catalyst and reacting for 30 min at -20 ºC. Under the conditions, the peak area percentages of products could exceed 95%. At the same time, the applicability of the derivative method was investigated by detecting products of mixture of A, G, U and C reacted with acetone. In addition, a quantification method was developed and validated to detect four acetonides of urinary nucleosides by using LC-MS/MS. The separation was improved dramatically with the derivatization method, comparing to directly analysis. The validation experiments showed that the averages of the correlation

coefficients for the four acetonides were greater than 0.9960, which indicated good linearity. The LOD of this method ranged from 0.01 to 0.15 ng mL^{-1} and LOQ from 0.02 to 0.63 ng mL^{-1}. The accuracy (RE%) was excellent with a range of -4.82% to 9.41%. The precision (RSD) was less than 4.68% for intra-day and inter-day analysis. The recoveries were ranged from 80.78% to 128.58%. The results indicated that the assay was reproducible and the products of urine reacted with acetone were stable during the analysis. The method could be used for the detection of all kinds of nucleosides. It was potentially useful for the analysis of modified nucleosides and other *cis*-diol-containing metabolites in biological samples.

Chapter 3 A novel method of liquid chromatography-mass spectrometry combined with chemical derivatization to study urinary ribonucleosides in hepatocellular carcinoma mice

3.1 Introduction

Hepatocellular carcinoma (HCC) is a primary malignancy of the liver. It is now the third leading causes of cancer-related death worldwide[179]. Over 500,000 people are affected by the disease. Each year, approximately 564,000 new cases are diagnosed, including 398,000 men and 166,000 women[180]. The commonly used and effective treatment method of the disease is to remove the tumors by surgical removal at the early stage. Unfortunately, limited to lack of specific clinical manifestations and detection means, early stage HCC is usually not easy to be noticeable. Therefore, a large number of HCC patients are not eligible for surgical intervention timely, leading to poor prognosis[181]. So, biomarkers are strongly essential for the diagnosis of HCC at early stages. Alpha fetal protein (AFP) is now the most specific biomarker for diagnosis of HCC. But the method still has false positive and false negative possibility. The AFP of serum was less than 20 μg L^{-1} in 30% HCC patients, which might not be considered as HCC positive[182]. Therefore, it is essential to find new biomarkers for HCC diagnosis to make up the existing approaches the insufficiency.

Ribonucleic acid (RNA) molecules play an important regulatory role in cell biology. RNA copies the genetic information from deoxyribonucleic acid (DNA), and then

translates them into proteins. After completing its assigned tasks, RNA is catabolized to nucleoside level. The main composition of these end products are unmodified ribonucleosides, namely adenosine (A), guanosine (G), urine (U) and cytidine (C), which are recycled to synthesize new RNA again. However, the modified ribonucleosides that cannot be catalyzed by the phosphorylases are excreted from the cell into the urine.

The levels of urinary ribonucleosides were fairly constant in normal healthy individuals with little difference[183]. The excretion of ribonucleosides was not affected by age and diet[51]. But elevated levels of ribonucleosides were observed in patients with physical illness, such as urogenital cancer[72, 73], hepatocellular carcinoma[74, 75], breast cancer[184], acquired immunodeficiency diseases (AIDS)[80, 81] and severe combined immunodeficiency diseases (SCID)[82]. Therefore, the levels of urinary ribonucleosides could be considered as a signal of disease status, especially as potential biomarkers for cancer diagnosis. Ribonucleosides have also been used for HCC diagnosis. Pseudouridine (Pseu) was considered as an important clinical detection index in HCC screening[185]. Some papers have reported high level of Pseu in HCC patients comparing to health controls[186, 187]. Except for Pseu, some other modified nucleosides have also been reported that they were affected by HCC[74]. Though the mechanism of nucleosides alteration in cancer patient urine remains unclear, the significant change of these compounds has aroused public attention for HCC diagnosis.

Many methods have been developed for the analysis of urinary ribonucleosides. The early used methods included high performance liquid chromatography (HPLC) coupled with UV detector[84] and enzyme-linked immunosorbent assay (ELISA)[95]. The currently favored methods were chromatography or capillary electrophoresis coupled with mass spectrometry (MS)[104, 188, 189]. Although MS was more specific and sensitive than UV detector, the extraction and enrichment methods were still necessary for the analysis of ribonucleosides due to the complex components of biological samples and low abundance of ribonucleosides. For example, on-line extraction was performed by connecting a pre-column and an analytical column via a six-way switching valve[64]. For off-line extraction, solid phase extraction (SPE) was the most common pretreatment approach for ribonucleosides[102, 190]. The SPE methods could pre-concentrate ribonucleosides but their specificity was poor. Affinity adsorbent approaches based on boronate materials could selectively capture compounds with *cis*-diol groups for the pretreatment of ribonucleosides. SPE packed column[112, 191] and magnetic nanoparticles[192] binding boronate groups have been used for the selective enrichment of modified ribonucleosides. These methods have good specificity for extraction of group of ribonucleosides. However, the subsequent separation and determination of intact ribonucleosides, especially the isomers, on reversed-phase LC were often challenging due to their extremely high polarity. Therefore, it is necessary to develop new methods for the determination of these metabolites.

Compounds containing *cis*-diol groups can react with acetone to form acetonides (isopropylidene ketal). The volatility of acetonides is much higher than the substrates. Therefore, this reaction has been used as a derivatization method for the analysis of carbohydrates by using GC[158, 193]. As described in the last chapter, nucleosides containing *cis*-diol groups could also react with acetone to form isopropylidene-ribonucleosides, which has been applied to protect group of *cis*-diol in organic synthesis[159]. However, the application of this specific reaction for the determination of ribonucleosides has not yet been reported. In addition, in the analysis of metabolites, it was a challenge to determine the structure of unknown compounds, especially isomers. Using isotope to selectively label target metabolites could effectively improve the accuracy of structure identification.

In this work, a derivatization method based on the reaction of ribonucleosides with acetone was established for urinary ribonucleosides analysis by liquid chromatography-mass spectrometry (LC-MS). The specificity of detection was achieved from the use of acetone-d_6 to label the target compounds. Multivariate statistical analysis method was applied for aided identification of ribonucleosides. And the method would be used to evaluate the urinary ribonucleosides in nude mice bearing HCC xenografts.

3.2 Material and methods

3.2.1 Chemicals

Ribonucleosides were purchased from Sigma-Aldrich (St. Louis, MO, USA),

including guanosine (≥ 98%, G), adenosine (≥ 99%, A), cytidine (≥ 99%, C) and uridine (≥ 99%, U). 8-Chloroguanosine (8ClG, internal standard, IS) was purchased from Carbosynth (Berkshire, UK). Hexadeuteroacetone (99.9 atom % D, acetone-d_6), formic acid (HPLC grade) and 70% perchloric acid ($HClO_4$) were also purchased from Sigma-Aldrich. HPLC grade methanol and acetone were obtained from Merck (Dermstadt, Germany). Acetone was used directly without further drying process. Water was purified by using a Milli-Q system (Millipore, Milford, MA).

3.2.2 Cell culture

HepG2, a human hepatocellular carcinoma cell line, were obtained from Type Culture Collection of Chinese Academy of Sciences, Shanghai. They were cultured in Dulbecco's Modified Eagle Medium (DMEM) containing 10% fetal bovine serum (FBS), 100 μg mL^{-1} streptomycin sulfate, and 100 unit/mL penicillin. The humidified incubator maintained with 5% CO_2 and 37 °C. Cells in logarithmic growth (85% confluence) were enzymolysis with 0.25% trypsin and washed with phosphate buffer saline (PBS) twice. Then the cells were centrifuged at 100 × *g* for 5 min. The pellet was resuspended in PBS (2.5×10^7 mL^{-1}) and injected into nude mice.

3.2.3 Animal models

Eighteen athymic BALB/c nude mice (6–8 weeks, 20–25 g, males) were used as model animals. They were purchased from the Center of Laboratory Animal of

Guangzhou University of Chinese Medicine, China. Mice were housed in a standard animal facility under SPF conditions with room temperature at 22 ± 2 °C and relative humidity 50 ± 5%. The mice were provided with food and water ad libitum for one week to adapt to the raising environment after arrival. Then they were randomly and equally divided into three groups. The first group was control group. The second group of mice were injected with HepG2 cells (HCC group). The third group was also injected with HepG2 cells, but after four weeks, they were treated with 5-Fluorouracil (5-FU) (HCCFU group). HCC and HCCFU groups were generated by subcutaneous injection of about 5×10^6 HepG2 cells in 0.2 mL solution. After four weeks, the xenografts reached about 1 cm in diameter. The HCCFU group was treated with 0.05 mL 5-FU (50 mg mL^{-1}) for five days. A 24-hour urine specimen for each mouse was collected for all the groups. The urine samples were centrifuged to remove suspended particles at 5, 000 × *g* for 10 min at 4 ℃. The supernatants were stored at -80 ℃ until they were used for analysis. The samples collected on the last two days were used for analysis. Animal protocols were approved by the Animal Care and Use Committee of Graduate School at Shenzhen, Tsinghua University. The animal experiment was performed by Prof. JIANG Yuyang who was at the Graduate School at Shenzhen, Tsinghua University.

3.2.4 Sample preparation

Quality control (QC) samples were prepared by mixing 200 μL aliquots of each individual rat urine sample to create a pooled sample. The pooled sample was

divided into multiple QC samples with 100 μL aliquots volume for each. The multiple QC samples were used to recognize modified nucleosides in urine. They were divided into two groups, which were reacted with equal amounts of acetone and acetone-d_6, respectively. The processed procedure of QC samples and each individual rat sample was the same as described in Chapter 2.

As a control, 600 μL methanol/water (3:1, v/v) was added to the residue of vacuum freeze-dried QC urine samples (100 μL). After vigorous vortex for 30 s, the mixture was set aside for 30 min at -20 °C. And then it was centrifuged at 12,000 × *g* for 10 min at 4 °C to remove the precipitation. The supernatant was dried with a stream of nitrogen. The residue was reconstituted with 100 μL methanol/water (5:95, v/v). The solution was centrifuged at 12,000 × *g* for 5 min at 4 ºC and the supernatant was used for LC-MS/MS analysis.

3.2.5 Ultra-performance liquid chromatography

UPLC coupled with a Waters Acquity^{TM} BEH phenyl column (100 mm × 2.1 mm, 1.7 μm) was employed for chromatographic separation. The mobile phases were water containing 0.05% formic acid (A) and methanol (B). Linearity gradient elution increased from 5% B to 20% within 2 min, then to 35% within 8 min, following increasing to 95% within 4 min and held for 1 min, then returned to 5%. Total running time was 20 min. The flow rate was 0.30 mL min^{-1}. The column temperature was set at 35 °C for all analyses. Injection volume was 10 μL.

3.2.6 Mass spectrometry

A Waters TQ detector (Waters, Manchester, UK) equipped with an electrospray ion source was employed for qualitative and quantitative analysis. Analyte was ionized in positive ion mode. Capillary voltage was 3.00 kV. Ion source temperature was 130 °C and desolvation gas temperature was 450 °C. Desolvation gas flow was 1000 L h^{-1}. Cone gas flow was 150 L h^{-1}. Neutral loss scanning was performed to screening the ribonucleosides in urine samples. Neutral loss was set as 132 u for samples to be analyzed directly, 172 u for samples reacted with acetone and 178 u for samples reacted with acetone-d_6. Cone voltage were 35 V and collision energy was set at 10.0 eV. Data were acquired in centroid mode with mass range from *m/z* 200 to 600. Both cycle time and scan duration were set as 1.00 s.

3.2.7 Data processing

MarkerLynx software (version 4.1, Waters Corporation, MA, USA) and SIMCA-P 13.0 software (Umetrics AB, UMEÅ, Sweden) were used for data processing. Raw data acquired in UPLC-MS was decomposed into retention time (RT), mass to charge ratio (*m/z*) and associated height intensities to form a three-dimensional matrix containing 14 observations (sample names) with 498 variables (peak intensities). After normalization, the data was exported into SIMCA-P for multivariate data analysis. Scale type for x-variables was Pareto and transformation was set as automatic. Principal component analysis (PCA), an unsupervised multivariate statistical approach, was used for variable reduction. Orthogonal

partial least square discriminant analysis (OPLS-DA) was performed to maximize class discrimination and to find out potential biomarkers. S-plot visualized the relationship of covariance and correlation that were generated by the OPLS-DA. S-plot was used to pick up variables that had significant contributions to discrimination between groups for further structural identification. Origin 9.0 version (OriginLab, Co., MA) was used to perform other statistical analysis.

3.2.8 Confirmation of ribonucleoside structure

To confirm structures of ribonucleosides, MS/MS spectrum was acquired under the same LC-MS conditions while the collision energy was set at 10.0, 20.0 and 40.0 V. Authentic standards were derivative with acetone. MS/MS spectrums of the products were acquired to use as references. Accurate molecular weights were obtained by coupling Waters Q-TOF premier mass spectrometry to the same UPLC. Full scans of the urine samples were performed with positive ion mode. Capillary voltage was set at 3.1 kV and cone voltage at 35 V. Cone gas flow was set at 50 L h^{-1} while desolvation gas flow was set to 500 L h^{-1}. The source temperature was 120 °C and the desolvation gas temperature was 300 °C. Data were collected in centroid mode between *m/z* 200 and 600, with a scan time of 0.15 s and interscan time 0.02 s. A leucine-enkephalin solution at 100 pg uL^{-1} in acetonitrile-water with 0.1% formic acid (50:50, v/v) was used as the lock-mass (*m/z* 556.2771) with a flow rate of 0.05 mL min^{-1}. The obtained accurate *m/z* values were deducted 40.0313, then searching against databases for candidate compounds. The structural formulas

of the candidate compounds were retrieved by comparing MS/MS spectrums of samples and authentic standards for the characteristic ions.

3.2.9 Application of the method to determine modified nucleosides in HCC

The changes of the identified modified nucleosides in HCC mice urine were studied by using the method. The urine samples of control, HCC and HCCFU groups were derivative with acetone as described above. Then the samples were analyzed by LC-MS. Neutral loss of 172 u was selected to detect the modified nucleosides. The raw data was processed with MarkerLynx. The difference of the three groups samples was visualized by using unsupervised principal component analysis (PCA) method. Volcano plot analysis was performed to highlight compounds that had significant contributions to the discrimination in PCA score plot. Compared to control group, compounds in HCC or HCCFU group that showed significant difference ($p < 0.01$) and intensity ratio was larger than 2.0 or smaller than 0.50 were preferentially considered as the significantly changed modified nucleosides. Heat maps were employed to present the level difference of these significant compounds (generated by using Multi Experiment Viewer 4.9).

3.3 Results and discussion

3.3.1 Derivatization with acetone

Cis-diol is characteristic functional groups of ribonucleosides. The presence of the polar group results in poor retention of ribonucleosides on a reversed phase column, which makes trouble to the separation and identification of these biological

molecules. *Cis*-diol group could react with anhydrous acetone to form acetonides by using acid as catalyst (Figure 3.1a). The polarity of the derivatization products increased, which might improve the retention of these compounds.

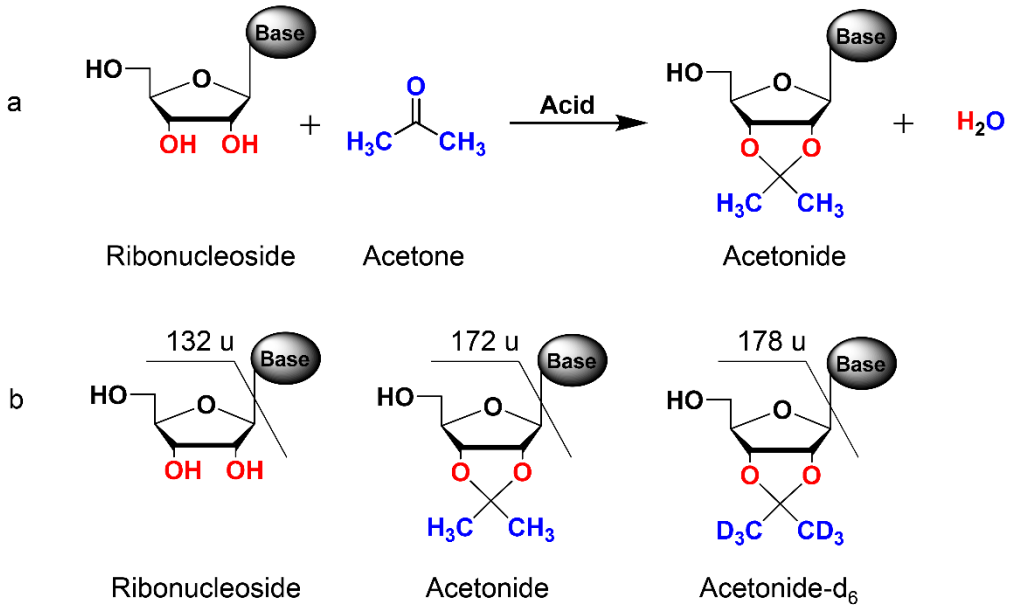

Figure 3.1 Reaction of ribonucleosides with acetone to form acetonides (a) and neutral loss of ribonucleosides, acetonides and acetonides-d_6 (b).

Besides, glycosidic bond of ribonucleosides could be easily broken in the second-order mass spectrum to form a neutral loss of 132 u (Figure 3.1b)[194]. The loss increased to 172 u for acetonide and 178 u for acetonide-d_6 which was generated by deriving ribonucleosides with acetone-d_6. Therefore, by using neutral loss scanning mode, ribonucleosides could be selectively detected by scanning the loss of 132 u for the sample without derivatization. And nucleosides that were labeled

with acetone (or acetone-d_6) could be determined by scanning the loss of 172 u (or 178 u) with mass spectrometry.

3.3.2 Liquid chromatography separation

The derivatization method was applied to label modified ribonucleosides in urine samples. The samples were reacted with acetone (or acetone-d_6) and detected by using LC-MS/MS. According to the reaction mechanism, *cis*-diol group in ribonucleosides is converted to isopropylidene group, which is more hydrophobic. It can be expected that the retention time of these derivatives will become better on a reversed phase column. Chromatograms in Figure 3.2a and 3.2b showed the differences of human urinary samples with and without derivatization. The sample without derivatization was scanned in neutral loss mode with a loss of 132 u (Figure 3.2a). The retention time of almost all the compounds eluted on reversed-phase column was less than 5 min, resulting in serious peak overlapping, even ion suppression. However, after reacted with acetone, all the peaks were evenly distributed across the whole chromatogram under the same chromatographic condition (Figure 3.2b). This result indicated that improvement of the chromatographic separation of polar nucleosides could be achieved by using derivatization method based on acetone.

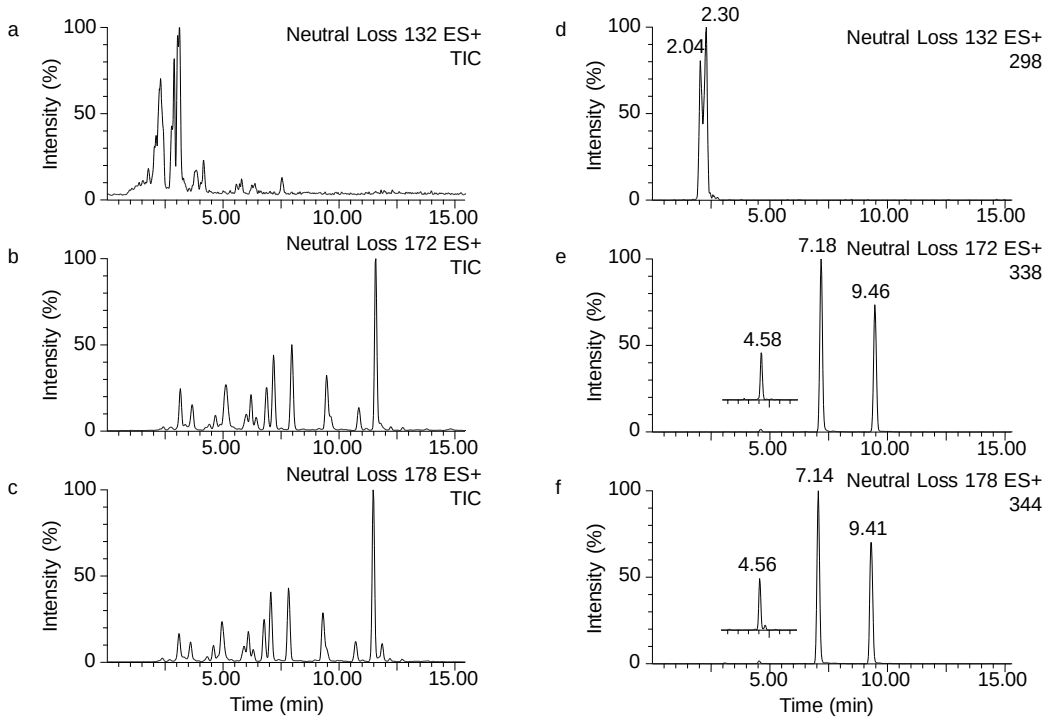

Figure 3.2 Total ion chromatogram (TIC) and extracted ion chromatograms (EIC) of human urine samples. TIC of samples by direct analysis (a), derivatization with acetone (b), and derivatization with acetone-d_6 (c). EIC of samples by direct analysis (d), derivatization with acetone (e) and derivatization with acetone-d_6 (f).

All the ribonucleosides have similar structures, a five-carbon sugar (ribose), and some of them are isomers. Therefore, it is a great challenge to determine these compounds by using traditional methods. For example, methylation of guanosine in the guanine ring forms three modified nucleosides, i.e. 1-methylguanosine (m^1G), N^2-methylguanosine (m^2G) and 7-methylguanosine (m^7G). The ion ($[M+H]^+$) at 298 *m/z* is corresponding to the three compounds. By extracting ion chromatogram of *m/z* 298 in Figure 3.2a, a broad peak with a small fork on the top was generated

(Figure 3.2d). It means that at least two compounds with the same M.W. were eluted through the column at almost the same time. It is hard to use the data to differentiate the isomers. In contrast, after derivatization with acetone, the M.W. of these isomers increased to 337 Da and the *m/z* became 338 Da. The extracted ion chromatogram of *m/z* 338 Da from Figure 3.2b showed that three baseline separated peaks were detected (Figure 3.2e). Similar results were obtained for the derivatization products of acetone-d_6 (Figure 3.2f). These results demonstrated that the method can not only separate co-elution peaks but also isolate small peaks from high concentration compounds. The improvement of chromatographic separation provided the foundation for the both qualitative and quantitative analysis of modified nucleosides.

3.3.3 Mass spectrometry analysis

An additional advantage of this approach was that it could effectively increase detecting signal intensity. By comparing the mass spectra of urinary samples that were analyzed directly (Figure 3.3a) and derivative with acetone (Figure 3.3b), it is found that the *m/z* of most peaks were added with 40 u after derivatization. Furthermore, intensity enhancement of most peaks was observed. For example, the intensity of *m/z* 312 was 2.25×10^4 when the sample was analyzed directly. While the sample was derivative with acetone, the intensity rose to 2.21×10^5, which was 9.8 times higher than the control. Figure 3.3d showed the distribution of fold change for all the peaks. Except for 4 peaks, the fold changes of peaks were all larger than

1.0. The largest was up to 31 times. The sensitivity enhancement was attributed to the reducing of matrix effect and elution in a higher-organic solvent. The derivative products could be dissolved in acetone and isolated with insoluble solid such as proteins, inorganic salts and other insoluble composition in urine samples. Thus, the samples were primarily purified and most of matrix was removed. Another factor was attributed to minimize matrix interferences and ion suppression by better chromatographic separation after derivatization. Furthermore, it is worth noting that improvement in signal was not related to urinary nucleotides degradation. Because nucleotides would not lose its phosphate group to convert to nucleosides under this conditions. An example of adenosine monophosphate (AMP) reacting with acetone was shown in Figure 3.4. The results showed that the derivatization method could help to enhance the intensity of mass spectra. It is conducive to detect low level ribonucleosides in urine.

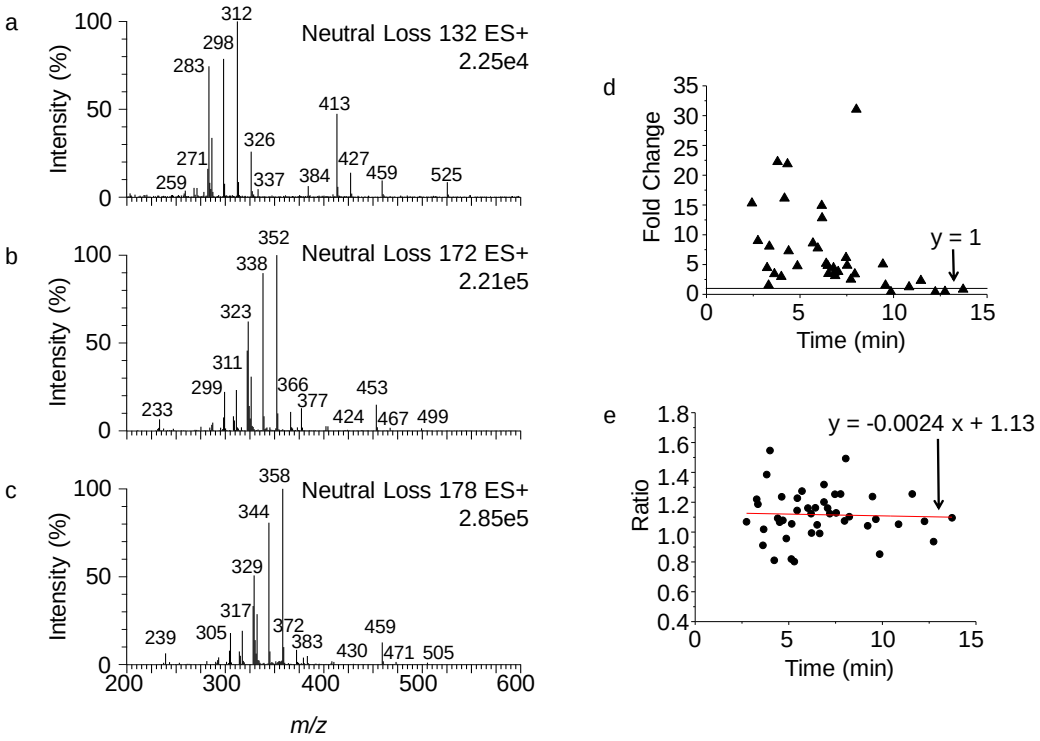

Figure 3.3 Mass spectra of human urine samples. (a) Direct analysis, (b) derivatization with acetone, (c) derivatization with acetone-d_6, (d) comparison of peak intensity between a and b, (e) comparison of peak intensity between b and c.

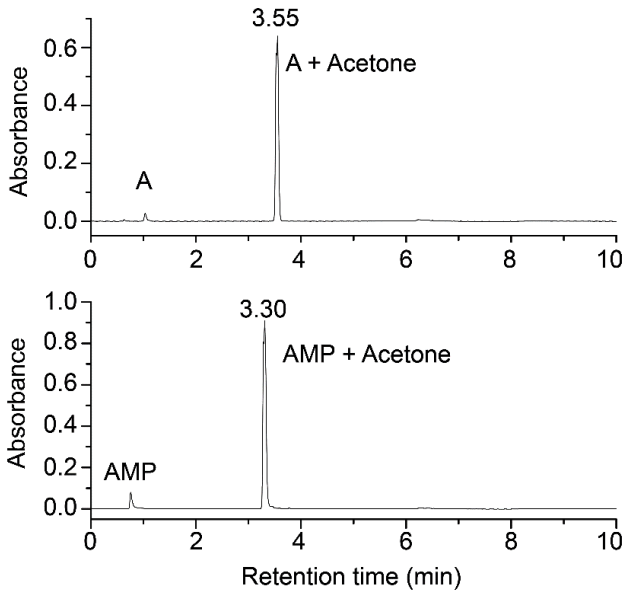

Figure 3.4 Chromatograms of derivative products of A and AMP.

3.3.4 Application of acetone-d_6 to assist ribonucleosides identification

Although the neutral loss scanning method could select ribonucleosides from a multitude of metabolites in urine after derivatization, it's very important to note that some metabolites without derivatization might also have a neutral loss of 172 u. Namely the metabolites could also display signals on the chromatogram to form false positive results. In order to eliminate these undesirable peaks, acetone-d_6 was applied to assist to identify ribonucleosides.

Ribonucleosides of urine samples were reacted with equal volume proportion of acetone and acetone-d_6 to form ordinary and deuterated acetonides. The products were analyzed by using LC-MS/MS with neutral loss scanning of 172 u (ordinary acetonides) or 178 u (deuterated acetonides) at the same time. Figure 3.2b and 3.2c showed the chromatogram of ordinary and deuterated products. The two chromatograms had similar peak distribution. This was because the ordinary and deuterated products had the same retention time. In addition, M.W. difference of acetone and acetone-d_6 was 6 u. After derivatization, the difference of the products for the same compound was also 6 u (Figure 3.3b and 3.3c). Because the reactants contained equal volumes of acetone and acetone-d_6, the intensity proportion of the two kinds of products was also close to 1:1. In fact, by comparing the peak intensity, the ratio of ordinary and deuterated products was between 0.8-1.6 and close to 1.1 on the whole (Figure 3.2e). Based on these features, by comparing the two

chromatograms (Figure 3.2b and 3.2c) and the two mass spectra (Figure 3.3b and 3.3c), those ions that matched the three features could be considered as nucleosides. As mentioned above, there may be some false positives signals by using neutral loss scanning mode to select ribonucleosides in urine samples. The three features distilled above could also be used to take unwanted signals out of results. There were two examples to show the distinction of false positive signals. A peak of *m/z* 232 was detected with neutral loss of 172 u (Figure 3.5a), but the corresponding peak, *m/z* 238 could not be seen in Figure 3.5b with neutral loss of 178 u. On the contrary, a signal of *m/z* 356 could be observed with 178 u neutral loss (Figure 3.6b), but the corresponding signal (*m/z* 350) could not be detected (Figure 3.6a). Both of the two examples were false positive signals. Other false positive results were ruled out in the same way.

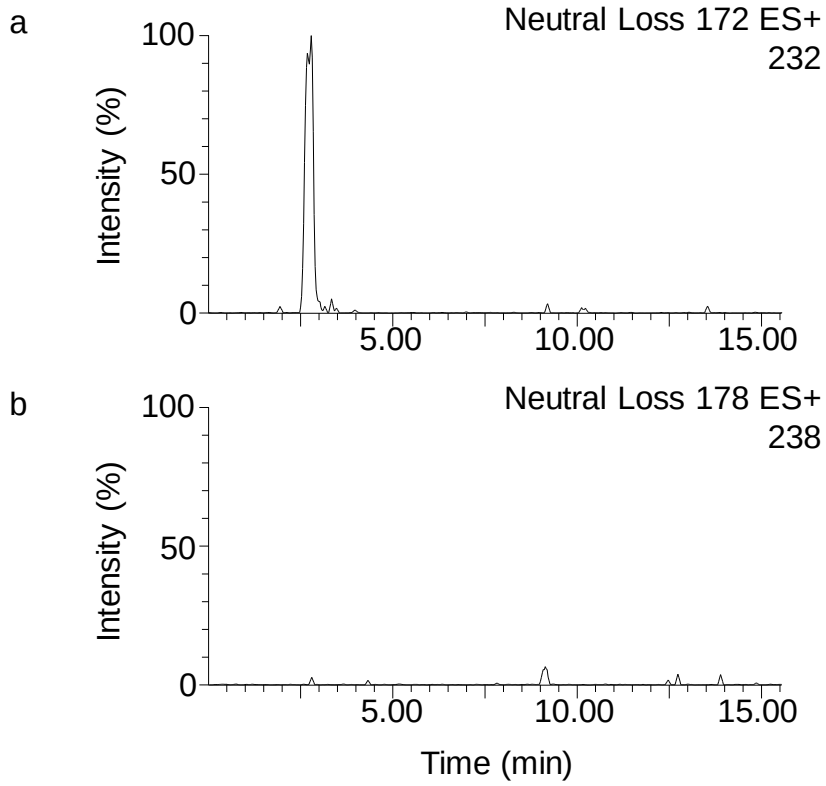

Figure 3.5 A sample of false positives signal showed in extracted ion chromatogram of *m/z* 232 from samples reacted with acetone (a), and *m/z* 238 from samples reacted with acetone-d_6 (b).

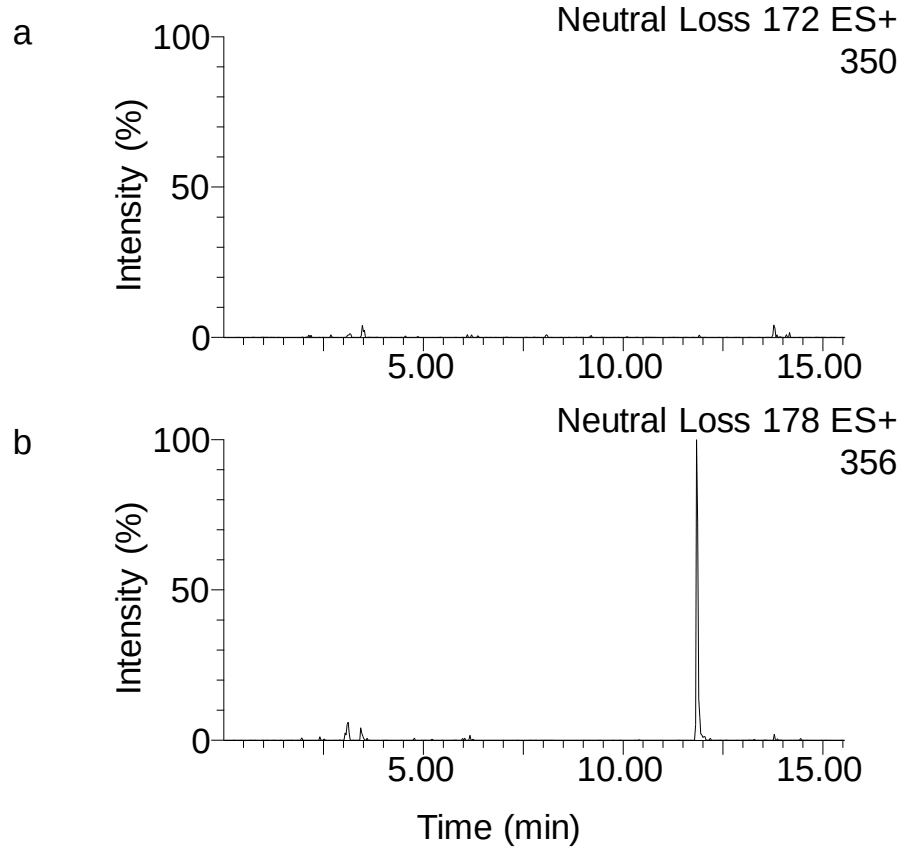

Figure 3.6 A sample of false positives signal showed in extracted ion chromatogram of *m/z* 350 from samples reacted with acetone (a), and *m/z* 356 from samples reacted with acetone-d_6 (b).

3.3.5 Data processing with multivariate statistical analysis method

Multivariate statistical analysis method, which was widely used in the metabolomic studies[66], was applied to carry out data processing. The raw data was pretreated with MarkerLynx software and then was visualized with Simca-P software. The classification results obtained from OPLS-DA score plot (Figure 3.7a) showed significantly separation between samples reacted with acetone and acetone-d_6. It

meant that the two groups contained some significantly different features.

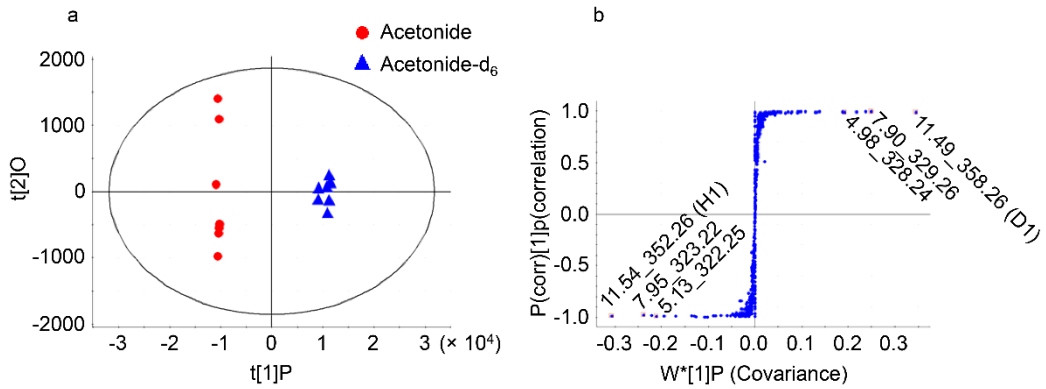

Figure 3.7 OPLS-DA score plot (a) and S-plot (b) of urine samples derivative with acetone and acetone-d_6. ●: Samples reacted with acetone; ▲: samples reacted with acetone-d_6. The label "11.54_352.26" meant R.T 11.54 min and *m/z* 352.26.

S-plot (Figure 3.7b) dictated a direct impression of features contributed to the classification. In Figure 3.7b, the farther away the point was from the origin, the greater contribution it made to the classification. In addition, S-plot could make pairs from the two groups according to the three features described above. For example, for the points H1 and D1, both their retention time was about 11.50 min; the *m/z* were 352.26 Da and 358.26 Da; the ratio of average signal strength was 0.89. The appearances of the ion pair matched to the features mentioned above. Therefore, it could draw a conclusion that the pair represented the same compound which were reacted with acetone and acetone-d_6, respectively. Other pairs such as 5.13_322.25 (R.T. 5.13 min and *m/z* 322.25, the same below) and 4.98_328.24, 7.95_323.22 and 7.90_329.26, and so on, could also be easily dug out in the S-plot.

These pairs were symmetrical about the center of the coordinates. On the basis of this characteristic, more pairs (i.e. ribonucleosides) could be visually found out in Figure 3.7b.

3.3.6 Identification of ribonucleosides in urine samples

It was not enough to confirm the structure of compounds only with the rough *m/z* values. Other information, including MS/MS spectra and accurate *m/z* values were needed. The ion H1 was used as an example to introduce the process of structure identification (Figure 3.8). The first step was to acquire accurate *m/z* value by using UPLC/Q-TOF MS. The accurate value of the ion was 352.1611. The accurate mass of the corresponding compound (without derivatization) was obtained by subtracting 40.0313. The minus result, i.e. 312.1298 was used to search against databases (HMDB, METLIN and MODOMICS). Three possible compounds, which were isomers, were retrieved, including N^2,N^2-dimethylguanosine, N^2,7-dimethylguanosine and 7-aminomethyl-7-deazaguanosine. MS/MS spectrum of *m/z* 352.1611 from urine samples was compared with that from authentic standards. The spectra that had similar MS fragments were considered as the same compound. Finally, the ion at 352.26 *m/z* and at RT 11.54 min was confirmed as N^2,N^2-dimethylguanosine. Similarly, other ribonucleosides were identified. Because not all the ribonucleosides could buy their authentic standards. For those compounds that authentic standards were unavailable, they were putatively identified based on mass match and MS/MS interpretation. The results were listed in Table 3.1.

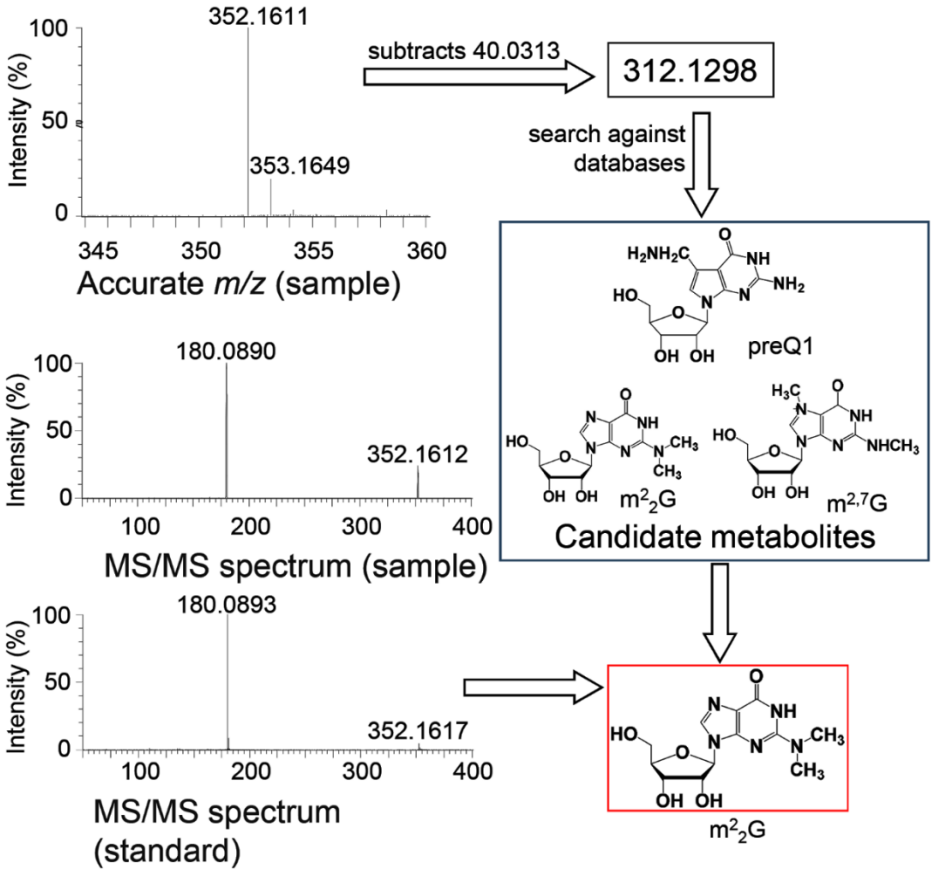

Figure 3.8 Process of structure identification and confirmation of ribonucleosides. $m^2{}_2G$: N^2,N^2-dimethylguanosine; preQ1: 7-aminomethyl-7-deazaguanosine; $m^{2,7}G$: N^2,7-dimethylguanosine.

Table 3.1 Ribonucleosides identified from urine samples.

No.	R.T.	*m/z* [a]	Accurate mass [b]	Error[c]	Formula	Name
1	3.80	284.1243	243.0852	-1.3	$C_9H_{13}O_5N_3$	Cytidine*
2	4.86	285.1077	244.0686	-3.8	$C_9H_{12}O_6N_2$	Uridine*

3	4.33	287.1255	246.0864	4.9	$C_9H_{14}O_6N_2$	Dihydrouridine
4	4.89	287.1245	246.0854	0.9	$C_9H_{14}O_6N_2$	2-Hydroxyluridine
5	2.75	295.1304	254.0913	3.9	$C_{11}H_{14}O_5N_2$	Nicotinamide riboside*
6	7.04	297.1448	256.1057	-0.9	$C_{11}H_{16}O_5N_2$	1-(beta-D-Ribofuranosyl)-1,4-Dihydronicotinamide
7	4.17	298.1409	257.1018	2.5	$C_{10}H_{15}O_5N_3$	3-Methylcytidine*
8	4.64	298.1403	257.1012	0.1	$C_{10}H_{15}O_5N_3$	5-Methylcytidine*
9	8.01	299.1248	258.0857	2.0	$C_{10}H_{14}O_6N_2$	3-Methyluridine*
10	5.12	299.1241	258.0850	-0.7	$C_{10}H_{14}O_6N_2$	5-Methyluridine*
11	3.66	299.1276	258.0885	12.8	$C_{10}H_{14}O_6N_2$	Imidazoleacetic acid riboside
12	6.40	308.1356	267.0965	-0.9	$C_{10}H_{13}O_4N_5$	Adenosine*
13	6.16	309.1189	268.0798	-3.6	$C_{10}H_{12}O_5N_4$	Inosine*
14	5.48	309.1182	268.0791	-6.2	$C_{10}O_5N_4H_{12}$	Isoinosine
15	6.18	311.1353	270.0962	-0.7	$C_{10}H_{14}O_5N_4$	6-Hydroxyl-1,6-dihydropurine ribonucleoside
16	7.46	312.1172	271.0781	-8.6	$C_{10}H_{13}O_6N_3$	5-Formylcytidine
17	9.20	312.1568	271.1177	3.2	$C_{11}H_{17}O_5N_3$	N^4,N^4-dimethylcytidine
18	5.69	322.1514	281.1123	-0.4	$C_{11}H_{15}O_4N_5$	N^6-methyladenosine*
19	5.08	322.1526	281.1135	3.9	$C_{11}H_{15}O_4N_5$	1-Methyladenosine*
20	8.51	322.151	281.1119	-1.8	$C_{11}H_{15}O_4N_5$	2-Methyladenosine*
21	7.39	322.152	281.1129	1.8	$C_{11}H_{15}O_4N_5$	8-Methyladenosine*

22	7.93	323.1354	282.0963	-0.4	$C_{11}H_{14}O_5N_4$	1-Methylinosine*
23	5.95	324.1306	283.0915	-0.6	$C_{10}H_{13}O_5N_5$	Guanosine*
24	5.29	324.1312	283.0921	1.4	$C_{10}H_{13}O_5N_5$	Isoguanosine
25	7.52	325.1173	284.0782	8.9	$C_{10}H_{12}O_6N_4$	Xanthosine*
26	6.84	326.1353	285.0962	0.4	$C_{11}H_{15}O_6N_3$	N^4-acetylcytidine
27	2.43	328.1269	287.0878	4.2	$C_9H_{13}O_6N_5$	Clitocine
28	4.22	328.1512	287.1121	1.3	$C_{11}H_{17}O_6N_3$	5-Methylaminomethyluridine
29	3.36	329.0997	288.0606	4.2	$C_{10}H_{12}O_8N_2$	Orotidine
30	6.52	336.1674	295.1283	0.9	$C_{12}H_{17}O_4N_5$	2,8-Dimethyladenosine
31	5.31	336.1652	295.1261	-6.6	$C_{12}H_{17}O_4N_5$	N^6,N^6-dimethyladenosine*
32	9.43	338.1464	297.1073	0.0	$C_{11}H_{15}O_5N_5$	7-Methylguanosine*
33	8.03	338.1458	297.1067	-2.0	$C_{11}H_{15}O_5N_5$	N^6-hydroxymethyladenosine
34	7.14	338.1465	297.1074	0.3	$C_{11}H_{15}O_5N_5$	N^2-methylguanosine*
35	4.58	338.1463	297.1072	-0.4	$C_{11}H_{15}O_5N_5$	1-Methylguanosine*
36	6.48	340.126	299.0869	1.0	$C_{10}H_{13}O_6N_5$	8-Hydroxyguanosine*
37	6.79	341.1097	300.0706	0.0	$C_{10}H_{12}O_7N_4$	Beta-D-3-Ribofuranosyluric acid
38	3.24	343.1157	302.0766	5.2	$C_{11}H_{14}O_8N_2$	5-Carboxymethyluridine
39	6.88	348.0467	307.0076	-0.2	$C_{11}H_5O_8N_3$	5-Carbamoylhydroxy methyluridine
40	13.80	348.1309	307.0918	0.4	$C_{12}H_{13}O_5N_5$	7-Cyano-7-deazaguanosine

41	3.32	350.146	309.1069	-1.4	$C_{12}H_{15}O_5N_5$	N^6-acetyladenosine
42	3.63	352.1613	311.1222	-2.5	$C_{12}H_{17}O_5N_5$	$N^{2,7}$-dimethylguanosine*
43	11.55	352.1623	311.1232	0.7	$C_{12}H_{17}O_5N_5$	N^2,N^2-dimethylguanosine*
44	12.62	352.1612	311.1221	-2.8	$C_{12}H_{17}O_5N_5$	7-Aminomethyl-7-deazaguanosine*
45	7.72	357.1304	316.0913	2.0	$C_{12}H_{16}O_8N_2$	5-Methoxycarbonyl methyluridine
46	9.57	366.178	325.1389	0.9	$C_{13}H_{19}O_5N_5$	N^2,N^2,7-trimethylguanosine
47	4.39	368.1368	327.0977	-7.4	$C_{12}H_{17}O_4N_5S$	2-Methylthio-N6-methyladenosine
48	11.46	373.1099	332.0708	9.0	$C_{12}H_{16}O_7N_2S$	5-Methoxycarbonylmethyl-2-thiouridine
49	5.71	373.1244	332.0853	-0.8	$C_{12}H_{16}O_9N_2$	5-(Carboxyhydroxymethyl) uridine methyl ester
50	3.12	373.1238	332.0847	-2.6	$C_{12}H_{16}O_9N_2$	Uridine 5-oxyacetic acid methyl ester
51	4.00	386.1561	345.1170	-0.6	$C_{13}H_{19}O_8N_3$	3-(3-Amino-3-carboxypropyl) uridine
52	9.86	424.1465	383.1074	-0.8	$C_{14}H_{17}N_5O_8$	Succinoadenosine
53	13.72	438.1817	397.1426	1.5	$C_{16}H_{23}O_5N_5S$	2-methylthio-N^6-(cis-Hydroxyisopentenyl)

						adenosine
54	10.83	453.1736	412.1345	0.6	$C_{15}H_{20}O_8N_6$	N^6-threonylcarbamoyl adenosine
55	12.23	467.1886	426.1495	-1.0	$C_{16}H_{22}O_8N_6$	N^6-methyl-N^6-threonylcarbamoyladenosine
56	12.75	499.1611	458.1220	0.0	$C_{16}H_{22}O_8N_6S$	2-Methylthio-N^6-threonylcarbamoyladenosine

[a] observed value.

[b] Accurate mass = observed value - 40.0313 - 1.0078.

[c] Mass error of accurate mass comparing with true value. Unit: ppm.

* Confirmation with authentic standards.

3.3.7 Evaluation of modified nucleosides in mice bearing HCC

The method was employed to analyze mice urine samples bearing HCC by detecting all the 56 nucleosides in the Table 3.1. The chromatograms of control, HCC and HCCFU samples showed obvious difference (Figure 3.9). It meant that some nucleosides were significantly changed among the three groups. The raw data was processed with MarkerLynx to obtain the information of ions, including RT, *m/z* and peak intensities. These information was imported into SIMCA-P to perform multivariate data analysis. Unsupervised principal component analysis (PCA) method was employed to evaluate the difference of the three groups of samples (Figure 3.10). The summary of the fit of the PCA model was manifest with R2X

and Q2. The R2X of PC1 was 74% and PC2 7.7%, with a cumulative value up to 81.7%. Correspondingly, the cumulative Q2 was 73% and for PC1 and PC2. The PCA score plot showed that the HCC group was appreciably separated from control group. It indicated that the effects of HCC xenograft had strong effects on urinary nucleoside metabolism. It also implied that some ions showed signification difference between the two groups. Two samples of HCC were outside the circle of PCA confidence intervals. It might be due to individual differences. The two mice might have subnormal responses to HCC, resulting in greater changes of nucleosides levels than other HCC mice.

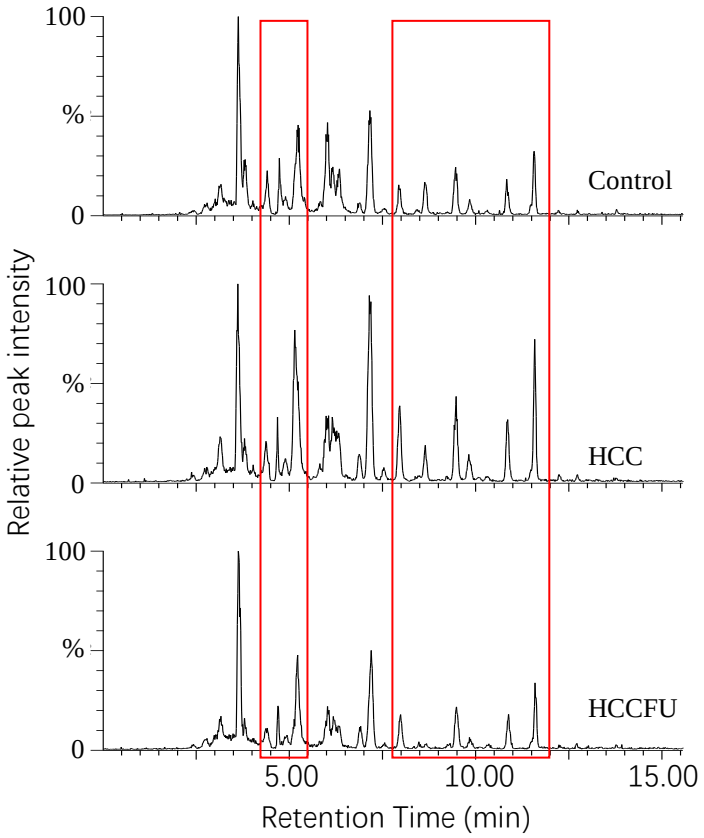

Figure 3.9 Chromatograms of nude mice urine samples. (a) control group, (b) HCC group and (c) HCCFU group.

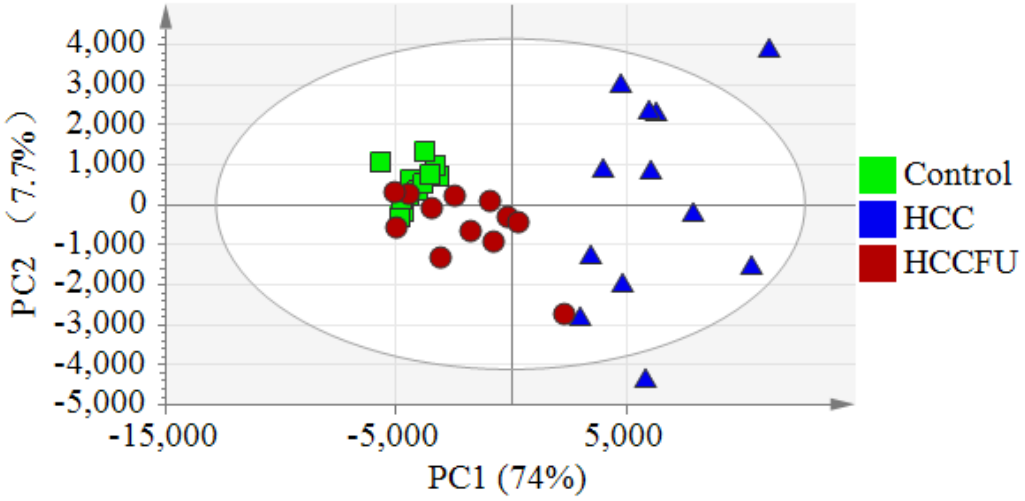

Figure 3.10 PCA score plot of nude mice urine samples.

The PCA score plot also implied that levels of some nucleosides changed significantly in HCC and HCCFU groups, because they were clearly separated from each other. But the HCCFU and control groups were a small overlapping. It indicated that the difference of nucleosides levels between the two groups might be small. In another word, treatment of 5-FU might have some positive effects on these mice.

Volcano plots were applied for quick visual identification of the most-meaningful changes (Figure 3.11 and 3.12). Points that displayed large magnitude fold changes (larger than 2.0) as well as high statistical significance ($p < 0.01$) were selected as candidates. Compared to control group, 26 candidates were found in HCC group (Figure 3.11a), while 3 was found in HCCFU (Figure 3.11c). All of these candidates in both groups were higher than in the control group. Particularly, the fold changes

in HCC group were generally greater than that in HCCFU group. Compared HCCFU group with HCC group, 21 candidates were found. And the levels of these candidates decreased in HCCFU group (Figure 3.11b). These results indicated that HCC strongly affected the levels of urinary modified nucleosides, leading to significant rise of this kind of metabolites. However, after treated with 5-FU, the cancer cells were killed by the anti-cancer drug. The modified nucleosides generated by the cells decreased, manifesting as lower levels in HCCFU group than in HCC group. Specific to each differential nucleoside, the largest differential occurred in HCC group, for compound isoinosine, which was 6.70 times higher than in control group.

To compare the HCCFU group with control group, three nucleosides showed statistical significance (Figure 3.11c and Figure 3.12c). It meant that although the 5-FU could kill most of cancer cells, resulting in decreasing of nucleosides levels (comparing to HCC group), some of them were still alive, which was presented as the nucleosides could not completely reach normal baseline levels. So the difference between HCCFU and control groups indicated the mice were not fully recovered from HCC.

Therefore, the changes of these nucleosides implied that modified nucleosides were valuable compounds to show the state of HCC. Quick growth of cancer cells led to fast catabolism of RNA and level increasing of nucleosides. When the cancer cells were killed by the drug, the level of nucleosides which were generated by the cells,

decreased. And the level gaps between normal and treatment mice represented the treatment effects of drugs. So the differential nucleosides could serve as potential biomarkers for HCC diagnosis

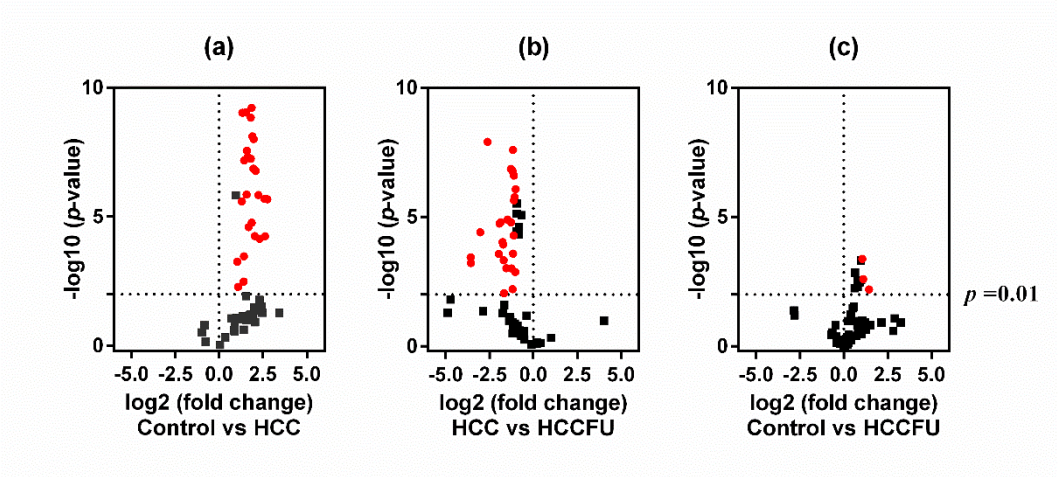

Figure 3.11 Volcano plot analysis of differential modified nucleosides between HCC or HCCFU with control group. The fold change in modified nucleosides levels between HCC or HCCFU group and control samples was plotted on the x axis (log2 scale), and the *p*-value of t-test was plotted on the y axis (–log10 scale). Compounds displayed statistical significance (fold change > 2.0 and $p < 0.01$) were indicated in red.

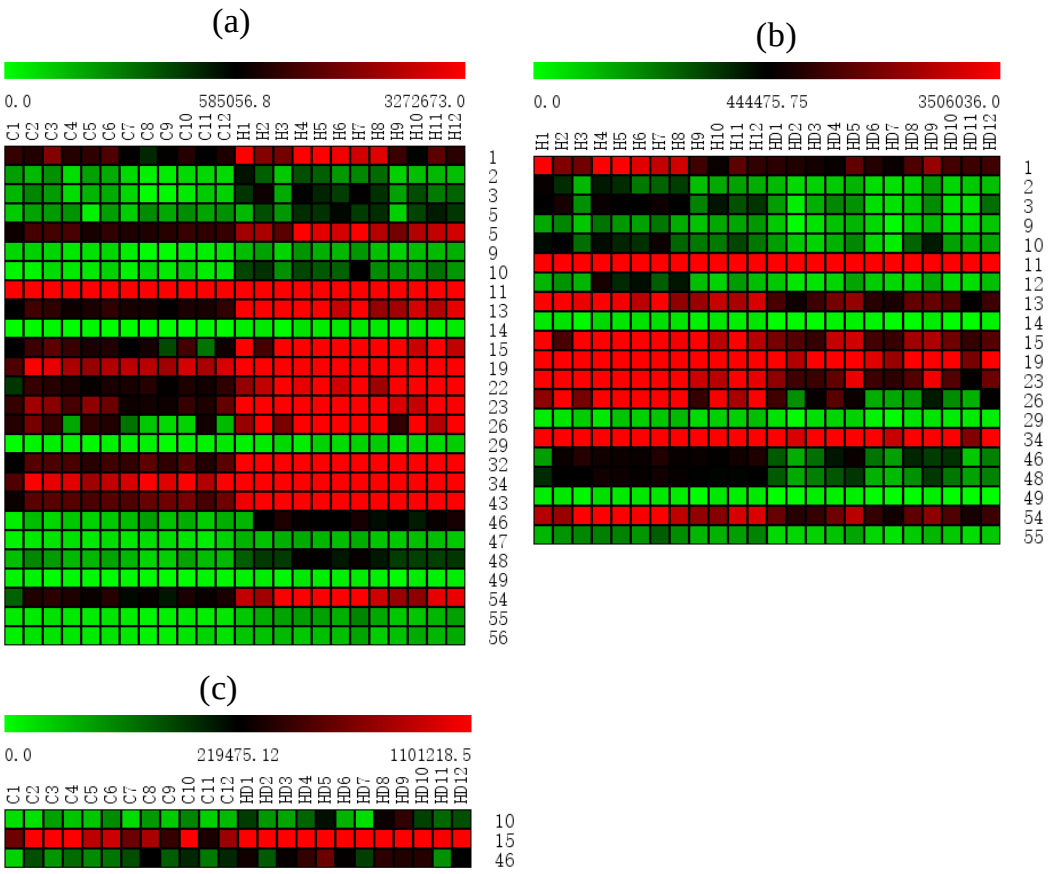

Figure 3.12 Comparison of differential modified nucleosides in urine samples of HCC mice. Heat map showed the differential modified nucleosides between control and HCC groups (a), between HCC and HCCFU groups (b) and between control and HCCFU groups (c).

3.3.8 Discussion

In this work, 56 nucleosides were detected in a single analysis by using acetone as derivatization agent. Among them, 52 compounds were identified as modified nucleosides. The error of M.W. was less than 15 ppm. The chemical type of modification of these compounds included methyl, carboxymethyl, acyl, and so on. Methylation was the most modification mode. The result indicated that the

derivatization method was an effective tool to identify modified nucleosides in urine samples.

Compared to other methods[192, 195, 196], the use of the derivatization method could help to detect more nucleosides. Comparison with sample pretreatment methods by using SPE or nanoparticles, although they could achieve highly selective extraction and enrichment of ribonucleosides, these methods required a large amount of samples in order to meet the testing requirements. This limited the application of these methods to samples that had low levels of nucleosides and very small samples, such like blood samples. In addition, the extracted nucleosides, which still contained free hydroxyl groups, were very polar, resulting in difficult separation for some isomers. However, by using the derivatization method described in this article, better chromatographic separation and higher mass spectrometric sensitivity were achieved. The improvements not only helped for qualitative detection and quantitative analysis, but also greatly reduced sample consumption. It was favorable for expanding the application of the method to other biological samples. Of course, this method also had some drawbacks. Since the data was acquired by using neutral loss scanning model, only metabolites that contained ribose groups could be detected. Other *cis*-diol compounds were ignored under these conditions. Addressing this issue, other types of technology, for example, full scanning with high-resolution mass spectrometry, could be employed to screen all *cis*-diol compounds.

3.4 Chapter summary

A derivatization method based on the reaction of ribonucleosides with acetone was established and applied for the determination of urinary ribonucleosides by liquid chromatography-tandem mass spectrometry, for the first time to our best knowledge. This method not only improved the retention of modified nucleosides on reversed-phase column, but also reduced the matrix effect of urine samples and enhanced detection sensitivity of mass spectrometry. Isotope labeling method with acetone-d_6 and multivariate statistical analysis enabled the positive identification of 56 ribonucleosides, including 52 modified nucleosides. The obtained results indicated that the derivatization method was practical, fast and effective for the identification of urinary nucleosides. The method was successfully applied to study the urinary nucleosides in nude mice of HCC. Several nucleosides were identified as significant change biomarkers. The developed method might be extended to determine modified nucleosides in other biological samples, such as cells, tissues, blood, etc. to support research of cancer-related biomarkers discovery.

Chapter 4 Determination of modified nucleosides via liquid chromatography-mass spectrometry with parallel reaction monitoring for study of RNA damage induced by bisphenol A exposure

4.1 Introduction

BPA is used to produce certain plastics which are applied to make a variety of common consumer goods[197,198]. Frequently contacting with these goods greatly increases the chance of BPA exposure. It has been reported that BPA had some effects on different diseases[199,200,201,202,203,204]. Studies of genomic, proteomic and metabolomics showed BPA exposure had influence on DNA, RNA, proteins, and even metabolites[151, 205, 206]. For example, it has been reported that BPA exposure could induce oxidative stress and cause DNA damage[207]. Due to the similar structure of RNA and DNA, BPA also has the potential to damage RNA. So far though, no one had published related results about the effects of BPA on RNA lesions.

RNA plays integral roles in information transfer from DNA to proteins. Similar to DNA methylation, posttranscriptional processing of RNA is also pervasive, conserved, and critical for many aspects of biology[208]. The modification on RNA produces an exceptional number and structural diversity of modified nucleosides. After the RNA is degraded, the modified nucleosides could not be reused by the organism. They are flushed out the body through urine. So the levels of urinary modified nucleosides are related to the degradation rate of RNA. In general, the

contents of these metabolites are stable, not affected by age and diet[51]. However, there are numerous factors that contribute to causing alteration of modified nucleosides. Either endomyocardial diseases or exogenous chemical exposure could cause an exception of RNA metabolism, resulting in changes of urinary modified nucleosides[209].

RNA damage induced by oxidative stress is one form of RNA modification, which is also related to fluctuations of urinary modified nucleosides. The level of oxidative stress in the cell is reflected by the quantity of reactive oxygen species (ROS). RNA can be oxidized by ROS via free radical which is referred to Fenton reaction[210]. The oxidation randomly damages RNA by attacking some susceptible residues in the nucleic strands. The hotspot sites have been identified as guanosine. The particular residues are oxidized to 8-hydroxyguanosine (8-oxoG) by ROS[211]. Therefore, 8-oxoG is considered as a biomarker of RNA lesions, which is used to elevate RNA damage. Following oxidative damage, 8-oxoG is cleared from the damaged RNA via turnover or degradation of these RNA[212]. In the meanwhile, other modified nucleosides of the RNA are released as well, leading to promotion of most of these compounds[213]. Therefore, by determining the contents of urinary modified nucleosides, the degradation of RNA in vivo could be monitored, especially the damage induced by ROS.

A number of methods have been reported to detect nucleosides in biological samples[109, 214-217]. These methods offered several alternatives for making a choice

of modified nucleosides determination. However, the sensitivity and selectivity of these methods could be improved with improved techniques, such as high resolution mass spectrometry (HRMS). HRMS, for example, Orbitrap-based machine, provides high analytical specificity for monitoring targeted species because of their high resolution ion detection capabilities[218, 219]. These instruments support to perform parallel reaction monitoring (PRM) scans in which all fragment ions from a precursor ion are monitored simultaneously[220]. The obtained high resolution MS/MS data could be employed for qualitative and quantitative analysis at high specificity and sensitivity[221]. Such a PRM assay may be practical to simultaneously monitor all the fragment ions that released from modified nucleosides.

Therefore, in this study, a LC-MS method was developed to determine the alteration of modified nucleosides in rats exposed to BPA, with the hope to study the effects of BPA exposure on RNA damage indirectly. The sample preparation was based on the derivatization method that was developed and validated in chapter 2. An ultra-high performance liquid chromatography (UHPLC) combined with a quadrupole-Orbitrap hybrid mass spectrometer (Q-Exactive MS) was employed for sample analysis.

4.2 Material and methods

4.2.1 Chemicals

Methanol (HPLC grade) was obtained from Merck (Dermstadt, Germany). Acetone

was also obtained from Merck and it was used directly without further drying process. Bisphenol A (BPA) was purchased from J&K Scientific Ltd. (Beijing, China). The internal standard, 8-chloroguanosine, (8ClG, IS) was purchased from Carbosynth (Berkshire, UK). Other chemicals, including nucleoside standards, acetone-d_6 (99.9 atom % D), formic acid (HPLC grade) and 70% perchloric acid ($HClO_4$) were purchased from Sigma-Aldrich (St. Louis, MO, USA). Water was purified by using a Milli-Q system (Millipore, Milford, MA).

4.2.2 Animal Protocols

Female Sprague-Dawley rats (180-220 g) were obtained from Guangdong Medical Laboratory Animal Center (No. 44007200014698, Guangdong, China). Animal protocols were approved by the Animal Care and Use Committee of Shenzhen Institute for Drug Control. Twenty rats were randomly divided into four groups with 5 rats for each: model control group and high, middle and lower dose BPA-exposed groups (simply as control, BPAH, BPAM and BPAL groups). All rats were housed under Specific Pathogen Free (SPF) conditions. The room temperature was set at 22 ± 2 °C with relative humidity at 50 ± 5% as well as a 12 h light/dark cycle. The rats were kept in separate metabolic cages and provided with commercial rat food and water ad libitum. After one-week adaptive feeding period, control, BPAL, BPAM and BPAH groups were administered with 0, 10, 30 and 50 mg BPA/kg body weight per day (in corn oil) by gastric gavaging, respectively. The administration of BPA was consecutive for four days. The animal experiment was performed by

Shenzhen Institute for Drug Control.

4.2.3 Sample collection and preparation

A 24-hour urine specimen for each rat was collected after four days of BPA exposure. The collected samples were centrifuged at 5, 000 × *g* for 10 min at 4 °C to remove suspended particles. The supernatants were stored in a -80 °C freezer until they were used for LC-MS analysis.

The urine samples were processed as previously described in chapter 2 with minor modifications. Briefly, in the four groups (control, BPAL, BPAM and BPAH), 100 μL aliquots of each urine sample was used for sample preparation. IS was added to each sample with final concentration of 50.00 ng mL^{-1}. The samples were dried completely by using an Ilshin Lab freeze dryer (Ilshin Co., Ltd., USA) for 5 h. The dried residue was reacted with 600 μL of HPLC grade acetone at the presence of 6 μL $HClO_4$ as catalyst. The mixture was well blended by vigorous vortex. The reaction lasted half an hour at -20 °C. Then 12 μL saturated potassium carbonate solution was added to neutralize the acid to form white precipitate, which contained inorganic salts, proteins and other substances insoluble in acetone. The precipitate was removed by centrifuging at 12,000 × *g* for 10 min at 4 °C. The supernatant was dried with a stream of nitrogen. The residue was reconstituted with 100 μL methanol/H_2O (5:95, V/V). Before injected into LC-MS, the reconstituted solution was centrifuged at 12,000 × *g* for 5 min at 4 °C to remove any possible particles.

Quality control (QC) samples were prepared by mixing 200 μL aliquots of each rat

urine sample to create a pooled sample. The pooled sample was divided into multiple QC samples with 100 μL aliquots volume for each. They were divided into two groups, i.e., QCH and QCD (for each group, n = 10), which were reacted with equal amounts of acetone and acetone-d_6, respectively. The processed procedure was the same as described above. The QCH and QCD samples were used to recognize modified nucleosides in urine.

4.2.4 Liquid chromatography parameters

Sample analysis was performed by using an Ultimate 3000 UHPLC controlled by Chromeleon 7.2 Software (Thermo Fisher Scientific, Waltham, MA, Germany). A Acquity UPLC BEH phenyl column (100 mm × 2.1 mm, 1.7 μm, Waters, USA) column was used for chromatographic separation. The composition of mobile phase was water (added 0.1% formic acid, A) and methanol (B). The linear gradient elution program used was as follows: 0 min, 5% B; 2 min, 20% B, 10 min, 35% B; 14 min, 95% B, 15 min, 95% B, 15.5 min, 5% B, and 20 min, 5% B. The flow rate was set at 0.30 mL min^{-1}. The column temperature was 35 °C. For each sample, the injection volume was 10 μL.

4.2.5 High resolution mass spectrometry parameters

Detection of targeted compounds was performed with a quadrupole-Orbitrap hybrid mass spectrometer (Q-Exactive, Thermo Fisher Scientific, Waltham, MA). A heated electrospray ionization source (HESI-II) was used in positive ionization mode. The parameters were set as follows: sheath gas flow rate 40, aux gas flow rate 10, spray

voltage 3.00 kV, S-lens RF level 55, capillary temperature 350 °C and aux gas heater temperature 320 °C. Parallel reaction monitoring (PRM) scans were at the resolution of 17,500 with AGC target set as 5×10^4 and maximum injection time set as 100 ms.

Inclusion lists were used to trigger PRM scans. The information of the targeted compounds in the lists were obtained from the databases of Metlin (https://metlin.scripps.edu/index.php), HMDB (http://www.hmdb.ca/), Modomics (http://modomics.genesilico.pl/) and the RNA modification database (http://mods.rna.albany.edu/home). In the databases, all the modified nucleosides that contained *cis*-diol groups were selected for subsequent screening. The accurate masses of the compounds were calculated by using Qualbrowser in Xcalibur 3.0. To analyze samples that reacted with acetone (control, BPAL, BPAM, BPAH and QCH groups), the *m/z* values used in the inclusion list were calculated by adding 40.0313 to the exact masses. While to analyze samples that reacted with acetone-d_6 (QCD group), the exact masses were added with 46.0689. It meant that there was a pair of *m/z* values for each nucleoside which belonged to QCH and QCD groups, respectively. These pairs were employed to recognize the modified nucleosides in QC samples.

The recognition was performed by using Qual browser in Xcalibur 3.0. Peaks that detected in QCH with a neutral loss of 172.0736 (mass tolerance 5 ppm) and in QCD groups with a neutral loss of 178.1112 (mass tolerance 5 ppm) were extracted.

The retention time, *m/z* values and intensities of the two groups' peaks were compared. If the retention time of two peaks between the two groups was consistent and the ratio of peak intensities was between 0.8-1.2, the two peaks would be considered as pairing peaks that represented a nucleoside which was reacted with acetone and acetone-d_6, respectively. These candidate compounds were confirmed by comparing their MS/MS spectra in QCH and QCD groups and validating with authentic standards if available. 66 compounds were found present in the QC samples (S/N > 10). The precursor ions of these validated compounds (reacted with acetone) were used to generate a new inclusion list to detect modified nucleosides in BPA exposure urine samples (control, BPAL, BPAM and BPAH groups).

4.2.6 Data processing and statistical analysis

Xcalibur 3.0 was used for raw data processing. ICIS peak detection algorithm was selected to specify peak integration and detection criteria. The mass values used for peak integration were the daughter ions which were generated from precursor ions with a neutral loss of 172.0736. The mass precision was set at 4 decimals and the mass tolerance was set as 5.0 ppm. The minimum peak height (S/N) was set as 10.0. The processing method was employed to integrate the peaks detected in control, BPAL, BPAM and BPAH groups.

The obtained peak area was normalized to the area of IS. The results, combining with associated retention time and *m/z* values, were used to build a three-dimensional matrix. The matrix was imported into SIMCA-P 13.0 (Umetrics AB,

UMEÅ, Sweden) to perform multivariate data analysis. The difference of the four groups samples was visualized by using unsupervised principal component analysis (PCA). Volcano plot analysis was performed to highlight compounds that had significant contributions to the discrimination in PCA score plot. Compared to control group, compounds in BPAL (or BPAM or BPAH group) that showed significant difference ($p < 0.05$) and intensity ratio was larger than 1.5 or smaller than 0.67 were preferentially considered as the significantly changed modified nucleosides. Heat maps were employed to present the level difference of these significant compounds (generated by using Multi Experiment Viewer 4.9).

4.3 Results and discussion

4.3.1 Primarily screening of modified nucleosides by PRM

A nucleoside consists simply of a nucleobase and a ribose. The base is bound to the ribose via a beta-glycosidic linkage. The glycosidic bond is not very stable, which makes it more prone to breakage in the second-order mass spectrum (MS/MS). After reacted with acetone, the derivatization products of nucleosides inherit the feature. As shown in Figure 4.1a, acetone-labeling adenosine lost the labeled ribose group to form a main fragment ion, which was the ionized nucleobase, adenine. The molecular weight of the neutral loss group was 172.0736. When the derivatization reagent was acetone-d_6, the value increased to 178.1112 (Figure 4.1b). Similar results were obtained for the derivatization products of guanosine, cytidine and uridine (Figure 4.2). Because of similar structure, other nucleosides derived from

the four common nucleosides also have similar fragment pattern. That is, nucleosides reacted with acetone (or acetone-d_6) could form a neutral loss of 172.0736 (or 178.1112) in MS/MS spectra. This feature could be applied to selectively screen nucleosides from complex biological samples.

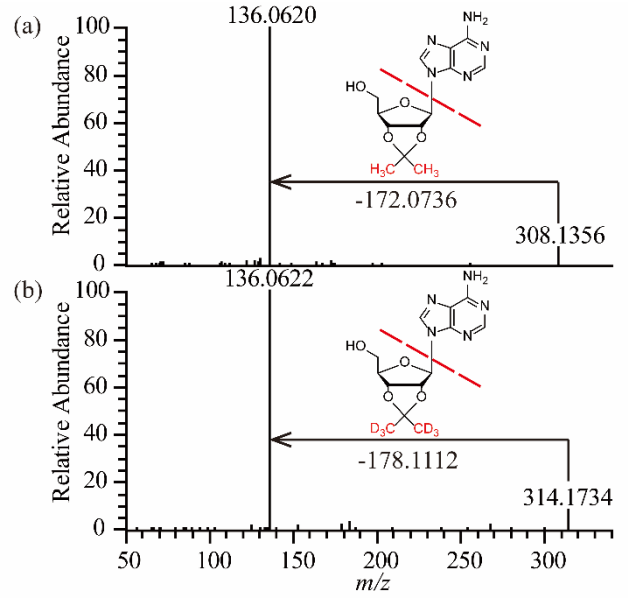

Figure 4.1 MS/MS spectra of derivatization products of adenosine reacted with acetone (a) and acetone-d_6 (b).

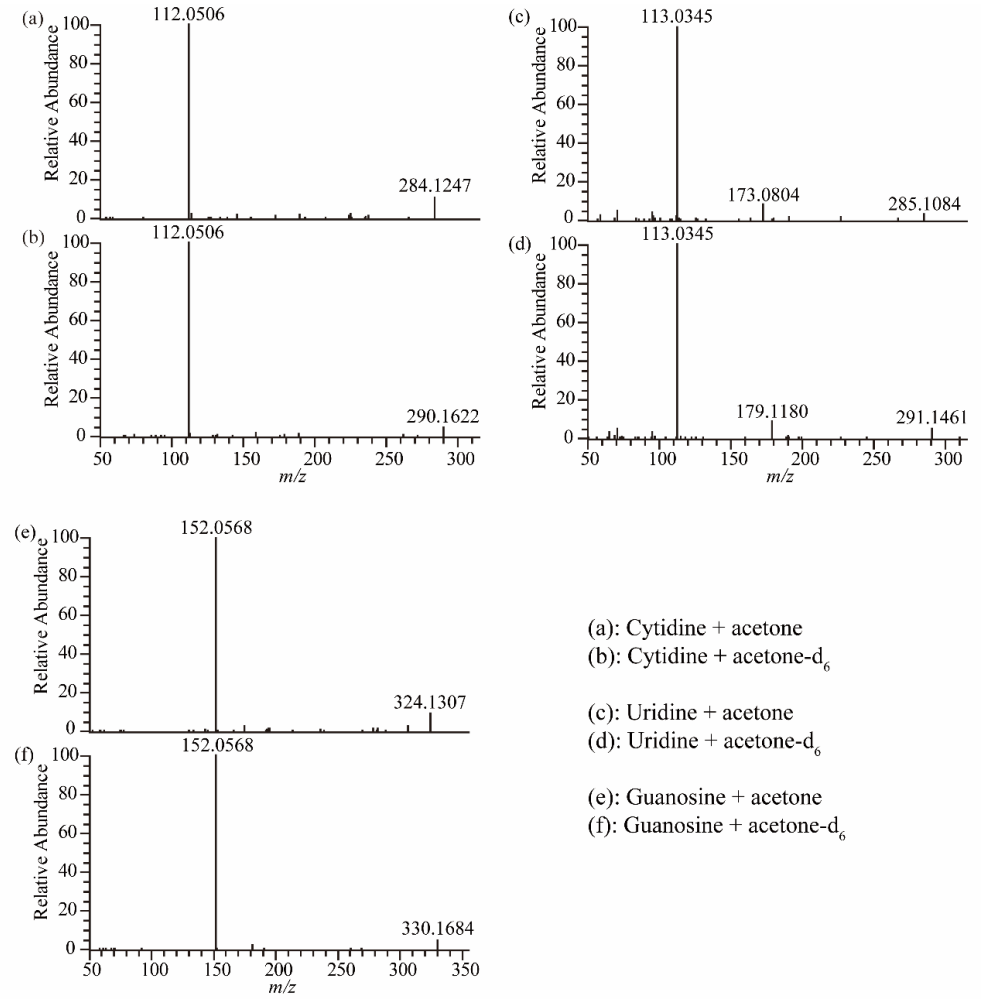

Figure 4.2 MS/MS spectra of derivatization products of three nucleosides reacted with acetone and acetone-d_6.

A Q-Exactive mass spectrometer was employed to perform nucleosides screening by using PRM model. The instrument used a quadrupole to filtrate ions that came from the ionization source based on the inclusion list. The passed ions were broken

in the higher-energy collisional dissociation (HCD) cell. All the fragment ions were detected by the orbitrap mass analyzer to generate high resolution MS/MS spectra. The isolation window of the quadrupole was set at 0.6 *m/z*. It means that, for a given ion value M in the inclusion list, *m/z* of ions that fell within the range of M-0.3 ~ M+03 could be selected by the quadrupole. Other ions which offset the specified values were not detected by the mass spectrometer. For example, for a given value of 499.1608 *m/z* in the inclusion list, ions between 498.1608 and 499.4608 generated peaks in the chromatograms. As the total ion chromatogram (TIC) shown in Figure 4.3a, at least 9 peaks were detected by scanning 499.1608 with the Q-Exactive mass spectrometer. Some of them might not be nucleosides signals which should be excluded. As mentioned above, nucleosides reacted with acetone could form a neutral loss of 172.0736. Accordingly, peaks that had a neutral loss of 172.0736 were extracted by using the software Xcalibur. Five peaks were observed to satisfy the criteria (Figure 4.3b). In other words, more than four peaks were filtered out, which were not nucleosides. Based on this method, other candidate nucleosides peaks could also be extracted. Of course, additional evidence should be provided to confirm the results.

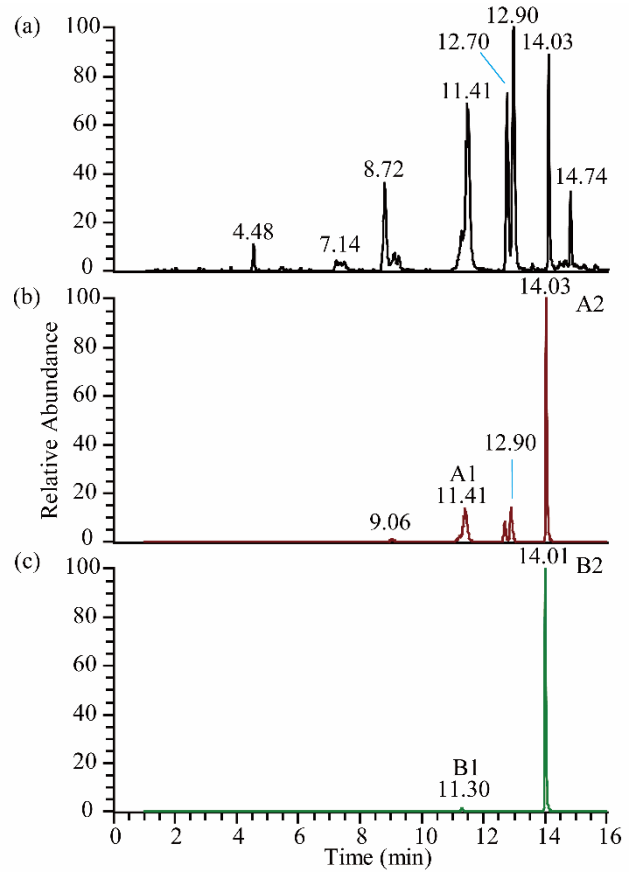

Figure 4.3 TIC of the specified ion value of 499.1608 in acetone-labeling QC samples (a), the extracted ion chromatogram with a neutral loss of 172.0736 from the TIC (b), and the extracted ion chromatogram with a neutral loss of 178.1112 in acetone-d_6-labeling QC samples (c).

4.3.2 Confirmation of modified nucleosides with chemical isotope labeling

The primarily screening results were verified by employing acetone-d_6 as derivatization reagent to assist modified nucleosides identification. QC samples were reacted with the same volume of acetone and acetone-d_6, respectively. The derivative products were analyzed by using Q-Exactive with PRM model. The acquired peaks with a neutral loss of 172.0736 or 178.1112 were extracted,

respectively. The extracted chromatograms were compared to recognize nucleosides peaks. Because the structures of acetone-labeling and acetone-d_6-labeling products were similar, their chromatographic behavior was also similar. Considering the isotope effects, retention time of acetone-d_6-labeling products might be a little shorter than acetone-labeling products. But the differences was very minor. It meant that the retention time of the two types of products was consistent. In addition, the volume of the derivatization reagents was the same, resulting in the same amount of derivative products. In other words, the intensity ratio of the two types derivative products was close to 1. Considering the instrumental error, the ratio ranges between 0.8 and 1.2 could be recognized as reasonable.

For instance, returning to the example of ion 499.1608, five peaks were detected by using a neutral loss scan of 172.0736 in QC samples reacted with acetone (Figure 4.3b). In the corresponding QC samples that reacted with acetone-d_6, two peaks were observed by scanning 505.1984 and extracting a neutral loss of 178.1112 from the obtained chromatogram (Figure 4.3c). Comparing the two extracted chromatogram, it was found that two pairs of peaks might be satisfied with the two conditions mentioned above, which were peaks of A1, B1 and A2, B2. For each pair, the retention time of paired peaks were close, with deviation less than 0.12 min. But the ratios of peak area were quite different, which were 17.6 for peak A1, B1 and 1.12 for peak A2, B2. The peak area ratio of A1 and B1 was extended far beyond the range of 0.8~1.2. So they didn't simultaneously match the two features

mentioned above. It meant that they didn't present the same compound. However, for peak A2 and B2, both the retention time and peak area ratio were satisfied with the two criteria. Therefore, it is very likely that they represented the pair of reaction products that generated by labeling a nucleoside with acetone and acetone-d_6, respectively.

More evidence could also be provided to support this conclusion. Due to the elements difference of acetone and acetone-d_6, the molecular weight of derivatization products of the two compounds reacted with nucleosides was also different. Acetone-d_6-labeling nucleosides differed by 6.0376 from acetone-labeling nucleosides, which was the same as the difference of acetone and acetone-d_6. In addition, the two types of derivatization products should have similar MS/MS spectra, which could also strongly support the identification. Figure 4.4 showed the MS/MS spectra of peak A1, A2, B1 and B2. It was obvious that the MS/MS spectra of A1 and B1 were quite different (Figure 4.4a and Figure 4.4b). It implied the structure of the two compounds were not similar. This was further proof that they didn't present the same compound. However, by comparing Figure 4.4c and Figure 4.4d, it was found that most of the fragment ions of the two MS/MS spectra were the same and the abundance distributions were similar. In the two figures, the highest fragment ions were both 327.0872, which was generated from the precursor ions by losing a neutral loss of 172.0736 (or 178.1112). In addition, the precursor ions of A2 and B2 were 499.1608 and 505.1984. The difference of the couple ions

was 6.0376, which was equal to the difference of acetone and acetone-d_6. The results implied that the chemical structure of A2 and B2 were similar. They were derived from the same nucleosides by reacting with acetone and acetone-d_6, respectively. In other word, the pair of peaks represented one nucleoside. Based on the information of database, the compound was identified as 2-methylthio-N^6-threonylcarbamoyladenosine.

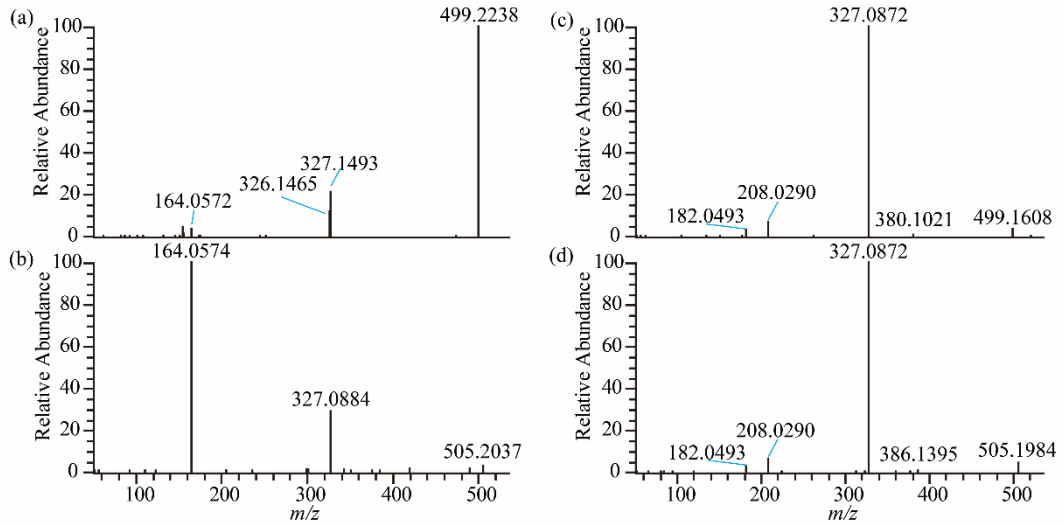

Figure 4.4 Application of MS/MS spectra to assistance appraise of nucleosides. The MS/MS spectra were corresponding to the peaks of Figure 4.3, which were labeled with A1 (a), B1 (b), A2 (c) and B2 (d).

After synthesized all kinds of information, modified nucleosides could be recognized by using acetone and acetone-d_6 labeling method. 66 nucleosides were identified in QC samples. After optimizing the collision energy for each compound, a new inclusion list was generated based on their information of retention time, *m/z*

values and collision energy. The list was employed to evaluate changes of modified nucleosides in rat urine samples exposed to BPA.

4.3.3 Evaluation of modified nucleosides in rats exposed to BPA

Based on the new list, PRM method was employed to analyze rat urine samples exposed to BPA. The raw data was processed with Xcalibur. The most abundance fragment ions which were generated by losing a neutral group of 172.0736 from precursor ions were used for integration of the peak areas. The areas were employed to assess effects of BPA on the urinary nucleoside by performing multivariate data analysis. Unsupervised PCA visually demonstrated the difference of the four groups of samples (Figure 4.5). The results showed that BPAL group overlapped with the control group. BPAM and BPAH were appreciably separated from the control group. And the distance of BPAH and control groups was farther than that of BPAM and control groups. It demonstrated that BPA had a stronger impact on rat urinary nucleosides at high and middle does than at low does. And it had the strongest effect on high does-exposure rats. The results indicated that the relationship of BPAL, BPAM and BPAH groups with the control group were dose-response reactions.

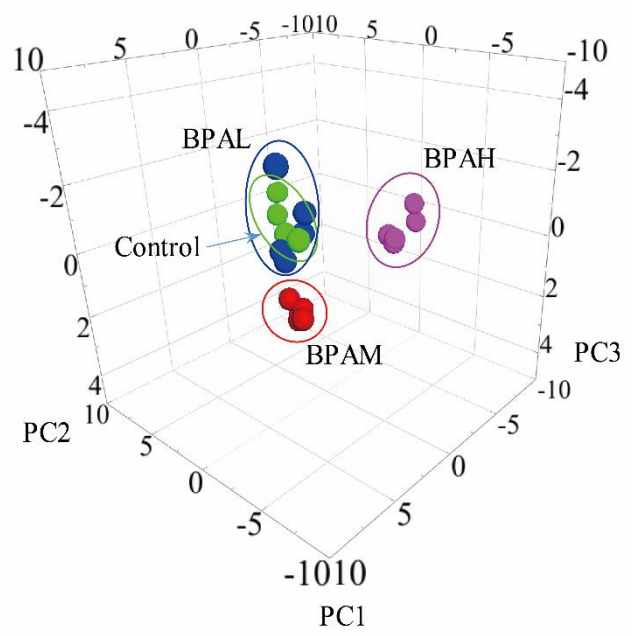

Figure 4.5 PCA score plot of four groups urine samples exposed to BPA. BPAL: low-dose, BPAM: middle-dose, BPAH: high-dose.

The PCA score plot also implied that levels of some nucleosides changed significantly in does-exposure groups, especially in BPAH group. Volcano plots were applied for quick visual identification of the most-meaningful changes (Figure 4.6). Points that displayed large magnitude fold changes (larger than 1.5) as well as high statistical significance ($p < 0.05$) were selected as candidates. 18 candidates were found in BPAH group (Figure 4.6c), while 2 and 5 were found in BPAL (Figure 4.6a) and BPAM (Figure 4.6b) groups, respectively. It indicated that BPA exposure disturbed the levels of nucleoside more strongly in high-dose exposure group than in low- and middle-dose groups. The results were well comparable to that of the previous conclusion drawn from PCA score plot.

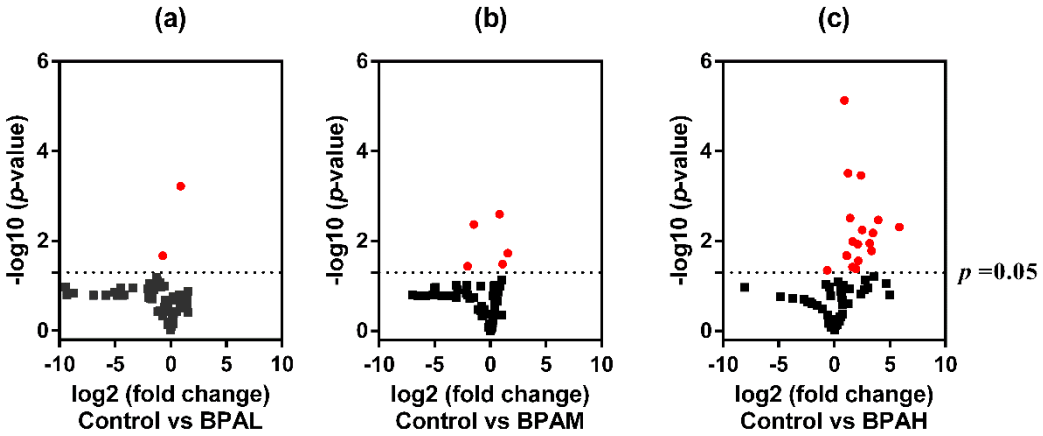

Figure 4.6 Volcano plot analysis of differential nucleosides in each BPA-exposed group. The fold change in modified nucleosides levels between BPA-exposed groups and control samples was plotted on the x axis (log2 scale), and the *p*-value of t-test was plotted on the y axis (–log10 scale). Compounds displayed statistical significance (old change > 1.5 and $p < 0.05$) were indicated in red.

Specific to each differential nucleoside, it could find that most the nucleosides tended to increase (Figure 4.7a, 7b, 7c and Table 4.1). The largest differential occurred in BPAH group, for compound 5-methylaminomethyluridine, which was 57.95 times higher than in control group. In addition, 8-oxoG was detected as significant compound in BPAH group but not in BPAL or BPAM groups. 8-oxoG was a biomarker of RNA damage[222]. The content elevation of the specific nucleoside indicated RNA was damaged under high-dose BPA exposure. The accident may be due to increased oxidative stress induced by BPA. It was reported that the environmental agent could induce statistically significant alterations in ROS level in cells [223, 224]. High levels of ROS oxidized RNA, primarily leading to

single strand breaks and base modifications[225]. Though the attack of oxidation at nucleic strands was random, particular residues, especially guanosine, were more susceptible to ROS. Such hotspot sites were hit by ROS with a great chance to form 8-oxoG, resulting in the consequent loss of integrity of RNA[226]. The damaged RNA was turnover or degraded to clear the 8-oxoG to protect cells from low translation efficiency and aberrant protein products[227]. The released free modified nucleosides were excreted out of the body via urine. Therefore, the damage of RNA could be deduced reversely from the level of 8-oxoG in the urine. In the groups of BPAL and BPAM, 8-oxoG did not show significant change, but they had the trend of increasing ($p > 0.05$). These tendencies of change were related to the increase of BPA dose (Figure 4.7d). The explanation is that the cells have a complete set of antioxidant system, such as superoxide dismutase, peroxidase, ascorbic acid, reduced glutathione, membrane lipid peroxidation, and so on[139, 224]. The production of ROS in the body could be countered by several antioxidative mechanisms via the system to reduce risk of oxidation-induced RNA damage. Some reports have demonstrated that decreased levels of antioxidants were found in BPA treated rats[228, 229]. However, when the oxidative stress exceeded a specified level which was far more than the body could endure, the chance of RNA suffered from damaging attacks greatly increased. The most immediate consequence was that the turnover or degradation of RNA were accelerated, leading to level alteration of 8-oxoG. As the damaged RNA was degraded, other modified nucleosides (except for 8-oxoG)

were released from the RNA, too. Because they could not be reused by the cells, they were also excreted to the urine. It means that while the RNA damage increased, the levels of modified nucleosides also increased. Therefore, by detecting the content of urinary modified nucleosides, especially 8-oxoG, the damage of RNA caused by BPA exposure could be indirectly surveyed.

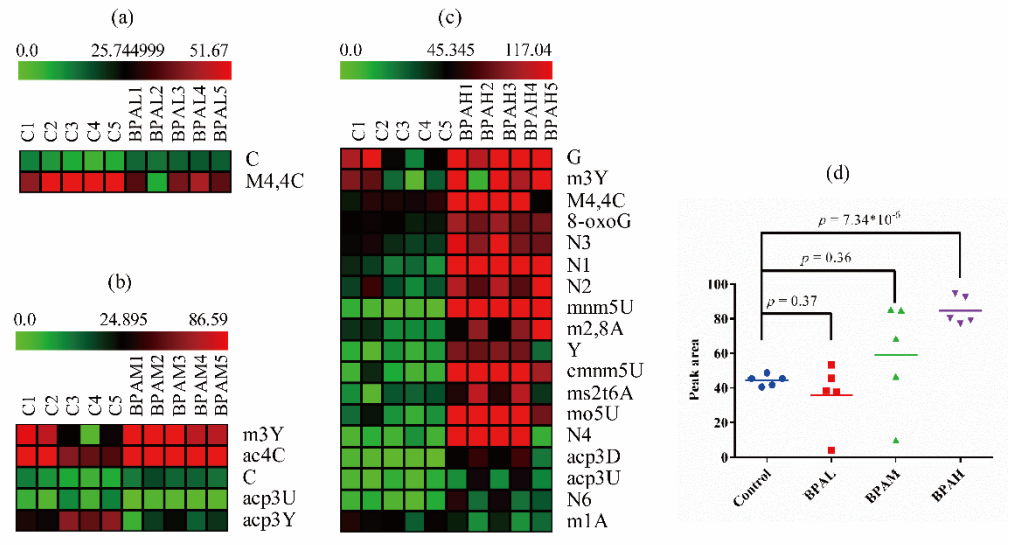

Figure 4.7 Comparison of differential nucleosides in urine samples of rats exposed to BPA. Heat maps showed the differential nucleosides between control and low-dose exposure group (a), middle-dose exposure group (b) and high-dose exposure group (c). And comparison of levels of 8-oxoG in the four group (d).

Table 4.1 Differential nucleosides detected in urine samples of rats exposed to BPA.

No.	R.T. /min	*m/z*	Name	Symbol	Fold change [a]	p-value [b]	Group

1	5.01	284.1243	Cytidine	C	1.86	0.00061	BPAL
2	4.80	312.1555	N^4,N^4-Dimethylcytidine	m4,4C	0.61	0.021	BPAL
3	3.62	299.1242	3-Methylpseudouridine	m3Y	2.15	0.032	BPAM
4	4.67	348.1168	N^4-Acetylcytidine	ac4C	2.99	0.019	BPAM
5	5.01	284.1244	Cytidine	C	1.78	0.0025	BPAM
6	5.45	386.1561	3-(3-Amino-3-carboxypropyl)uridine	acp3U	0.24	0.036	BPAM
7	9.49	386.1562	3-(3-Amino-3-carboxypropyl)pseudouridine	acp3Y	0.36	0.0043	BPAM
8	6.00	324.1305	Guanosine	G	2.16	0.021	BPAH
9	3.62	299.1240	3-Methylpseudouridine	m3Y	3.92	0.041	BPAH
10	4.80	312.1557	N^4,N^4-Dimethylcytidine	m4,4C	2.23	0.022	BPAH
11	8.31	340.1254	8-Hydroxy guanosine	8-oxoG	1.90	0.0000073	BPAH
12	8.88	297.1446	1-(beta-D-Ribofuranosyl)-1,4-dihydronicotinamide	N3	2.34	0.00031	BPAH
13	3.79	295.1291	Nicotinamide riboside	N1	5.36	0.00035	BPAH
14	3.79	296.1131	Nicotinate D-ribonucleoside	N2	2.71	0.0031	BPAH
15	3.24	328.1503	5-Methylaminomethyluridine	mnm5U	57.95	0.0049	BPAH
16	8.20	336.1665	2,8-Dimethyladenosine	m2,8A	3.12	0.038	BPAH
17	6.40	285.1086	Pseudouridine	Y	5.74	0.0056	BPAH

18	6.49	372.1407	5-Carboxymethylaminomethyluridine	cmnm5U	11.12	0.0065	BPAH
19	14.02	499.1608	2-Methylthio-N^6-threonylcarbamoyladenosine	ms2t6A	3.16	0.010	BPAH
20	4.06	315.1191	5-Methoxyuridine	mo5U	9.07	0.011	BPAH
21	8.67	333.1174	6-Hydroxyl-1,6-dihydropurine ribonucleoside	N4	10.19	0.016	BPAH
22	4.92	388.1718	3-(3-Amino-3-carboxypropyl)-5,6-dihydrouridine	acp3D	15.62	0.0034	BPAH
23	5.45	386.1559	3-(3-Amino-3-carboxypropyl)uridine	acp3U	4.53	0.028	BPAH
24	8.35	341.1092	beta-D-3-Ribofuranosyluric acid	N6	4.34	0.012	BPAH
25	6.63	322.1516	1-Methyladenosine	m1A	0.65	0.045	BPAH

a Fold change was obtained by comparing does groups with control group, respectively.

b *p*-Value was obtained from t-test by comparing the does groups with control group, respectively.

In recent years, RNA damage was attracting more and more attention[230-232]. However, in people or animals, direct detection of RNA damage was not easy as it was difficult to collect tissue samples. Therefore, indirect measuring methods became the most important means. RNA damage could be evaluated via measuring its specific biomarker, i.e., 8-oxoG. But due to the complex components of blood

or urine, low level and high polarity of 8-oxoG and other modified nucleosides, sample preparation was necessary to analyze these compounds. In the paper, derivatization method was employed to solve these issues. Acetone was used as a derivatization reagent to block the *cis*-diol groups in the nucleosides. The polarity of the reaction products decreased, leading to improvement of chromatographic separation on reversed-phase columns. Simultaneously, in reaction process, the samples were clean-up with the solvent of acetone by precipitating most of matrix, including inorganic salts, proteins and other biomacromolecules. Whereafter, the derivatized nucleosides were selectively detected by using PRM assay combining with isotope labeling to confirm the results. The PRM assay provided a wealth of information, such as high resolution precursor ions, high resolution MS/MS and neutral loss of the precursor ions. These data were valuable for compound identification. Comparing with previously reports, the current method showed better selectivity and sensitivity. As a result, 66 nucleosides were detected in one running, which was more than the previous reports[233, 234]. The results suggested that PRM was a powerful analytical tool for the detection of modified nucleosides. By using the method, various change trends of modified nucleosides were observed in rats with different dose BPA exposure. Specifically, significant change of 8-oxoG was observed in BPAH group, which proved that RNA was damaged when the dose of BPA was beyond a certain amount. To the best of our knowledge, it is the first time to report that BPA exposure could damage RNA. It provides new evidence for

toxicological research of BPA exposure.

4.4 Chapter summary

In summary, a PRM method based on high resolution MS was developed to detect urinary modified nucleosides in rats exposed to BPA. Combining with acetone derivatization, the high specificity and sensitivity of the method enabled positive identification of 66 nucleosides in urine samples. The level changes of the detected nucleosides in the rats exposed to BPA were studied. Various trends of modified nucleosides were observed with different dose BPA exposure. Specifically, the high-dose exposure group was the most strongly affected. The biomarker of RNA oxidation, 8-oxoG, showed significant change in this group. It proved that BPA exposure could induce RNA damage when the dose of BPA was beyond a certain amount. This study opened a new view on the mechanism of toxicity of BPA. It might be valuable for the risk assessment study of BPA exposure. The results also suggested that PRM was a powerful analytical tool for the detection of modified nucleosides.

Chapter 5 Urinary profiling of *cis*-diol-containing metabolites in rats with bisphenol A exposure by liquid chromatography-mass spectrometry and isotope labeling

5.1 Introduction

BPA is widely applied in daily life[235]. Human is constantly exposed to BPA from a variety of sources[236, 237]. The common exposure sparked concern about its safety in some consumer products and food containers. It was reported that BPA may alter hormone regulation due to its hormone-like properties, resulting in a wide range of diseases[144, 147, 238-242]. A few studies have linked the environmental contaminant exposure to endogenous metabolic disorders[150-152, 243].

Cis-diol-containing metabolites perform numerous roles in living organisms as important intermediate metabolites and information molecules for cell recognition and signal transduction[244,245-247]. BPA could alter the levels of *cis*-diol-containing metabolites in organism. Although several *cis*-diol compounds were mentioned in just a few articles that they were affected by BPA exposure[154, 248], there were no papers describing the effects of BPA on the profiling of *cis*-diol metabolites. That may be because these metabolites were not readily detected due to their low abundance, high polarity and serious matrix interferences in biological samples. These characteristics made them poor separation on reversed-phase column, serious ionic interference and low sensitivity of mass spectrometric detection. These factors have posed a grave challenge to determine *cis*-diol metabolites.

The chemical labeling was an alternative strategy to solve these problems. By introducing lipophilic group(s) to the analytes, chemical labeling can improve the chromatographic separation of polar or ionic compounds[249, 250]. Conversely, adding ionizable functional groups to the metabolites that were hard ionization could enhance their ionization efficiencies[251, 252]. Hydroxyl groups of *cis*-diol-containing metabolites make these compounds very polar. Therefore, it may decrease the polarity by introducing lipophilic groups to block the *cis*-diol groups to improve the separation on reversed-phase column. In addition, chemical labeling could be further extended to chemical isotope labeling. The method usually applies a light chemical tag to label targeted analytes in samples and mixes them to aliquots of comparative control samples labeled with a heavy isotopic analog. The pooled samples were then analyzed by using liquid chromatography-mass spectrometry (LC-MS). Due to the similar structure, the heavy- and light-labeled substrates were co-eluted from columns. The pair of peaks has a defined mass difference which is derived from the characteristic mass difference of the light and heavy isotopic tags. The peak pair could be distinguished from noises and background peaks which are detected as singlet peaks[253]. Based on these characteristics and advantages, the method could be applied to overcome ion suppression, instrument drift and other technical problems for chromatographic analysis[254]. The techniques were often used for relative quantification by determining intensities ratio of peak pair[255-258]. It was particularly helpful to compare differences of certain compounds which

could not find suitable internal standard for absolute quantitation. In some case, the techniques were employed to recognize analytes with a common functional group, such as amine, acid, phenol, etc[259-261]. This method may also be used to detect *cis*-diol-containing metabolites by selecting a pair of proper isotope labeling reagents. Based on the results mentioned above, acetone could selectively react with *cis*-diol group of ribonucleosides to form acetonide. The reaction has been validated and proved a robust derivatization method. Therefore, in this chapter, the method was employed to label *cis*-diol metabolites with acetone and deuterium acetone (acetone-d_6) to recognize these compounds in urine samples. The results were used to evaluate the changes of urinary *cis*-diol-containing metabolites in rats with BPA exposure.

5.2 Material and methods

5.2.1 Chemicals

HPLC grade methanol and acetone were obtained from Merck (Dermstadt, Germany). Acetone was used directly without further drying process. Water was purified by using a Milli-Q system (Millipore, Milford, MA). Bisphenol A (BPA) was purchased from J&K Scientific Ltd. (Beijing, China). Hexadeuteroacetone (99.9 atom % D, acetone-d_6), formic acid (HPLC grade), 70% perchloric acid ($HClO_4$) and other authentic standards were purchased from Sigma-Aldrich (St. Louis, MO, USA).

5.2.2 Animal models

The animal protocols and sample collection were the same as mentioned in chapter 4. Briefly, Sprague-Dawley rats were divided into four groups randomly with 5 rats for each: control, low-dose (BPAL), middle-dose (BPAM) and high-dose (BPAH) groups. For the four groups, 0, 10, 30 and 50 mg BPA/kg body weight were administered every day for four days, respectively. A 24-hour urine specimen for each rat was collected after four days of BPA administration for the analysis.

5.2.3 Sample preparation

The method used for sample preparation was the same as described in chapter 2. Briefly, urine samples in the four groups (Control, BPAL, BPAM and BPAH) were labeled with acetone by using $HClO_4$ as catalyst. The derivatization products were separated from matrix and analyzed by using LC-MS.

Quality control (QC) samples were used to recognize *cis*-diol metabolites from urine. They were prepared by combining and thoroughly mixing 200 µL aliquots of urine from each sample of BPA-exposed rats to create a pooled QC sample. 100 µL aliquots of this pooled samples were applied to prepare multiple QC samples. The multiple QC samples were divided into three groups (QCH, QCD and QC0) with 10 samples for each group. QCH and QCD groups were reacted with acetone and acetone-d_6, respectively, following the procedure described above. In the last step of centrifugation, the supernatant was mixed with equal volume and used for LC-MS analysis. The third group (QC0) was treated by using methanol/water (4:1, V/V)

for protein precipitation. After centrifuged to remove the precipitation, the supernatant was dried with a stream of nitrogen. The residue was reconstituted as described above. The QC0 and QCH groups were compared to study the effect of acetone labeling on the chromatographic separation.

5.2.4 Ultra-performance liquid chromatography–mass spectrometry

Sample analysis was performed by using Waters Acquity ultra-performance liquid chromatography coupled with Waters Q-TOF Premier Mass Spectrometer (UPLC-Q-TOF MS). The chromatographic separation was accomplished on a Acquity UPLC BEH phenyl column (100 mm × 2.1 mm, 1.7 μm, Product Number: 186002885). Linearity gradient elution program was set up with the mobile phases containing water (added 0.1% formic acid, A) and methanol (B). The initial mobile phase was composed of 95% A and 5% B. Within 2 min, percentage of B increased from 5% to 20%, then to 35% within 8 min, following increasing to 95% within 4 min and held for 1 min, then returned to 5% within 0.5 min and kept for 4.5 min. A complete running took 20 min for one sample. The flow rate was 0.30 mL min^{-1}. The column temperature was 35 ℃. For each sample, injection volume was 10 μL. A Q-TOF MS was used to acquire accurate mass to charge ratio (*m/z*). The analyte was detected in full scan under positive ion mode. The parameters of MS method were as follow: capillary voltage 3.5 kV, cone voltage 20 V, cone gas flow 100 L h^{-1}, desolvation gas flow 600 L h^{-1}, source temperature 130 ℃, desolvation gas temperature 350 ℃. Data was acquired with a mass range from *m/z* 100 to 1000 in

centroid mode. The scan time was set at 0.2 s and interscan time 0.02 s. The lock-mass was a 100 pg uL^{-1} leucine-enkephalin solution in acetonitrile-water (50:50, v/v) with a flow rate of 0.05 mL min^{-1}.

5.2.5 Data processing and statistical analysis

The raw data was converted to NetCDF format by using Databridge software. The raw data of six group samples (QCH, QCD, Control, BPAL, BPAM and BPAH) was processed by using XCMS online[262] at the same time. After nonlinear alignment and automatic integration, peak intensities were extracted. The variables that presented in more than 80 % of the samples were used to build a three-dimensional matrix which contained retention time (RT), *m/z* and associated ion intensities. The matrix was divided into two parts (A and B). Part A contained data of samples of QCH and QCD and part B contained samples of Control, BPAL, BPAM and BPAH. Part A was imported into ShiftedIonsFinder[263] to select candidate labeled peaks by comparing the mass spectra in the two groups. The specified mass difference was set at 6.0376. The parameter of Max. Fold was set to 3. The *m/z* difference threshold was set at 15 ppm and RT difference threshold was 0.25 min. The filter criterions were that RT difference must be smaller than 0.25 min and *m/z* difference must be 1 ,2 or 3 multiples of 6.0376 with a threshold smaller than 15 ppm. By comparing samples that reacted with acetone (light labeled) and acetone-d_6 (heavy labeled), peaks in the two groups matched the filter criterions were selected as “hits”. To calculate the intensities of peaks in the two groups, each

hit that had intensity ratio between 0.8 and 1.2 was considered as an "ion pair" that represented one metabolite containing *cis*-diol group(s). All the ion pairs were used to build a data set for practical sample analysis.

For the samples of part B (containing samples of Control, BPAL, BPAM and BPAH), the intensity of each peak was normalized by using the summation of response of all metabolites in one sample. The resulting new matrix was compared to the data set which was built from samples of QCH and QCD. Peaks that could find in the data set were imported into SIMCA-P to perform multivariate data analysis. Unsupervised principal component analysis (PCA) method was employed to evaluate the difference of the four groups of samples. To highlight variables that had significant contributions to discrimination between groups, a one-way ANOVA was performed followed by a Least Significant Difference (LSD) test among the groups. Variables that were significant difference ($p < 0.05$) and fold changes were larger than 1.5 were selected as candidates. Subsequently, the target ions were identified with high resolution MS/MS and confirmed by authentic standards. The certified variables were preferentially considered as the significantly changed compounds.

The pathway analysis (integrating enrichment analysis and pathway topology analysis) module were performed by using MetaboAnalyst[264]. The metabolic network was built by MetScape which provided a bioinformatics framework for the visualization and interpretation of metabolomic data using Cytoscape[265].

5.3 Results and discussion

5.3.1 Selectivity of the labeling methodology

Cis-diol-containing metabolites are widely distributed in living organisms. These groups provide extensive functionality in biological metabolism. However, other polyhydroxy groups, such as *tran*-diol and *1,3*-diol, make it a challenge to selectively determine *cis*-diol metabolites due to a large number of isomers. In this study, by using chemical labeling method, *cis*-diol compounds were tagged with acetone and distinguished from other polyhydroxy compounds. Comparison of three authentic references, i.e. adenosine, deoxyadenosine and vidarabine, which have *cis*-diol, *trans*-diol and *1,3*-diol, respectively, showed that only *cis*-diol group could react with acetone to form acetonide (Figure 5.1). But *trans*-diol and *1,3*-diol did not show any changes before and after reacting. It suggested the method had the advantage of a high selectivity.

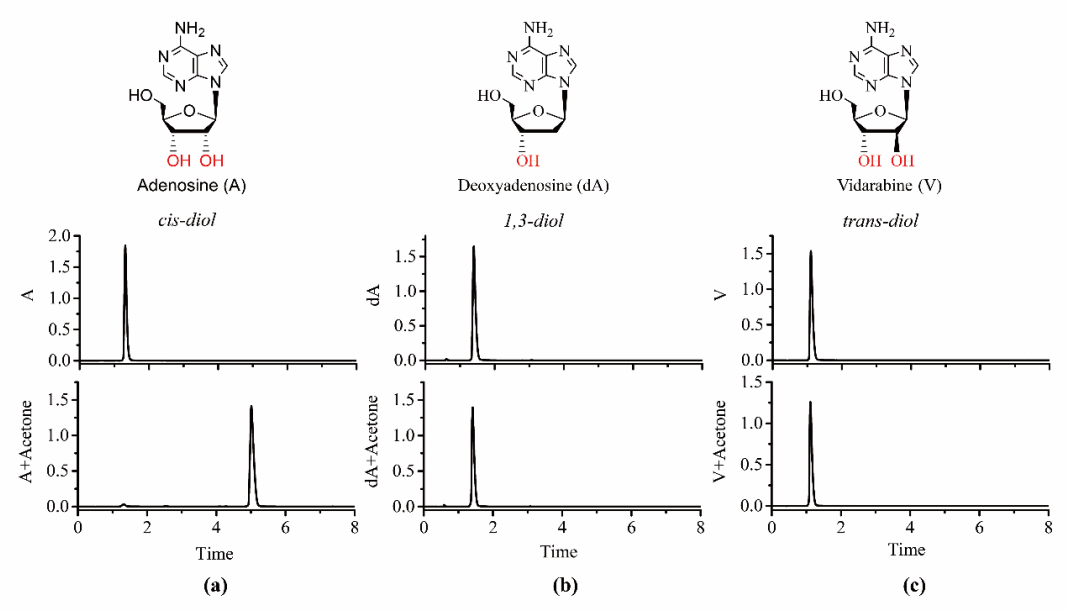

Figure 5.1 Selectivity evaluation of the chemical labeling reaction by using acetone to label (a) adenosine, (b) deoxyadenosine and (c) vidarabine. The chromatographic separation was accomplished with ACQUITY UPLC system equipped with a PDA detector. Ultraviolet detection was set at 260 nm.

5.3.2 Improvement of LC-MS detection after acetone labeling

The hydroxyl groups in *cis*-diol compounds are very polar, resulting in poor retention on reversed-phase column. Especially for some isomers, the remarkably similar properties caused unsatisfactory separation and made it hard to conduct qualitative and quantitative analyses. By blocking the *cis*-diol with acetone, the polarity of formed isopropylidene ketal decreased, which could be expected to improve the chromatographic behavior of the targeted analytes. The cloud plot (Figure 5.2) generated by XCMS, showed noticeable difference of chromatograms of urine samples with and without acetone labeling, i.e., QCH and QC0 groups. In

the figure, the upper bubbles represented emerging peaks in labeled samples, while the lower bubbles represented disappearing peaks which had been reacted with acetone. The radius scale of each bubble delegated intensity of peaks. And significant difference of peaks between the two groups was represented with *p*-value by shade of color. All the *p*-values were smaller than 0.001. By comparing the two chromatograms, it was found that peaks detected in labeled samples were much more than in directly analyzed samples. It may be ascribed to the clean-up processing during the sample preparation. Because the samples were reacted with acetone in anhydrous solvent, the inorganic salts, proteins and other biomacromolecules were precipitated and removed by centrifugation. The samples were cleansed to reduce matrix effects and ion suppression, leading to enhancement of ionization efficiency. Therefore, more metabolites could be detected, even for some substances with low abundance.

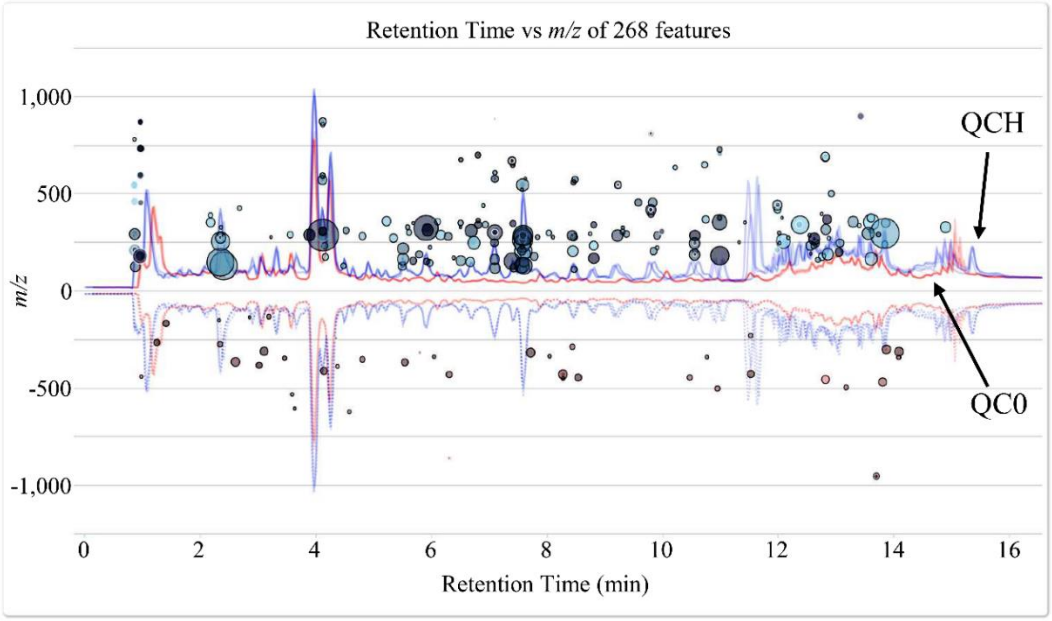

Figure 5.2 Cloud plot showing difference of chromatograms of urine samples with (upper) and without (lower) acetone labeling. The blue line corresponded to the acetone-labeled QC sample (QCH), and the red line to the non-labeled sample, QC0.

In addition, peak number increased in acetone-labeled samples were also related to the improvement of chromatographic separation. Introduction of acetone to *cis*-diol metabolites decreased their polarity and increased retention time on reversed-phase column. In Figure 5.2, only a small portion of peaks distributed in mid and later sections of gradient eluting procedure (in lower area). But after reacted with acetone, more peaks appeared in the region (in upper area). In such circumstances, analytes were eluted by high percentage of organic mobile phase, which was conducive to electrospray ionization and enhancement of sensitivity. Moreover, decreasing the polarity of *cis*-diol-containing metabolites also contributed to separate co-eluted

components, especially for some isomers. A simple example is that uridine and pseudouridine, two isomers with very similar structures, had the same retention time when they were analyzed directly (Figure 5.3a). In contrast, after reacted with acetone, the two metabolites were baseline separation (Figure 5.3b). Differentiation of the two substance could be realized under such condition. Furthermore, the intensity of main peak (at 4.08 min) in acetone-labeled sample was much higher than that in directly analyzed sample. That was consistent with previous statement. The results demonstrated that the method could not only separate components of closely similar properties, but also increase the intensities. It offered an available alternative for the determination of low abundance *cis*-diol-containing metabolites based on these characteristics and advantages.

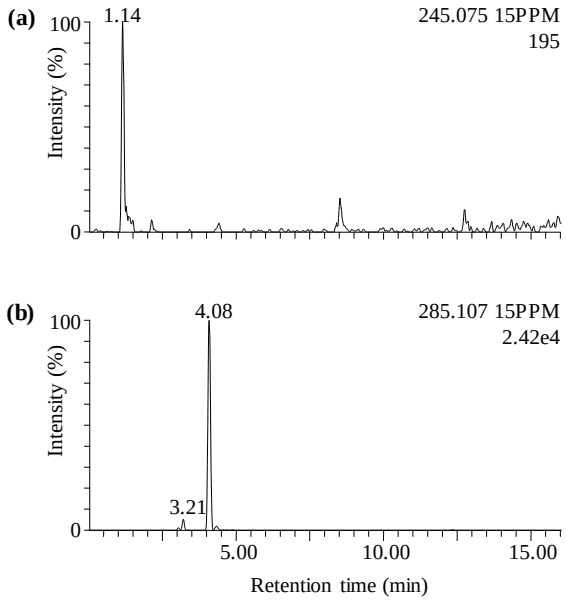

Figure 5.3 Chromatographic separation of uridine and pseudouridine on reversed-phase column. Extracted ion chromatograms of samples by direct analysis (a) and labeling with acetone (b).

5.3.3 Recognition of *cis*-diol metabolites by using stable isotope labeling

Because the chromatograms of urine samples with and without acetone were quite different, it was not easy to identify *cis*-diol signals by directly comparing the two kinds of chromatograms. Therefore, stable isotope reagent was applied to assist the recognition of *cis*-diol metabolites combined with ShiftedIonsFinder software. Acetone and acetone-d_6 were used to label the same samples, respectively. The labeled samples were mixed with equal volume and used for LC-MS analysis. First, because of the similar structures of ordinary and deuterated acetonides, they would be co-eluted from the column. In other words, the retention time of the two kinds of products was consistent. Second, the molecular weight difference of acetone and acetone-d_6 is 6.0376. Therefore, based on the number of *cis*-diols in the molecular, the difference of *m/z* was an integer multiple of 6.0376. Third, the samples were mixed with equal volume, leading to the same peak intensities. Considering the error of method and instrument, the intensities ratio between 0.8~1.2 was acceptable. The three features were assessment standards to recognize "ion pair" of acetonide and acetonide-d_6 which were generated from the same compound. The filtration of ions was performed by using ShiftedIonsFinder according to the first two features, following with selecting ion pairs which matched to the third feature.

An example in Figure 5.4 showed the processes of recognition. A pair of peaks, whose retention time was both at about 7.70 min (Figure 5.4a and 5.4b), was found by ShiftedIonsFinder. The *m/z* of the two peaks were 278.1598 and 290.2345

(Figure 5.4c and 5.4d), respectively. It meant that the *m/z* difference was about 2 times of 6.0376. And the intensity ratio was 0.98 which was very close to 1. The data revealed that the two peaks matched the three features mentioned above. And they represented a metabolite containing two *cis*-diol groups. In fact, after confirmed by MS/MS and authentic standards, it was identified as galactose. The results demonstrated another advantage of the method. That is, it could be used to decide the number of *cis*-diols in the molecular by comparing the *m/z* difference of ion pairs with 6.0376. The multiples were the number of *cis*-diols. The feature reduced the workload of searching against databases. That is only those compounds which contained *cis*-diol group(s) should be selected as candidates.

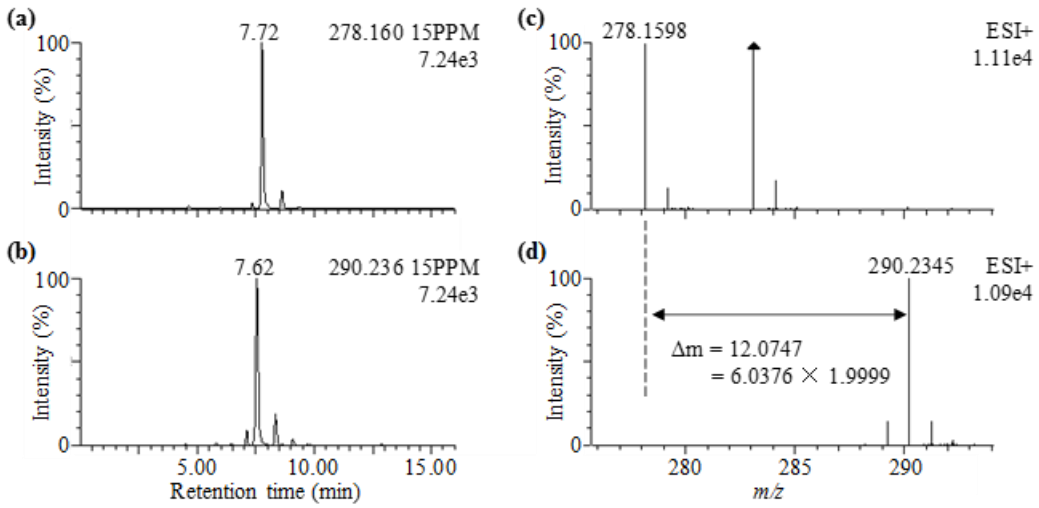

Figure 5.4 An example to show the processes of *cis*-diol metabolite recognition. Extracted ion chromatogram (a) and its corresponding mass spectra (c) of *m/z* 278.1598 from sample reacted with acetone. Extracted ion chromatogram (b) and

its corresponding mass spectra (d) of *m/z* 290.2345 from sample reacted with acetone-d_6.

Besides, MS/MS spectra of "ion pair" of acetonide and acetonide-d_6 provided further evidences for *cis*-diol metabolite recognition. Using labeled galactose as example again, due to the similar structures, the MS/MS spectra of "ion pair" had similar fragment ions and relative abundances (Figure 5.5). Fragment ions that did not contain *cis*-diol group(s) were the same in the two kinds of MS/MS spectra, just as ions of *m/z* 127.0394 (or 127.0400) and 97.0298 (or 97.0287) in Figure 5.5a and 5.5b. By contrast, differences could be observed for these ions contained *cis*-diol*(s)*, for example, ion of *m/z* 203.0911 in Figure 5.5a and *m/z* 209.1287 in Figure 5.5b. The mass difference of the two ions was 6.0376, which was equal to the difference of acetone and acetone-d_6. It implied that the ions contained one labeling tag connecting to the *cis*-diol group. In other word, it was formative from the parent ion by losing one acetone-labeled fragment (Figure 5.5c). Similarly, ion of *m/z* 243.1361 in Figure 5.5a and *m/z* 255.2022 in Figure 5.5b contained two labeling tags. They were generated through losing the adduct of NH_4^+ and one molecule of H_2O from the parent ions (Figure 5.5c). Hence, a wealth of information was acquired from these ions. They provided structural information for identification of interest metabolites. The recognition of other *cis*-diol metabolites was performed following the procedures described previously. The ion pairs that met the

requirements (in total 945 pairs) were selected to build a data set to study the influence of BPA exposure on *cis*-diol metabolites in rat urine samples.

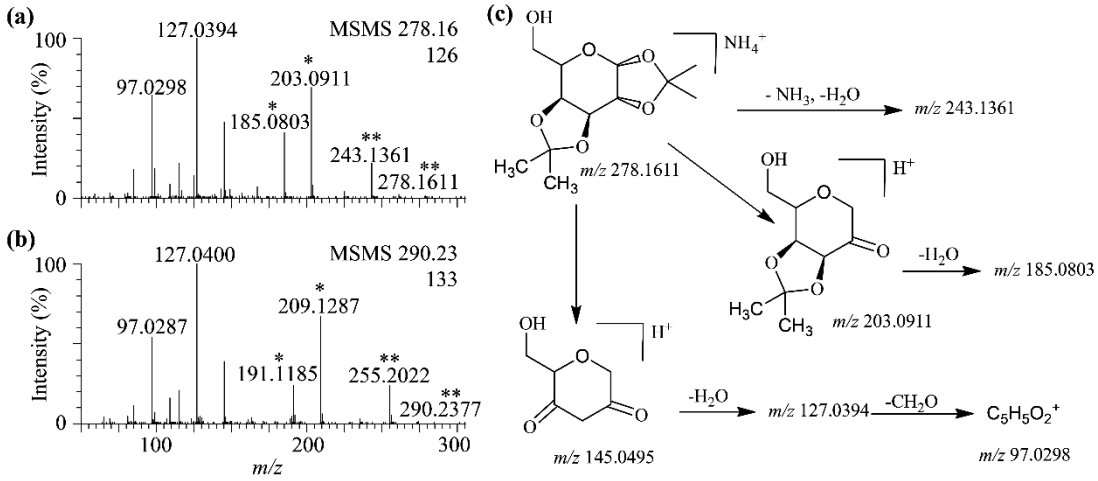

Figure 5.5 MS/MS spectra of galactose labeled with acetone (a), acetone-d_6 (b) and the possible fragmentation behavior of acetone-labeled galactose (c). * Fragment ions contained one labeling tag, ** fragment ions contained two labeling tags.

5.3.4 Influence of BPA exposure on *cis*-diol metabolites in rat urine samples

After exposed to BPA, the rat urine samples were collected for LC-MS analysis. The samples were prepared and analyzed as described above. Via treated with XCMS, information of ions in the previous dataset were obtained, including RT, *m/z* and peak intensities. These information was imported into SIMCA-P to perform multivariate data analysis. Unsupervised principal component analysis (PCA) method was employed to evaluate the difference of the four groups of samples (Figure 5.6). The summary of the fit of the PCA model was manifest with R2X and Q2. The R2X of PC1 was 40.0% and PC2 14.5%, with a cumulative value up to

54.5%. Correspondingly, the cumulative Q2 was 39.9% and for PC1 and PC2, the values were 32.4% and 7.5%, respectively. The PCA score plot showed that BPAH and BPAM groups were appreciably separated from control group, but BPAL group overlapped the control group. It indicated that the effects of BPA on rat urine were much stronger at high and middle does than at low does. It also implied that some ions showed signification difference between the does-exposure and control groups.

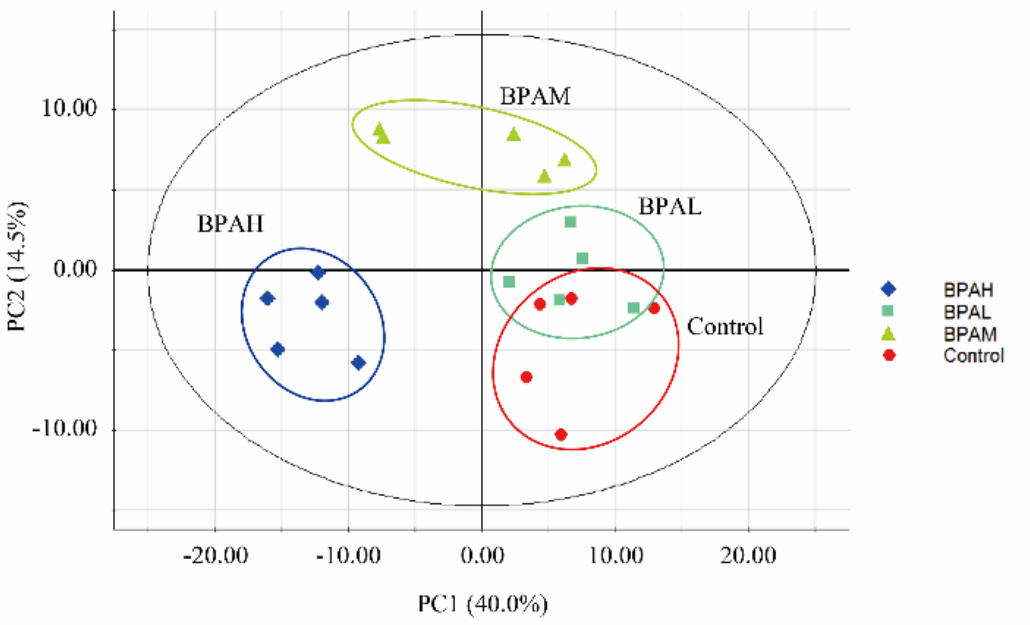

Figure 5.6 PCA score plot of urine samples of rats exposed to BPA with low-dose (BPAL), middle-dose (BPAM), high-dose (BPAH) and their control.

To highlight these ions, a one-way ANOVA was performed followed by a LSD test among the groups. Ions that were significant difference ($p < 0.05$) and fold changes were larger than 1.5 were selected as candidates. Subsequently, the target ions were

identified with high resolution MS/MS and confirmed by authentic standards. Throughout the process, 31 *cis*-diol metabolites were identified (Table 5.1). Only three differential *cis*-diol metabolites, i.e., gulonolactone, α-D-galacturonic acid and ribonolactone were found in BPAL group. In BPAM group, six metabolites showed noticeable difference. But in BPAH group, up to twenty-eight metabolites were identified with $p < 0.05$ and fold change > 1.5. The data demonstrated that BPA showed strong effect on *cis*-diol compounds metabolism at high-dose exposure and the effect on BPAL and BPAM group was smaller. It was in concordance with the result of PCA discussed earlier.

Table 5.1 Differential *cis*-diol metabolites in rat urine samples with BPA exposure.

ID	RT.	*m/z*	Adducts	Δppm	Name	Fold change (vs control)		
						BPAL	BPAM	BPAH
1	5.77	259.1179	$[M+H]^+$	-0.93	Gulonolactone	3.7 ***	5.1 *	3.5 ***
2	8.25	275.1121	$[M+H]^+$	-3.5	α-D-Galacturonic acid	1.9 *	1.9 *	/
3	3.78	211.0571	$[M+Na]^+$	-5.6	Ribonolactone	1.8 *	/	/
4	13.79	239.0912	$[M+H]^+$	-3.0	3-(3,4-Dihydroxyphenyl)lactate	/	3.2 *	2.2 *
5	13.31	274.1069	$[M+Na]^+$	4.9	Methyldopa	/	2.5 ***	/
6	4.38	284.1230	$[M+H]^+$	-5.7	Cytidine	/	2.4 *	2.1 *

7	5.00	313.1383	$[M+NH_4]^+$	-5.4	Nicotinate D-ribonucleoside	/	3.6 *	6.1 *
8	8.92	173.0806	$[M-H_2O+H]^+$	-4.8	D-Ribose	/	/	2.2 **
9	10.75	190.0857	$[M+H]^+$	-5.7	5,6-Dihydroxyindole	/	/	3.6 *
10	9.86	203.0905	$[M-H_2O+H]^+$	-7.3	α-D-Glucose	/	/	2.2 ***
11	8.88	203.0906	$[M-H_2O+H]^+$	-6.8	D-Mannose	/	/	1.7 *
12	1.89	215.0313	$[M+K]^+$	-4.1	Threonate	/	/	2.9 *
13	12.64	227.0897	$[M+Na]^+$	0.56	L-Rhamnulose	/	/	1.9 ***
14	12.64	246.1097	$[M+Na]^+$	-3.8	(-)-Epinephrine	/	/	2.0 *
15	2.58	259.0581	$[M+K]^+$	-1.1	Myoinositol	/	/	2.1 ***
16	2.85	262.1285	$[M+NH_4]^+$	-2.2	3-o-Ethyl-L-ascorbic acid	/	/	1.8 *
17	7.56	269.0986	$[M+Na]^+$	-5.7	Ribonic acid	/	/	2.1 **
18	2.01	275.0525	$[M+K]^+$	-2.9	Gluconic acid	/	/	5.9 *
19	1.63	275.0528	$[M+K]^+$	-1.8	L-Gulonate	/	/	8.8 *
20	6.41	278.1233	$[M+H]^+$	-7.2	Biopterin	/	/	1.9 *
21	7.72	278.1599	$[M+NH_4]^+$	-0.67	D-Galactose	/	/	1.5 ***
22	6.84	297.1436	$[M+H]^+$	-4.8	1-(beta-D-Ribofuranosyl)-1,4-dihydronicotinamide	/	/	1.9**
23	2.55	300.0847	$[M+K]^+$	-0.80	N-Acetyl-D-	/	/	1.9 *

					galactosamine			
24	9.02	301.1069	$[M+K]^+$	5.2	Sorbitol	/	/	3.6 ***
25	4.47	309.1042	$[M+Na]^+$	-6.8	5,6-Dihydrouridine	/	/	2.5 *
26	8.58	313.1062	$[M+H]^+$	3.2	D-Pinitol	/	/	2.2 *
27	3.63	326.1381	$[M+H]^+$	8.9	N^4-Acetylcytidine	/	/	2.3 *
28	12.41	338.1276	$[M+H]^+$	-3.1	5'-Deoxy-5'-(methylthio)adenosine	/	/	2.1 **
29	12.53	382.1008	$[M+NH_4]^+$	-2.0	Uridine monophosphate	/	/	1.9 ***
30	9.55	453.1720	$[M+H]^+$	-3.0	N^6-Carbamoyl-L-threonyladenosine	/	/	3.2 ***
31	12.52	499.1607	$[M+H]^+$	-0.76	2-Methylthio-N^6-threonylcarbamoyladenosine	/	/	2.7 **

Fold change was obtained by comparing the mean value of *cis*-diol metabolites in different dose group with control group. The asterisk indicated significant difference between dose group and control group. * $p < 0.05$, ** $p < 0.01$, *** $p < 0.005$.

5.3.5 Pathway analysis

To get some insight into how the BPA exposure affected *cis*-diol metabolites, network building and pathway analysis was performed with the metabolites

detected in BPAH group. Figure 5.7 showed that 13 metabolites were recognized by the software and matched to the database to build a metabolic network. Six of these metabolites, including D-galactose, α-D-glucose, D-sorbitol, D-mannose, myo-inositol and uridine monophosphate were at a critical juncture. These key nodes were related to many metabolic processes and may play important roles in cell metabolism. The pathways that these significantly different metabolites belonged to were studied by using MetaboAnalyst. The result showed that the most relevant pathways influenced by BPA exposure were galactose metabolism, fructose and mannose metabolism, ascorbate and aldarate metabolism, amino sugar and nucleotide sugar metabolism, pyrimidine metabolism, nicotinate and nicotinamide metabolism, and so on (Figure 5.8). Galactose metabolism showed the highest pathway impact ($p = 2.44 \times 10^{-5}$) among them. Five metabolites in the pathway were emphasized, including D-galactose, D-mannose, L-rhamnulose, myo-inositol and α-D-glucose (Figure 5.9). The levels of these metabolites were at least 1.5 times higher than control group. To our best knowledge, there was currently no paper reported that BPA exposure could alter galactose metabolism. But, some indirect evidence could explain the phenomenon. Published papers suggested that endocrine-disrupting chemicals induced the beta-galactosidase activity[266-268]. As an endocrine disruptor, BPA may also exhibit potential to activate the expression of β-galactosidase[269-271]. In fact, it has been reported that the relative estrogenic activity of BPA could be detected through a β-galactosidase colorimetric

assay[272, 273]. β-Galactosidase, a hydrolase enzyme, could catalyze the hydrolysis of beta-galactosides such as ganglioside GM1, lactosylceramides, lactose, and various glycoproteins into monosaccharides. The most important function of the enzyme is to cleave lactose to glucose and galactose to provide source for cell energy metabolism. Therefore, when exposed to high-dose BPA, the activity of β-galactosidase was induced, leading to an alter the beta-galactosides' hydrolysis to form increase of galactose as well as other monosaccharides. The studies implied that BPA exposure might influence galactose metabolism in some extent.

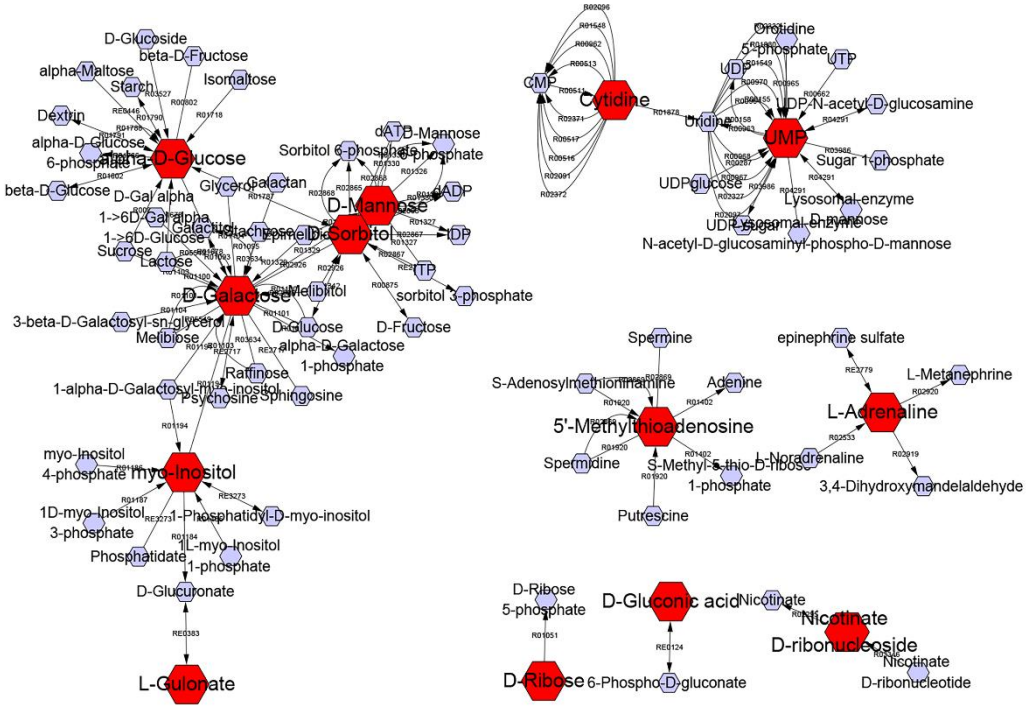

Figure 5.7 Network of the significantly differential metabolites detected in high-dose BPA exposure group.

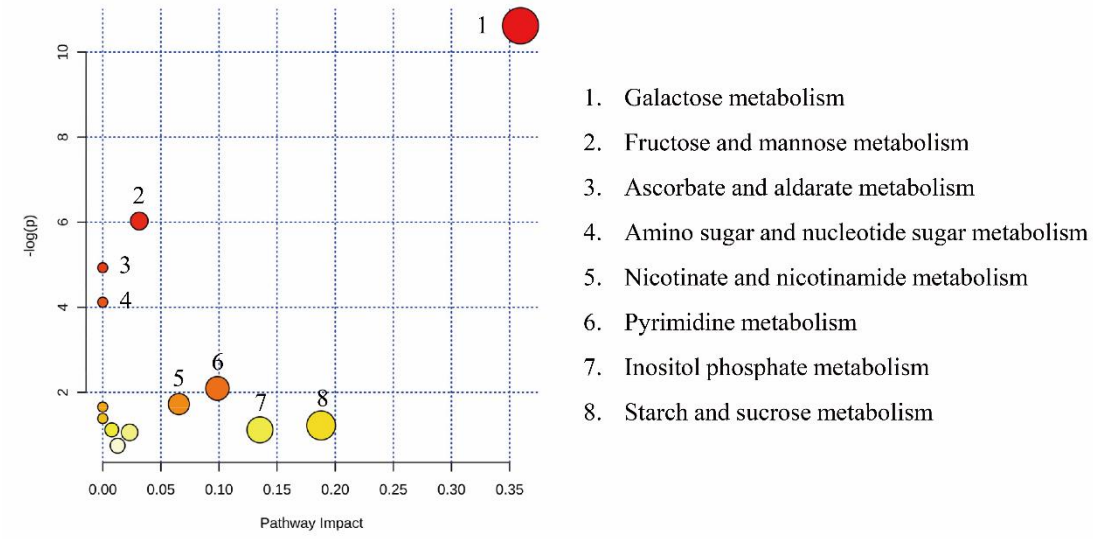

Figure 5.8 Pathway analysis of the BPA toxic effects.

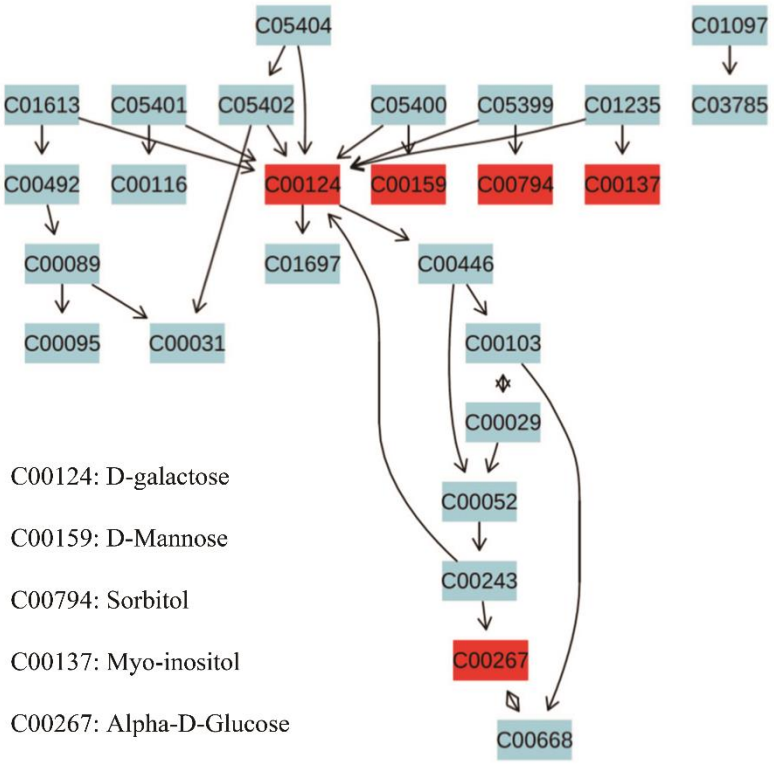

Figure 5.9 Differential metabolites in galactose metabolism pathway affected by BPA.

Except for galactose metabolism, other pathways, for example, amino sugar and nucleotide sugar metabolism, pyrimidine metabolism, nicotinate and nicotinamide metabolism were also affected by BPA (Figure 5.8). The three pathways were closely related to the metabolism of nucleoside and its analogues. In this experiment, nine nucleosides and its analogues were detected, including cytidine, nicotinate D-ribonucleoside, 1-(beta-D-ribofuranosyl)-1,4-dihydronicotinamide, 5,6-dihydrouridine, N^4-acetylcytidine, 5'-deoxy-5'-(methylthio)adenosine, uridine monophosphate, N^6-carbamoyl-L-threonyladenosine and 2-methylthio-N^6-threonylcarbamoyladenosine (Table 5.1). BPA promoted the levels of these ribose-containing substances, which was consistent basically with the previous reports[154, 243]. After treated with BPA, the toxic effects of BPA made rats suffer from excessive oxidant stress, resulting in RNA damage[274]. It accelerated RNA metabolism to form increased levels of nucleosides and its analogues in urine. The pathway analysis made a preliminary impression of effects of BPA administration on *cis*-diol metabolites in rat urine samples. However, the results were adequate to support fully understanding of the toxic effects of BPA. More data are still needed to gain some insight into the toxic mechanism of the endocrine disruptor.

The chemical isotope labeling was often used for relative quantification by comparing the intensities of labeled analytes. This is especially convenient when there are only two groups of samples, because to find one isotope labeling reagent

is fairly easy. However, if the research topic involves in multiple groups of samples, relative quantification with isotope labeling is hard to perform. Since it is not easy to prepare several appropriate isotope labeling reagents at the same time. Therefore, in the study, considering the difficulty of reagent synthesis and cost, only acetone and acetone-d_6 were selected as labeling reagents to react with QC samples. After comparing the mass spectra of light and heavy labeled samples, *cis*-diol signals were recognized and used to build a data set. In the practical samples, by contrasting level changes of signals fallen in the data set, significantly differential *cis*-diol metabolites could be identified. This strategy eased the difficulty level than to prepare multiple isotope labeling reagents. Meanwhile, using equal amounts of reagents to label the same samples could provide more information for signal recognition, i.e., equal intensity of signal pairs between light and heavy labeled samples. This feature offered more evidence to conform the labeled analytes improving the accuracy and efficiency of *cis*-diol metabolite identification.

It should be noticed that the list of significant metabolites found in this chapter was somewhat different from that in Chapter 4. Especially the number of detected nucleosides was smaller in the chapter than in Chapter 4. Probably, the differences were mainly due to technical differences. In Chapter 5, the instrument used for *cis*-diol compounds screening was Q-TOF MS and the scanning mode was full scan. While in Chapter 4, Orbitrap was employed to detect nucleosides and the detection mode was PRM. The latter had better sensitivity and selectivity. So it could detect

more nucleosides. But it could only provide the information of nucleosides. It could not detect other *cis*-diol compounds such as carbohydrates under its used condition. Therefore, in Chapter 5, Q-TOF MS was applied to screen all the ions of the samples with full scan. Although its lower sensitivity resulted in losing some information of low abundance nucleosides, other *cis*-diol compounds (primary carbohydrates) were observed. Each method has its own advantage. Application of them was only according to requirement.

5.4 Chapter summary

In summary, a chemical isotope labeling method was performed to study the effects of BPA exposure on *cis*-diol metabolites. After acetone and acetone-d_6 labeling, chromatographic separation and mass spectrometry detection of *cis*-diol metabolites were improved. By using the method, *cis*-diol metabolites were recognized easily from urine samples. Influence of BPA exposure on these metabolites was investigated by comparing different dose administration on rats. Analytes showed noticeable difference were highlighted. Pathway analysis indicated that galactose metabolism, nucleoside and its analogues metabolism were disturbed by BPA. To our best knowledge, it is the first time to report that BPA could alter galactose metabolism in rats. The obtained results may open a new point for exploring the toxic effects of BPA exposure.

Chapter 6 Strategies for quantitation of ribonucleotides in plasma using in situ derivatization on titania and reversed-phase liquid chromatography-mass spectrometry

6.1 Introduction

Ribonucleotides have distinctive structure which endows them with unique functions and properties. They play key roles in cell regulation, cell signaling, energy metabolism and enzymatic reactions[21,25,26,27]. Because of the great importance of nucleotides in the fields of biochemistry, determination of these metabolites provides valuable information for understanding their function in cellular physical activities. However, there are many challenges for the detection of nucleotides, such as serious matrix interferences, poor retention on reversed-phase columns, in-source fragmentation, and peak tailing causing by interacting with specific parts of the LC–MS setup[275,29,276]. These problems greatly limited the detection of nucleotides. Therefore, efficient sample pre-treatment, completely chromatographic separation and high sensitive, high selective detections technologies are necessary for the analysis of these compounds.

A variety of sample preparation and detection techniques have been developed to analyze nucleotides. For sample preparation, Solid-phase extraction (SPE), strong Anion Exchange (SAX) SPE, combined phenol-chloroform LLE and ion-pair reverse phase SPE, or weak anion exchange (WAX) SPE[34,33,31,32,35]. However, the limitation of the methods was that it was poor selectivity, low recoveries, laborious

and time-consuming to perform multiple extraction and sample transfer steps, and fairly high cost for per sample. Therefore, a rapid, high efficient method for sample pre-treatment is still a major bottleneck for extracting nucleotides with good reproducibility and recovery. For chromatographic separation, methods included RPLC with UV detection by adding phosphate buffer to the mobile phases[36], strong anion exchange (SAX) columns combined with high concentrations of non-volatile salt buffer[37], LC-MS/MS with volatile ion-pairing agents as mobile phase[40,41]. Although the methods could achieve good separation for nucleotides, the incompatibility of the mobile phase or persistent residues ion-pair agents caused contamination of the mass spectrometer, resulting in significant signal suppression and requiring frequent cleanings of ionization source[42,43]. Therefore, a suitable LC-MS method is eager for sensitive and selective detection of nucleotides under acceptable chromatographic condition with low concentration and volatile buffer salts, but without using ion-pairing agents.

Titania (TiO_2, also known as titanium dioxide) is an amphoteric compound. It has great mechanical strength and chemical stability, as well as excellent resistance to acid and alkali (pH 1~14)[277]. It acts as an anion exchanger at low pH and a cation exchanger at high pH[278]. It means that it can be used as a Lewis acid or a Lewis base. It showed ion-exchange and ligand-exchange properties to charged compounds. In particular, it plays a selective adsorption role with respect to phosphate compounds such as phosphorylated proteins and peptides, nucleic acids

and its intermediates, phospholipids, etc[279, 280]. So as a new separated medium, TiO_2 has a good application prospect. In recent years, TiO_2 has been widely applied in the study of posttranslational modification of proteins. It was often used to selectively enrich and extract phosphorylated proteins and peptides in biological samples[281]. However, publications were very limited about the utilization of the material on small molecules containing phosphate groups, such as nucleotides[282]. Due to the huge potential of TiO_2 in phosphorylated compounds adsorption, it is very feasible to employ this material to selectively extract nucleotides from a complex biometrics. After extraction, considering the high polarity of nucleotides, derivatization could be performed to the targeted compound to improve their retention on reversed-phase columns.

Therefore, in this study, TiO_2 was used as packing materials to prepare micro-columns for the selective adsorption metabolites containing phosphate groups. Then, in situ derivatization was performed on the surface of TiO_2. Reaction products were analyzed by using reversed-phase liquid chromatography-mass spectrometry. The method was applied to measure twelve ribonucleotides in plasma of rats exposed to BPA.

6.2 Material and methods

6.2.1 Chemicals and materials

HPLC grade methanol (MeOH) and acetonitrile (ACN) were obtained from Merck (Dermstadt, Germany). Bisphenol A (BPA) was purchased from J&K Scientific Ltd.

(Beijing, China). Fetal bovine serum (FBS) was obtained from Gibco (Thermo Fisher Scientific). The following compounds were purchased from Sigma-Aldrich (St. Louis, MO, USA): 1,1-Dimethoxycyclohexane (DMCH, 99%), formic acid (FA, HPLC grade), 70% perchloric acid ($HClO_4$), trifluoroacetic acid (TFA), ammonium bicarbonate (> 99%), ammonium hydroxide solution (28% NH_3 in H_2O, ≥ 99.99%), adenosine 5'-triphosphate disodium salt hydrate (ATP, 99%), adenosine 5'-diphosphate sodium salt (ADP, ≥ 95%), adenosine 5'-monophosphate sodium salt (AMP, ≥ 99%), guanosine 5'-triphosphate sodium salt hydrate (GTP, ≥ 95%), guanosine 5'-diphosphate sodium salt (GDP, ≥ 96%), guanosine 5'-monophosphate disodium salt hydrate (GMP, ≥ 99%), cytidine 5'-triphosphate disodium salt (CTP, ≥ 95%), cytidine 5'-diphosphocholine sodium salt dehydrate (CDP, ~98%), cytidine 5'-monophosphate disodium salt (CMP, ≥ 99%), uridine 5'-triphosphate trisodium salt hydrate (UTP, ≥ 96%), uridine 5'-diphosphoglucuronic acid trisodium salt (UDP, 98-100%), uridine 5'-monophosphate disodium salt (UMP, ≥ 99%). Internal standard (IS) was adenosine-$^{15}N_5$ 5'-diphosphate sodium salt (98 atom % ^{15}N, 90%, ADP-$^{15}N_5$). Water was purified by using a Milli-Q system (Millipore, Milford, MA).

TiO_2 beads were obtained from GL sciences Inc. (Cat.No.: 5020-75010, 10 μm). Hydropholic UHMW-PE frits were provided by Biocomma (Cat.No.: BF066-16-02, diameter 6.6 mm, thickness 1.6 mm, pore size 5 μm, Shenzhen, China). Pipette tips (200 μL, yellow color) were obtained from Brand (Germary).

Composition of working solution were as follow: Loading solution: 25% H_2O, 75% ACN and 5% FA. Washing solution 1: 50% H_2O, 50% ACN and 2% FA. Washing solution 2: H_2O contained 5% MeOH. Eluting solution: H_2O contained 10% MeOH and 10 mM NH_4HCO_3 (pH = 10.5).

6.2.2 Preparation of packed TiO_2 micro-columns

The schematic of micro-columns preparation was shown in Figure 6.1. The UHMW-PE frits were cut into about 0.5 mm pieces. The pieces were put at the cusp of the 200 μL pipette tip as a filter. TiO_2 beads were stirred and suspended at ACN/H_2O (80/20, V/V) with a final concentration of 10 mg mL^{-1}. 200 μL of the suspension was then loaded to the tip (about 2 mg TiO_2 per tip). After 30 minutes' standing, the packed tips were centrifuged at 1,000 × *g* for 3 min. Then 100 μL ACN/H_2O (80/20, V/V) was added to the tips. After rotating the tips 180 degrees, the packed tips were centrifuged at 1,000 × *g* for 3 min once again. This process was repeated for 3 times to compress TiO_2 beads. The obtained TiO_2 micro-columns were activated by washing them with 200 μL 1 M NaOH and 200 μL 1 M HCl and 200 μL Loading solution**.** The activated micro-columns were used for method optimization and sample preparation.

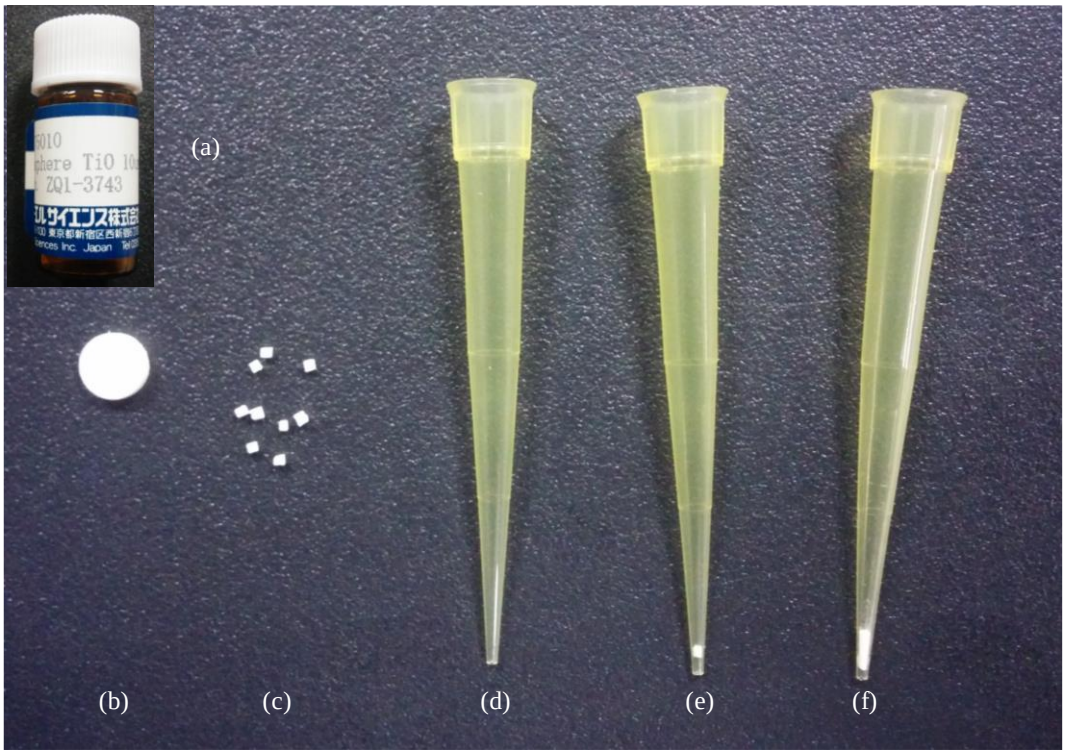

Figure 6.1 The schematic of micro-columns preparation. (a) TiO_2 beads. (b) UHMW-PE frits. (c) Pieces of the frits. (d) 200 μL pipette tip. (e) A tip with a filter at the cusp. (d) Packed tips with TiO_2.

6.2.3 Optimization of the loading and eluting conditions

Both the loading and eluting conditions were optimized, respectively. An AMP solution at a concentration of 5 μM was chosen as the test solution. When optimizing the loading conditions, FA was added to the AMP solution to adjust the pH values. The test solution (100 μL) was loaded to the micro-columns. The micro-column was centrifuged at 1,000 × *g* for 20 min, and then rinsed with 100 μL of washing solution 1 and 100 μL of washing solution 2 via centrifuging at 3,000 × *g* for 10 min. After that, the micro-columns were eluted with 100 μL of Eluting

solution via centrifuging at 1,000 × g for 20 min. When optimizing the eluting conditions, the micro-columns which had adsorbed AMP under the optimized loading condition were eluted with different volume of Eluting solution. All the eluates were analyzed by ultraviolet detection at 260 nm.

6.2.4 Selectivity evaluation of the micro-columns

The model solution used to evaluate the selectivity of the tip micro-columns contained 5 μM AMP, A and 5% FA. A was used as interfering structural analogue and its concentration was 0.1, 1.0, 10 and 100 times of AMP. The model solution (100 μL of each) was loaded the micro-column and rinsed with 100 μL of washing solution 1 and 100 μL of washing solution 2, respectively. Then it was eluted with 100 μL of eluting solution. The eluates were analyzed by ultraviolet detection at 260 nm.

6.2.5 Adsorption capacity evaluation of the micro-columns

The solution contained 0.5, 1.0, 5.0, 10, 50, 100, 500, 1000, 2000 μM of AMP and 5% FA was used as the model to evaluate the adsorption capacity of the tip micro-columns. The solution (100 μL of each) was loaded to the micro-column and rinsed with 100 μL of washing solution 1 and 100 μL of washing solution 2, respectively. Then it was eluted with 100 μL of eluting solution. The eluates were diluted by 10 times and detected by ultraviolet detection at 260 nm.

6.2.6 Optimization of the derivatization conditions

The solution included AMP (or ADP or ATP) at concentrations of 5 μM was used as the model to optimize the in situ derivatization conditions on the tip micro-columns. The nucleotides were loaded to the micro-columns and washed with 100 μL of washing solution 1 and 100 μL of washing solution 2, respectively. Then 100 μL of ACN was used to carry the water away on the micro-columns. Derivatization reagents which contained DMCH and FA were added to block the *cis*-diol groups of the nucleotides. The residual derivatization reagents were washed with 100 μL ACN. The residual ACN was washed with 100 μL washing solution 2. The nucleotides were eluted with 100 μL eluting solution. The released nucleotides were detected by ultraviolet detection at 260 nm. The ratios of DMCH/FA and the volume of derivatization reagents were optimized. When optimizing the ratios of DMCH/FA, 0.2 mL of derivatization reagents were used. Based on the obtained ratio, the volume of derivatization reagents was optimized.

6.2.7 Preparation of calibration standards and QC solutions

The stock solution contained 12 ribonucleotides. It was prepared as follows: first, pipetted all of the standard solutions (10 mg mL^{-1}), each 100 μL, and transferred them into a centrifuge tube (total volume 1.2 mL for 12 compounds), and then adding 0.8 mL water to the tube to obtain a concentration of 50 μg mL^{-1} for each compound. FBS was used as matrix and was spiked with the stock solution of ribonucleotides to achieve the following calibration standard concentrations: 0.050,

0.10, 0.50, 1.0, 5.0 and 10 μg mL^{-1}. Quality control (QC) samples, with the concentration of 0.10, 1.0, and 10 μg mL^{-1}, were also prepared in the same way and were run in each assay.

6.2.8 Sample preparation

0.05 mL of IS was pooled into 0.05 mL of calibration standard or QC solutions. 0.3 mL ACN and 0.02 mL FA was added to the sample. Then, the sample was vigorous vortex for 30 s and centrifuged at 12,000 × *g* for 10 min at 4 °C to remove the precipitation. The supernatant was loaded to the activated micro-columns. After washing with 0.2 mL of washing solution 2, the micro-columns were washed with 0.2 mL ACN to carry the water away. 0.2 mL DMHC/FA (1:1, V/V) was used as derivatization reagents to block the *cis*-diol groups of the nucleotides. The residual derivatization reagents were washed with 0.2 mL ACN. The residual ACN was washed with 0.2 mL washing solution 2. The nucleotides were eluted with 0.06 mL eluting solution 1 for three times**.** The eluates were combined and centrifuged at 12,000 × g for 10 min at 4 °C to remove any possible particles. The supernatant was analyzed by liquid chromatography–mass spectrometry (LC-MS).

6.2.9 Method validation

Quantitative analysis of 12 ribonucleotides was performed to validate the method. Calibration of the method was performed by analyzing the derivate working solutions to establish calibration curves. The limit of detection (LOD) and limit of quantification (LOQ) of this method were defined as the concentration where the

signal-to-noise ratio of one peak was 3 and 10, respectively. Recoveries of all the ribonucleotides were evaluated by analyzing QC samples. Stability of four nucleoside derivatives were evaluated by analyzing the QC samples in five replicate runs. The intra-day stability was performed with a 4 h interval in the same day. And inter-day stability was determined after the samples were stored at −20 °C for 72 h.

6.2.10 Detection of nucleotides in plasma of rats exposed to BPA

Twenty female Sprague-Dawley rats (180-220 g) were used as model animals. They were housed in a standard animal facility as described previously. Briefly, rats were randomly and equally divided into four groups as control, and low, middle and high dose BPA-exposed groups (referred to as simply control, BPAL, BPAM and BPAH groups). The four groups of rats were administered 0, 10, 30 and 50 mg BPA/kg body weight (in corn oil) per day, respectively. After four days' BPA exposure, rats were sacrificed. The blood samples were collected and centrifuged at 2500 × g for 10 min (4 °C). The plasma samples (supernatants) were used for nucleotides analysis. The samples were prepared as the same as the calibration standard and QC solutions.

6.2.11 Ultra-performance liquid chromatography

Waters ACQUITY UPLC system coupled with a Waters Acquity™ BEH C_{18} column (50 mm × 2.1 mm, 1.7 μm) was applied for chromatographic separation. The mobile phases were water containing 10 mM NH_4HCO_3 at pH = 10.5 (A) and methanol (B). Linearity gradient elution program was as follow: increased from 10%

B to 15% within 1.5 min, then to 25% within 2.5 min, following increasing to 95% within 2.5 min, then returned to 10% within 0.3 min and held for 3.2 min. Total running time was 10 min. The flow rate was 0.30 mL min^{-1}. The column temperature was set at 30 °C for all analyses. Injection volume was 10 μL. For method optimization, samples were analyzed by an ACQUITY UPLC Photodiode Array (PDA) Detector at 260 nm.

6.2.12 Mass spectrometry

Ribonucleotides quantitation was performed by employing a Waters TQ detector (Waters, Manchester, UK) equipped with an electrospray ion source (ESI). Data was acquired in positive ion mode and in multiple reaction monitoring (MRM) scanning mode. The capillary voltage was set at 3.00 kV. Ion source temperature and desolvation gas temperature were 130 °C and 450 °C, respectively. Desolvation gas flow was 1000 L h^{-1}. Cone gas flow was 150 L h^{-1}. Dwell time was 0.05 s. The precursor to product ion transitions, cone voltage, and collision energy for each analyte were listed in Table 6.1. Waters QuanLynx software was used for data processing, using peak area ratio (compared to IS) for quantification.

Table 6.1 Ion transitions for MRM scan of ribonucleotide derivatives and IS.

Ribonucleotides	Abbreviation	Parent ion	Daughter ions	Cone (V)	Collision Energy
Adenosine nucleotides	AMP	428	136	30	30

	ADP	508	136	30	30
	ATP	588	136	30	40
Guanosine nucleotides	GMP	444	152	30	25
	GDP	524	152	30	25
	GTP	604	152	30	30
Cytidine nucleotides	CMP	404	112	30	20
	CDP	484	112	30	20
	CTP	564	112	35	20
Uridine nucleotides	UMP	405	177	30	25
	UDP	485	177	30	25
	UTP	565	177	35	35
Internal standards	ADP-$^{15}N_5$	513	141	30	30

6.3 Results and discussion

6.3.1 Performance evaluation of micro-columns

TiO_2 is a common amphoteric metal oxide. It is a Lewis base under acidic conditions while Lewis acid under alkaline conditions. Under acid condition, it can form reversible complexes of five or six-membered cyclic esters with the hydroxyl of phosphate groups, and the complexes could be dissociated if the conditions are switched to alkaline[283]. Therefore, the pH value would greatly affect the

performance of TiO_2. For the best performance, both the loading and eluting conditions were optimized for maximize efficiencies of extraction with TiO_2 packing micro-columns. Different proportion of FA in the loading solutions were tested. It was found that when the proportion of FA was greater than 3%, the adsorption ability of the micro-columns was the best and the adsorptive rate reached 99.0% (Figure 6.2). Considering the complexity of biological samples, in particular, plasma samples showed buffer capacity, 5% FA was chosen to ensure that the loading solution had enough acidity. In the process of elution, the eluent containing 5% methanol and 10 mM NH_4HCO_3 in water (pH = 10.5) was used, rather than common eluent containing ammonia. This purpose was to make the composition of elution consistent with the initial mobile phase, which could be directly injected for LC-MS analysis. Several eluting modes were compared. It was found that when the micro-columns were eluted with 60 μL eluting solution for 3 times, more than 98% targeted compounds could be recovered (Figure 6.3). When the volume of eluting solution was larger than 60 μL (80 or 100 μL), the recoveries were equivalents. To minimize the volume of eluting solution, the mode, i.e., eluting with 60 μL eluting solution for 3 times was selected. As a result, the optimal loading condition was the sample solution containing 5% FA. And the targeted compounds were eluted from the micro-columns with 60 μL eluting solution for 3 times.

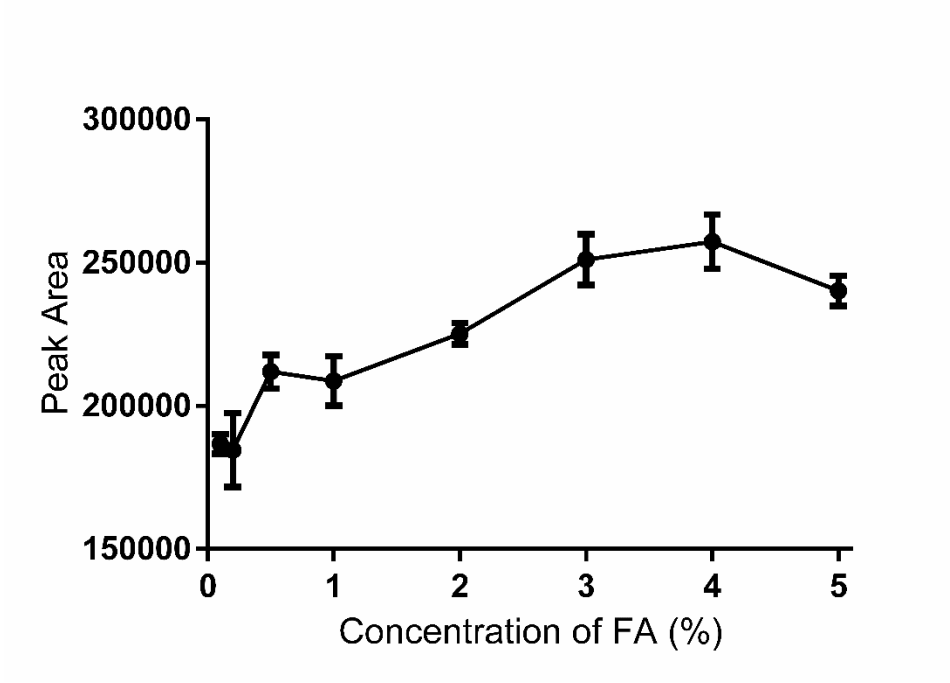

Figure 6.2 The effect of formic acid concentration on the micro-column adsorption.

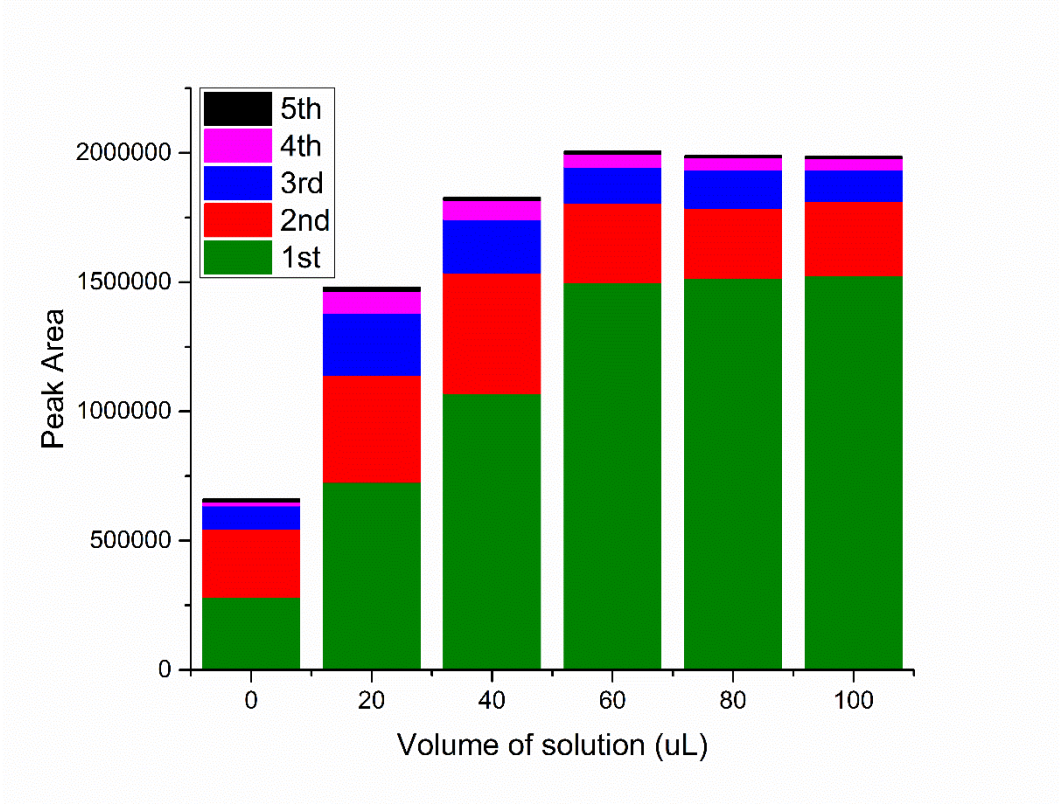

Figure 6.3 The effect of eluting models on the micro-column desorption.

Under such conditions, the adsorption capacity of TiO_2 material was evaluated by using AMP as model solution. The results showed that the maximum adsorption capacity was 363 μM AMP per milligram TiO_2 (Figure 6.4). To study the specificity of TiO_2 materials for phosphorylated compounds, solutions contained AMP and its interfering structural analogue, adenosine, were treated with micro-columns. Results showed that under different disturbance, TiO_2 revealed high affinity to AMP, even the concentration of interferent up to 100 times (Figure 6.5). It illustrated that TiO_2 had very high selectivity for the extraction of phosphorylated compounds. It could be applied to isolate nucleotides from the complex plasma samples.

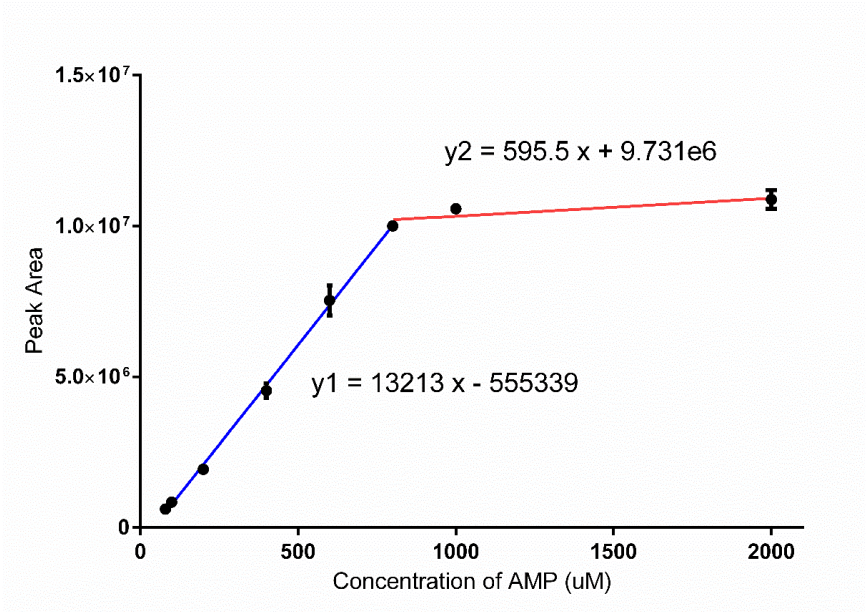

Figure 6.4 The evaluation of adsorption capacity of the micro-column.

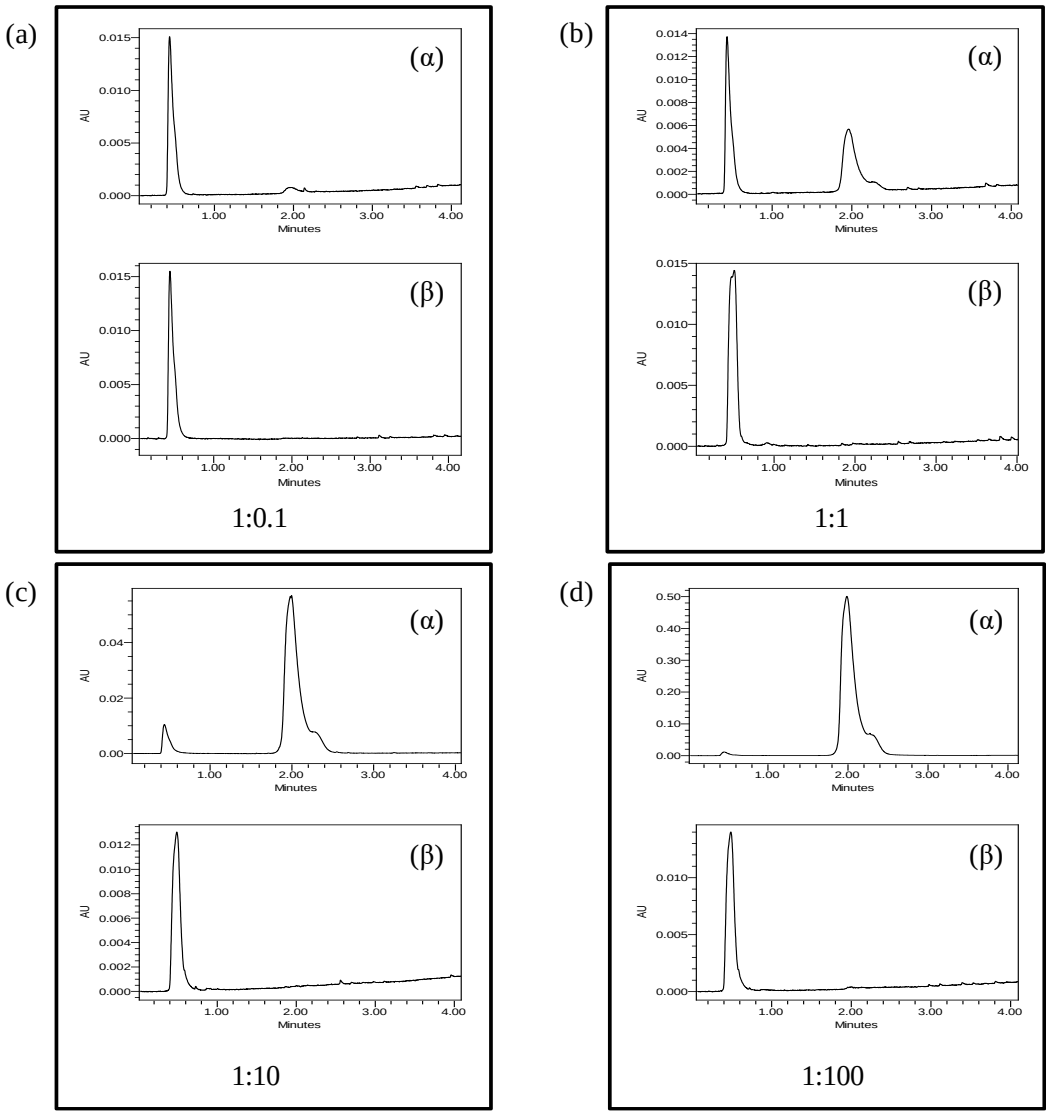

Figure 6.5 Chromatograms of the mixture of adenosine monophosphate and the interfering molecule, adenosine. Analyzed (α) directly and (β) after enrichment by the micro-column with molar ratios of 1:0.1, 1:1, 1:10 and 1:100.

6.3.2 Evaluation of in situ derivatization on TiO_2

TiO_2 material adsorbed ribonucleotides via affinity of phosphate groups. The *cis*-diol groups of the ribonucleotides were free. Therefore, they could be derived through chemical reaction. In this experiment, DMCH was chosen as derivatization

reagent and FA as catalyst. Because it was an exothermic reaction, low temperature was propitious to promote the reaction. Therefore, in the whole process of sample preparation, the temperature was set to 4 °C. AMP was used as a model compound to optimize the dosage of derivatization reagent and catalyst. The results showed that when the volume ratio of DMCH and FA was 1.5:1, and the dosage of FA/DMCH was 200 μL, the derived results were the best. More than 90.0% of the AMP was converted to the corresponding derivative product (Figure 6.6).

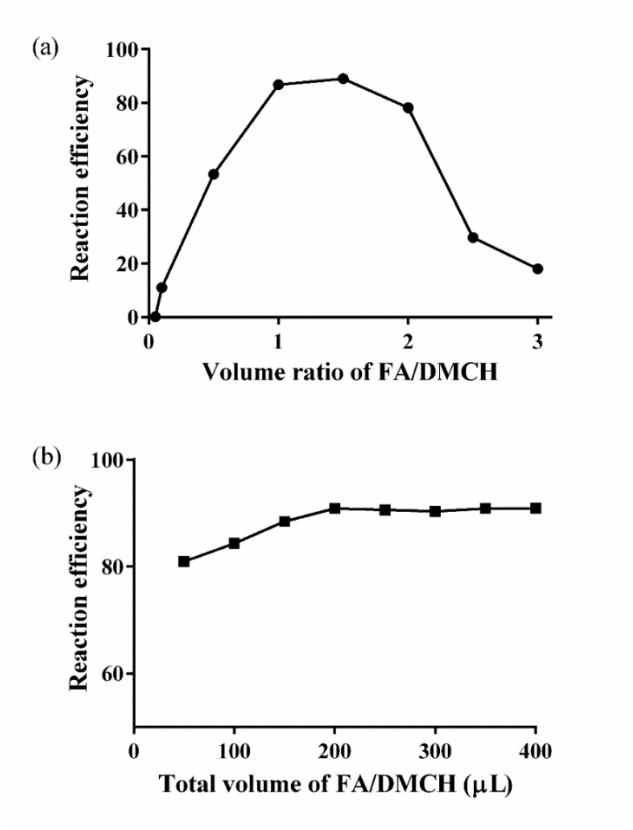

Figure 6.6 Optimization of in situ derivatization conditions. (a) Volume ratio of formic acid (FA) and 1,1-Dimethoxycyclohexane (DMCH). (b) Total volume of FA/DMCH with a ratio of 1.5:1.

The catalyst used in the reaction was a moderate acid, but not strong acids such like perchloric acid, hydrochloric acid or sulfuric acid which were commonly applied in similar reaction in organic synthesis[284]. This mild reaction condition could avoid the degradation of the instability nucleotides. It was manifested as no other by-products were generated in the reaction, i.e., a single product peak in the chromatogram (Figure 6.7). The reaction product was confirmed by high resolution mass spectrometry. The results showed that detected molecular weight was 428.1331, which was accorded with the theoretical value and the fragment ions were also matched (Figure 6.8). Similarly, the reaction efficiency of ATP, ADP and other ribonucleotides with different base was also higher than 90.0%, which was better than the same reactions in organic synthesis[285]. In addition, by comparing the AMP and dAMP, it was found that only AMP could react with DMCH but dAMP could not. That means the reaction was selective to *cis*-diol-containing compounds. Accordingly, ribonucleotides could be isolated from deoxyribonucleotides.

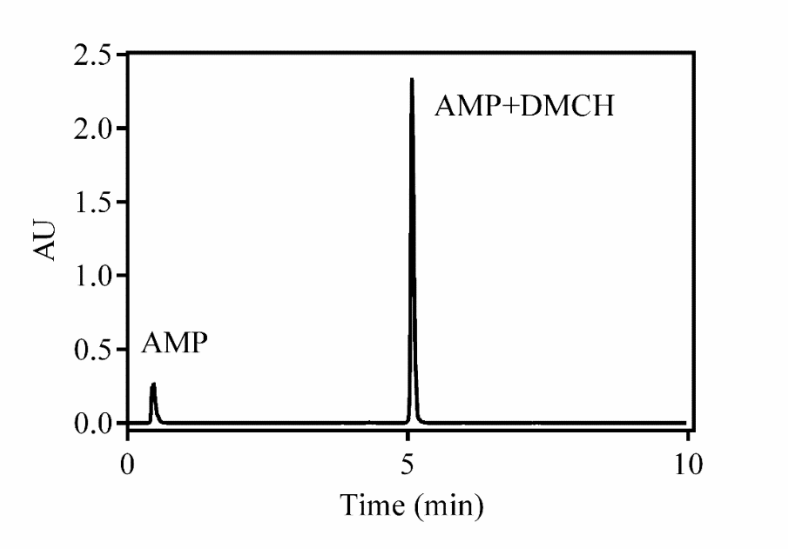

Figure 6.7 Chromatogram of AMP reacted with DMCH.

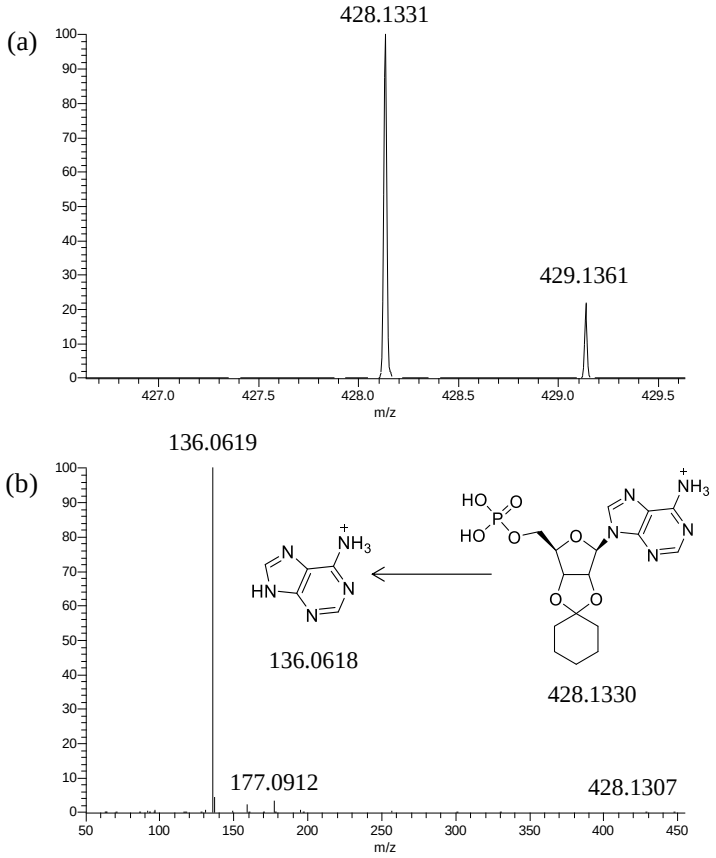

Figure 6.8 High resolution MS (a) and MS/MS (b) spectra of derivatization product of AMP with DMCH.

6.3.3 Evaluation of recoveries

Further, the method was validated through quantitative analysis of 12 nucleotides. In the linearity study, All the correlation coefficients for the analyte were greater than 0.98, which indicated acceptable linearity (Table 6.2). The LOD of this method ranged from 0.0012 to 0.072 μg mL^{-1} and LOQ from 0.0033 to 0.22 μg mL^{-1}. The results demonstrated that the method was sensitive enough for nucleotide detection. The recoveries of the compounds were ranged from 87.4 to 94.4%. These values were consistent with the derivatization reaction efficiency as mentioned above. This suggested that the loss of the recoveries should be attributed to the incomplete derivative reaction. In the other sample preparation steps, i.e., adsorption, washing and elution processes, nucleotides adsorbed on the surface of the TiO_2 gave no significant loss. The results indicated that the assay was reproducible and robust. It could be employed to determine ribonucleotides in plasma samples.

Table 6.2 Validation of the derivatization method.

Compound	Cure	r^2	LOQ (μg mL^{-1})	LOD (μg mL^{-1})	Recovery	
					Mean (%)	RSD (%)
AMP+DMCH	y=0.9247x-0.1098	0.9916	0.0033	0.0012	90.2	3.3
ADP+DMCH	y=1.1276x-3.551	0.9842	0.071	0.025	92.3	6.7

ATP+DMCH	y=0.9989x-5.262	0.9927	0.18	0.053	91.5	10.5
GMP + DMCH	y=0.9506x-1.107	0.9917	0.0046	0.0017	91.0	9.5
GDP+DMCH	y=1.264x-5.068	0.9869	0.12	0.055	94.4	5.8
GTP+DMCH	y=1.103x-5.951	0.9901	0.20	0.065	92.0	6.1
UMP+DMCH	y=0.9274x-2.603	0.9909	0.0091	0.0033	88.9	2.9
UDP+DMCH	y=1.152x-5.356	0.9878	0.13	0.047	89.8	4.3
UTP+DMCH	y=0.9880x-6.083	0.9904	0.22	0.066	90.5	7.0
CMP+DMCH	y=0.9263x-0.9141	0.9958	0.0047	0.014	87.4	3.3
CDP+DMCH	y=1.619x-4.191	0.9962	0.15	0.072	89.2	7.1
CTP+DMCH	y=0.89993x-4.156	0.9845	0.085	0.022	88.5	8.0

r^2: Correlation coefficient.

6.3.4 Evaluation of chromatographic separation and MS detection

When analyzing nucleotides with LC-MS, in-source fragmentation of these compounds required baseline separation to avoid mutual interference. But separation with reversed-phase LC faced great challenges duo to their high polarity. As illustrated in Figure 6.9, all the peaks of nucleotides were overlapped, forming a broad peak at early time point of the chromatogram. It displayed the poor retention of these compounds. By introducing a nonpolar group into the molecule, the

polarity of nucleotides decreased, leading to better retention on reversed-phase columns. Although baseline separation of all the nucleotides was not yet realized, completely separation of nucleotides with the same base was achieved as showed in Figure 6.10. And based on the high selectivity of MRM mode, nucleotides contained different bases did not interfere with each other. Under this situation, in-source fragmentation would not affect the quantitation of these compounds.

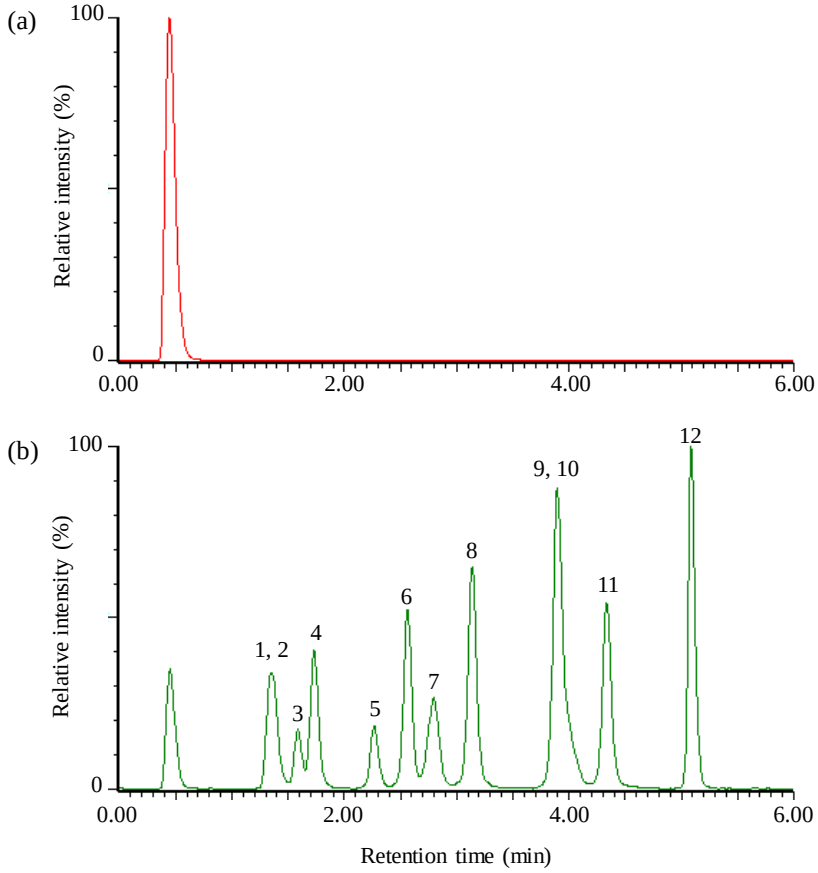

Figure 6.9 Chromatograms of ribonucleotides (a) and their derivatization products with DMCH (b). Compounds: 1-CTP, 2-UTP, 3-UDP, 4-CDP, 5-UTP, 6-CTP, 7-GTP, 8-GDP, 9-GMP, 10-ATP, 11-ADP and 12-AMP.

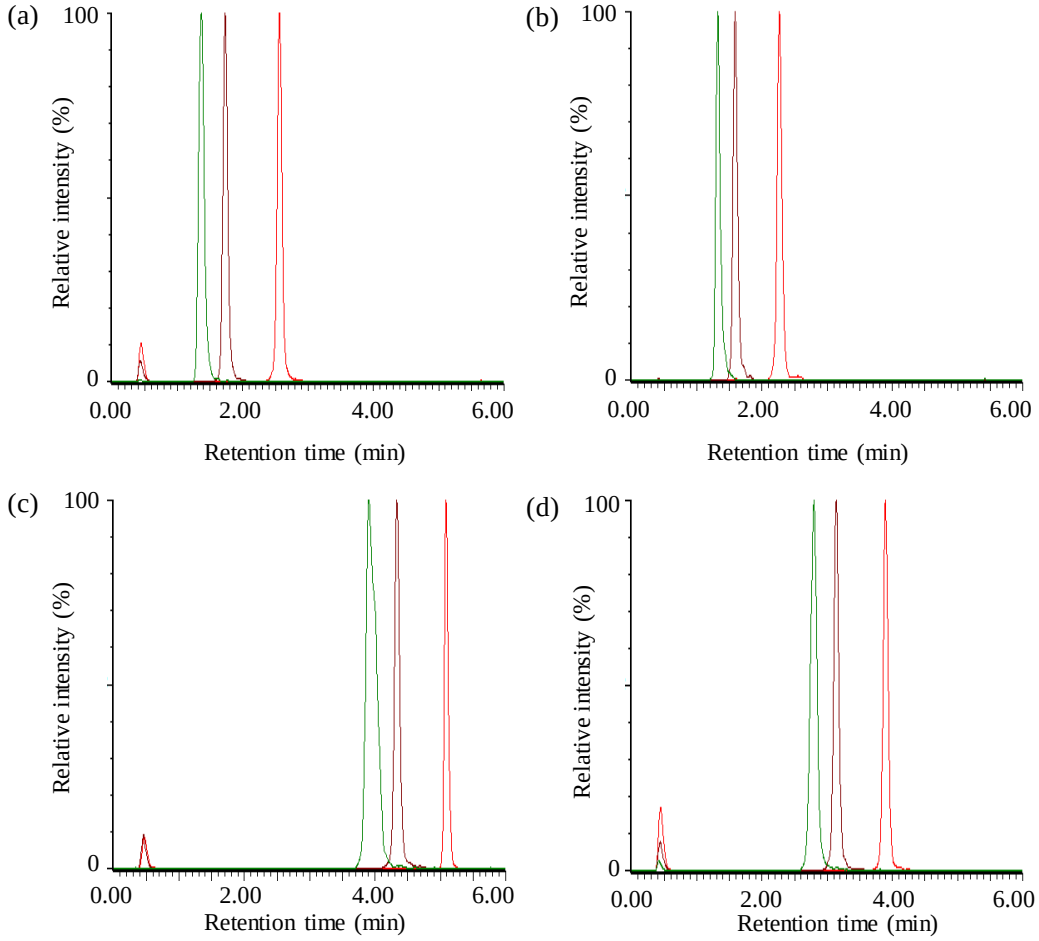

Figure 6.10 Chromatograms of ribonucleotides with the same base. (a) Cytidine nucleotides, (b) uridine nucleotides, (c) adenosine nucleotides and (d) guanosine nucleotides.

The pH values of mobile phase had great effect on the chromatographic separation. As shown in Figure 6.11(a), peak tailing was serious when the mobile phase was acidic. To settle the problem, high pH mobile phase was employed for gradient elution. As the pH increased, tailing was eliminated. When the pH was 10.5, sharp and symmetric peaks were observed for each nucleotide (Figure 6.11(c)). In

addition, comparing the chromatograms obtained with different pH mobile phase, it was found that the higher the pH, the better peak intensities. It meant that improvement of peak shape could enhance the detection sensitivity. It could help reduce the demand for sample size.

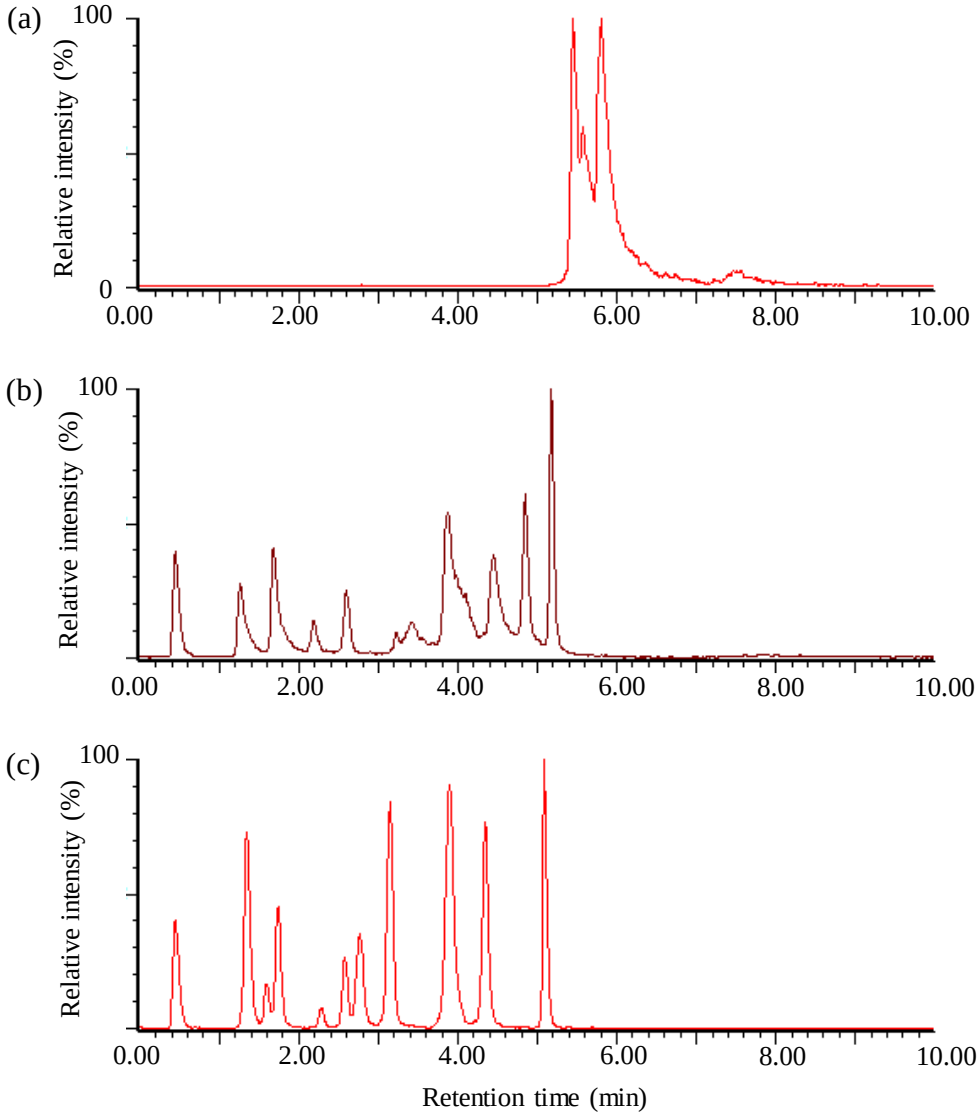

Figure 6.11 Separation of ribonucleotide derivatization products with mobile phase at pH 3.0 (a), 8.7 (b) and 10.5 (c).

The improvement of chromatographic separation was also contributed to MS detection. After derivatization, longer retention time of ribonucleotides could make them stagger the interference from other polar metabolites, which were eluted at the forepart of gradient, such as deoxyribonucleotides. This could reduce matrix effects. In addition, in the mid and latter stages of the gradient, high proportion of organic solvent in mobile phase may enhance ionization efficiency of the analyte. Moreover, comparing the chromatograms obtained with different pH mobile phase, it was found that the higher the pH, the better peak intensities. It meant that improvement of peak shape could also enhance the detection sensitivity. Based upon the interaction of all of these factors, the sensitivity of mass spectrometry could be improved.

6.3.5 Quantification of ribonucleotides in plasma samples of rats exposed to BPA

The method was applied to quantify ribonucleotides in plasma samples of rats exposed to BPA. Table 6.3 showed that BPA administration had some effects on these metabolites. Especially, compounds of AMP, ATP and CDP showed significant decrease in BPAH group compared to control group. This showed that BPA exposure altered the energy charge in rats, resulting in disorder of energy metabolism. It also suggested that BPA was an energy balance disruptor, which was consistent with previous reports.[286]

The concentration variations of a given nucleotide within a group were a little large. It might be due to individual differences. The effects of BPA exposure might have different effects on the energy metabolism of rats. Even the dose of BPA was the same, each rat might display different response to the hormone disruptor. The factor made the concentration variations of a given nucleotide large within a group.

Table 6.3 Concentrations of nucleotides in control and BPA-treated rat plasma.

Compound	Control	BPAL	BPAM	BPAH
AMP	27.85 ± 6.65	28.33 ± 14.78	20.38 ± 6.21	18.43 ± 3.84*
ADP	59.32 ± 32.24	53.87 ± 22.49	50.68 ± 15.42	46.86 ± 18.88
ATP	382.41 ± 108.49	291.95 ± 132.53	363.07 ± 171.51	177.85 ± 26.76*
GMP	4.57 ± 1.81	4.06 ± 1.76	3.68 ± 1.14	3.91 ± 1.20
GDP	9.31 ± 4.35	7.87 ± 4.32	6.34 ± 2.45	6.00 ± 2.46
GTP	68.25 ± 64.03	50.86 ± 29.75	66.33 ± 30.95	30.08 ± 20.51
CMP	20.30 ± 10.88	39.48 ± 18.95	14.50 ± 2.36	28.35 ± 7.93
CDP	4.47 ± 0.97	3.62 ± 2.01	3.24 ± 1.49	1.90 ± 1.10*
CTP	29.15 ± 20.05	16.67 ± 12.55	21.84 ± 19.49	26.50 ± 15.98
UMP	7.09 ± 5.71	4.88 ± 3.85	4.41 ± 1.94	4.35 ± 3.89
UDP	3.57 ± 0.98	3.60 ± 2.55	2.81 ± 1.56	4.03 ± 3.30

UTP	18.02 ± 12.00	15.61 ± 12.47	12.22 ± 5.61	16.20 ± 6.43

*$p < 0.05$. *p*-value of t-test obtained by comparing BPA treated groups with control.

Concentration unit: μM.

Five biological replicate samples were used for each group.

6.3.6 Discussion

The phosphate and *cis*-diol groups of ribonucleotides are the key factors that affect their retention on reversed-phase columns. Therefore, it should focus on the two factors to develop methods for the improvement of chromatographic separation of nucleotides. First, based on the features that TiO_2 could selectively adsorb phosphorylated compounds, the nucleotides were extracted from the complex matrixes. Then the mobile phase was adjusted to high pH value. Under the condition, the phosphate groups were ionized, reducing their interactions with LC-MS system. For the *cis*-diol groups, it was protected via derivatization with DMCH. Due to the selectivity of the reaction, ribonucleotides and deoxyribonucleotides were distinguished. At the same time, the reaction induced a nonpolar group to the ribonucleotides to block the *cis*-diol groups. It also reduced the interaction of the hydroxyl groups with LC-MS system, avoiding peak tailing, spreading and bifurcation. Meanwhile, introducing of the nonpolar groups enhanced the retention of ribonucleotides on reversed-phase columns. Therefore, ribonucleotides with the same base could reach baseline separation, avoiding interference caused by in-

source fragmentation. It enhanced the accuracy of the qualitative and quantitative analysis. The improvement of retention and peak shape could increase the sensitivity of mass spectrometry and reduce the demand for sample size.

In addition, TiO_2 extraction combined with derivatization made the sample processing simple and easy to carry out. The TiO_2 material was manufactured in micro-columns, which could be used for small amount samples. It was very practical for cells, blood, tissues and other samples which were difficult to collect. In addition, by using micro-columns, batch operation was probably preferable. So it was convenient to test large numbers of samples simultaneously.

The micro-columns also provided an appropriate venue for derivatization reaction. To keep anhydrous conditions was the most important factor for the reaction. In general cases, the water in samples should be freeze-dried with lyophilizers or dried under nitrogen. This was very time-consuming. In addition, the derivatization reagents and catalysts also needed to be separated from the reaction products to ensure compatibility with LC-MS systems. Usually, it required steps of neutralization, desalination, drying and redissolving, which were inconvenient and time consumption, too. In this approach, however, TiO_2 could firmly adsorbed phosphorylated compounds, even in organic solvent. Therefore, the water in samples could be carried off by using acetonitrile to wash the micro-columns, creating a non-water environment for the derivatization reaction. Similarly, after the reaction, derivatization reagents and catalysts were taken away by acetonitrile,

without needing neutralization, desalination and drying. It greatly simplified the process of operation steps. Moreover, phosphorylated compounds could be adsorbed by the TiO_2 in the acidic medium. And the derivatization was a typical acid catalyst reaction. That is to say, during the derivatization, the targeted analyte could retain on the surface of the TiO_2 material, but not be released to the solvent, avoiding decreasing of recoveries. And finally, reaction products were eluted with alkaline elution solution, in which the products were stable. The comprehensive effect of these factors made the selective extraction and derivatization reaction be conducted on the same carrier. It ensured the operability and the processing speed while maintaining selectivity and stability for the extraction of ribonucleotides.

6.4 Chapter summary

In short, a quantitative method of nucleotides was established in this article. Tip micro-columns were prepared with TiO_2. The micro-columns were used for selective adsorption of the nucleotides in the plasma. Then in-situ derivatization were carried out to change the polarity of targeted compounds, following with LC-MS analysis of the derivative products without using ion-pairing reagents. This method exhibited a high selectivity for the extraction of nucleotides. After derivatization, retention of nucleotides on reversed-phase C_{18} column was improved. Complete separation of nucleotides with the same base was achieved. The peak shape was symmetrical and the tailing was eliminated by using high pH mobile phase. The method settled the problems of nucleotide detection, which were

poor retention, trailing, in-source fragmentation and contamination of ion-pairing reagents. The quantitative method was successfully applied to determine the content of ribonucleotides in rats' plasma exposed to BPA. It was simple and fast, as well as good selectivity and stability. It could be extended to detection of other phosphorylated metabolites with similar structure.

Chapter 7 Conclusions and Future Studies

In this project, chemical derivatization methods were developed for *cis*-diol-containing metabolite detection by using liquid chromatography-mass spectrometry. These methods were optimized and validated to achieve the optimal reaction conditions. Then they were applied for qualitative and quantitative analysis of *cis*-diol-containing metabolites in biological samples, including HCC and BPA exposure samples.

Firstly, the derivatization reaction of ribonucleosides with acetone was optimized and validated. The reaction temperature was discovered as the key factor affected reaction efficiency. The results of validation showed that the approach had good linearity, accuracy, precision and recoveries. It indicated that the assay was reproducible. The robust method should be potentially useful for the analysis of modified nucleosides and other *cis*-diol-containing metabolites in biological samples.

Then, the validated method was applied to determine urinary ribonucleosides by LC-MS. This method not only improved the retention of modified nucleosides on reversed-phase column, but also reduced the matrix effect and enhanced detection sensitivity of mass spectrometry. Combined with isotope labeling and multivariate statistical analysis, 56 ribonucleosides were positively identified. The practical, fast and effective method was applied to study the level changes of urinary modified nucleosides in nude mice bearing HCC. Some of them were identified as

significantly changed biomarkers.

Subsequently, this approach was improved by employing PRM method based on high resolution MS to detect urinary modified nucleosides in rats exposed to BPA. The technology showed higher specificity and sensitivity. More nucleosides were identified in urine samples by using the method. The changes of these modified nucleosides were studied in the rats exposed to BPA. Various trends of the compounds were observed with different dose BPA exposure. Specifically, the high-dose exposure group was the most strongly affected. The biomarker of RNA oxidation, 8-oxoG, showed significant change in this group. It proved that BPA exposure could induce RNA damage when the dose of BPA was beyond a certain amount.

Except for modified nucleosides, other *cis*-diol-containing metabolites were also studied by using the derivatization method. By using acetone and acetone-d_6 labeling, *cis*-diol metabolites were easily recognized from urine samples. Application of the method showed that different dose administration of BPA on rats had diverse influence on *cis*-diol-containing metabolites. Some analytes with noticeable difference were highlighted. Pathway analysis indicated that these metabolites belonged to galactose metabolism, nucleoside and its analogues metabolism.

The derivatization method was extended to quantify ribonucleotides in plasma samples. Tip micro-columns prepared with TiO_2 were used for selective adsorption

of nucleotides and to perform in-situ derivatization. The targeted compounds were analyzed by LC-MS without using ion-pairing agents. The method settled the problems of traditional methods for nucleotide detection. The peak shape was symmetrical and the tailing was eliminated. It exhibited high selectivity of extraction and good retention on reversed-phase column. The method was simple and fast, as well as good selectivity and stability. It was successfully applied to quantify ribonucleotides in plasma samples of rats exposed to BPA.

To our best knowledge, it was the first time to detect *cis*-diol-containing metabolites by using derivatization methods with acetone or dimethyl ketal. The methods may be extended to determine other *cis*-diol-containing metabolites in biological samples, such as cells, tissues, blood, etc. It can also be applied to analyze real clinical samples, hoping to discover notably different metabolites of diseases as new biomarkers.

REFERENCES

1. A. Pigneux, V. Perreau, E. Jourdan, N. Vey, N. Dastugue, F. Huguet, J. J. Sotto, L. R. Salmi, N. Ifrah and J. Reiffers. Adding lomustine to idarubicin and cytarabine for induction chemotherapy in older patients with acute myeloid leukemia: the BGMT 95 trial results. *Haematologica*, **2007**, 92, 1327-1334.
2. W. S. Wang, C. H. Tzeng, T. J. Chiou, J. H. Liu, R. K. Hsieh, C. C. Yen and P. M. Chen. High-dose cytarabine and mitoxantrone as salvage therapy for refractory non-Hodgkin's lymphoma. *Jpn. J. Clin. Oncol.*, **1997**, 27, 154-157.
3. H. P. Jiang, C. B. Qi, J. M. Chu, B. F. Yuan and Y. Q. Feng. Profiling of cis-diol-containing nucleosides and ribosylated metabolites by boronate-affinity organic-silica hybrid monolithic capillary liquid chromatography/mass spectrometry. *Sci. Rep.*, **2015**, 5, 7785.
4. S. T. Wang, D. Chen, J. Ding, B. F. Yuan and Y. Q. Feng. Borated titania, a new option for the selective enrichment of cis-diol biomolecules. *Chem.-Eur. J.*, **2013**, 19, 606-612.
5. T. Zaunmuller, M. Eichert, H. Richter and G. Unden. Variations in the energy metabolism of biotechnologically relevant heterofermentative lactic acid bacteria during growth on sugars and organic acids. *Appl. Microbiol. Biotechnol.*, **2006**, 72, 421-429.

6. K. Kato, H. Yagi, M. Utsumi, N. Takahashi and Y. Yamaguchi. A structural biology approach to sugar recognition at the neural cell surface. *Neurosci. Res.*, **2008**, 61, S17-S17.
7. P. A. Sieling, A. M. Kuhlman, K. M. Dobos, N. Banaiee, P. J. Hill, J. D. Ernst, J. T. Belisle and R. L. Modlin. Human T cell recognition of a mycobacterial lipoglycoprotein: The role of sugar and lipid moieties in the T cell response to mycobacterial LprG. *J. Immunol.*, **2006**, 176, S115-S115.
8. K. Asanuma-Date, Y. Hirano, N. Le, K. Sano, N. Kawasaki, N. Hashii, Y. Hiruta, K. Nakayama, M. Umemura, K. Ishikawa, H. Sakagami and H. Ogawa. Functional regulation of sugar assimilation by N-glycan-specific interaction of pancreatic alpha-amylase with glycoproteins of duodenal brush border membrane. *J. Biol. Chem.*, **2012**, 287, 23104-23118.
9. L. Cao, L. Yu, Z. Guo, A. Shen, Y. Guo and X. Liang. N-Glycosylation site analysis of proteins from Saccharomyces cerevisiae by using hydrophilic interaction liquid chromatography-based enrichment, parallel deglycosylation, and mass spectrometry. *J. Proteome. Res.*, **2014**, 13, 1485-1493.
10. A. Kirwan, M. Utratna, M. E. O'Dwyer, L. Joshi and M. Kilcoyne. Glycosylation-Based Serum Biomarkers for Cancer Diagnostics and Prognostics. *Biomed Res. Int.*, **2015**, 2015, 490531.
11. M. Ines and G. Dhouha. Glycolipid biosurfactants: Potential related biomedical and biotechnological applications. *Carbohydr. Res.*, **2015**, 416, 59-69.

12. D. Shorthouse, G. Hedger, H. Koldso and M. S. Sansom. Molecular simulations of glycolipids: Towards mammalian cell membrane models. *Biochimie*, **2016**, 120, 105-109.
13. K. Furukawa, Y. Ohmi, Y. Kondo, Y. Ohkawa, O. Tajima and K. Furukawa. Regulatory function of glycosphingolipids in the inflammation and degeneration. *Arch. Biochem. Biophys.*, **2015**, 571, 58-65.
14. O. Kovbasnjuk, R. Mourtazina, B. Baibakov, T. Wang, C. Elowsky, M. A. Choti, A. Kane and M. Donowitz. The glycosphingolipid globotriaosylceramide in the metastatic transformation of colon cancer. *Proc. Natl. Acad. Sci. U. S. A.*, **2005**, 102, 19087-19092.
15. T. Togawa, T. Kodama, T. Tsukimura, I. Kawashima, T. Tanaka, T. Shiga, A. Sato and H. Sakuraba. Measurement of glycosphingolipids by means of tandem mass spectrometry and evaluation of them as a biomarker of Fabry disease. *Mol. Genet. Metab.*, **2016**, 117, S112-S113.
16. S. Holst, K. Stavenhagen, C. I. Balog, C. A. Koeleman, L. M. McDonnell, O. A. Mayboroda, A. Verhoeven, W. E. Mesker, R. A. Tollenaar, A. M. Deelder and M. Wuhrer. Investigations on aberrant glycosylation of glycosphingolipids in colorectal cancer tissues using liquid chromatography and matrix-assisted laser desorption time-of-flight mass spectrometry (MALDI-TOF-MS). *Mol. Cell. Proteomics*, **2013**, 12, 3081-3093.

17. F. Jacob, M. Anugraham, T. Pochechueva, B. W. Tse, S. Alam, R. Guertler, N. V. Bovin, A. Fedier, N. F. Hacker, M. E. Huflejt, N. Packer and V. A. Heinzelmann-Schwarz. The glycosphingolipid P(1) is an ovarian cancer-associated carbohydrate antigen involved in migration. *Br. J. Cancer*, **2014**, 111, 1634-1645.

18. K. Bum-Erdene, H. Leffler, U. J. Nilsson and H. Blanchard. Structural characterization of human galectin-4 C-terminal domain: elucidating the molecular basis for recognition of glycosphingolipids, sulfated saccharides and blood group antigens. *FEBS J.*, **2015**, 282, 3348-3367.

19. K. Suzuki, A. Tobe, S. Adachi, S. Daikoku, Y. Hasegawa, Y. Shioiri, M. Kobayashi and O. Kanie. N-Hexyl-4-aminobutyl glycosides for investigating structures and biological functions of carbohydrates. *Org. Biomol. Chem.*, **2009**, 7, 4726-4733.

20. S. Ceunen and J. M. Geuns. Steviol glycosides: chemical diversity, metabolism, and function. *J. Nat. Prod.*, **2013**, 76, 1201-1228.

21. H. Ihara, T. Sawa, Y. Nakabeppu and T. Akaike. Nucleotides function as endogenous chemical sensors for oxidative stress signaling. *J. Clin. Biochem. Nutr.*, **2011**, 48, 33-39.

22. J. A. Yalowitz and H. N. Jayaram. Molecular targets of guanine nucleotides in differentiation, proliferation and apoptosis. *Anticancer Res.*, **2000**, 20, 2329-2338.

23. G. Schneider, T. Glaser, C. Lameu, A. Abdelbaset-Ismail, Z. P. Sellers, M. Moniuszko, H. Ulrich and M. Z. Ratajczak. Extracellular nucleotides as novel, underappreciated pro-metastatic factors that stimulate purinergic signaling in human lung cancer cells. *Mol. Cancer*, **2015**, 14, 201.

24. I. A. Radichev, A. G. Remacle, N. E. Sounni, S. A. Shiryaev, D. V. Rozanov, W. Zhu, N. V. Golubkova, T. I. Postnova, V. S. Golubkov and A. Y. Strongin. Biochemical evidence of the interactions of membrane type-1 matrix metalloproteinase (MT1-MMP) with adenine nucleotide translocator (ANT): potential implications linking proteolysis with energy metabolism in cancer cells. *Biochem. J.*, **2009**, 420, 37-47.

25. Y. Xing, K. Gopalrao Rajesh, R. Suzuki, M. Yamamoto, P. Rao and S. Sasaguri. Supplementation of nucleoside-nucleotide mixture enhances functional recovery and energy metabolism following long-time hypothermic heart preservation. *J. Surg. Res.*, **2005**, 127, 144-150.

26. T. Sawa, H. Ihara, T. Ida, S. Fujii, M. Nishida and T. Akaike. Formation, signaling functions, and metabolisms of nitrated cyclic nucleotide. *Nitric Oxide*, **2013**, 34, 10-18.

27. T. Noguchi, A. Dawn, D. Yoshihara, Y. Tsuchiya, T. Yamamoto and S. Shinkai. Selective detection of NADPH among four pyridine-nucleotide cofactors by a fluorescent probe based on aggregation-induced emission. *Macromol. Rapid Commun.*, **2013**, 34, 779-784.

28. G. G. Yegutkin. Enzymes involved in metabolism of extracellular nucleotides and nucleosides: functional implications and measurement of activities. *Crit. Rev. Biochem. Mol. Biol.*, **2014**, 49, 473-497.

29. Y. F. Xu, W. Lu and J. D. Rabinowitz. Avoiding misannotation of in-source fragmentation products as cellular metabolites in liquid chromatography-mass spectrometry-based metabolomics. *Anal. Chem.*, **2015**, 87, 2273-2281.

30. R. F. Steinhoff, J. Krismer, K. Eyer, S. R. Fagerer, A. Ibanez, M. Pabst and R. Zenobi. Rapid estimation of the energy charge from cell lysates using matrix-assisted laser desorption/ionization mass spectrometry: role of in-source fragmentation. *Anal. Biochem.*, **2014**, 447, 107-113.

31. O. Magdenoska, J. Martinussen, J. Thykaer and K. F. Nielsen. Dispersive solid phase extraction combined with ion-pair ultra high-performance liquid chromatography tandem mass spectrometry for quantification of nucleotides in Lactococcus lactis. *Anal. Biochem.*, **2013**, 440, 166-177.

32. J. Rabina, M. Maki, E. M. Savilahti and R. Renkonen. Ion-pair solid-phase extraction and reversed-phase HPLC analysis of nucleotide sugars from cell lysates. *Glycobiology*, **2001**, 11, 924-925.

33. B. D. Gill and H. E. Indyk. Analysis of Nucleotide 5'-Monophosphates in Infant Formulas by HPLC-UV: Collaborative Study, Final Action 2011.20. *J. AOAC Int.*, **2015**, 98, 971-979.

34. S. H. Chen, M. X. Qian, J. M. Brennan and J. M. Gallo. Determination of antisense phosphorothioate oligonucleotides and catabolites in biological fluids and tissue extracts using anion-exchange high-performance liquid chromatography and capillary gel electrophoresis. *J. Chromatogr. B,* **1997**, 692, 43-51.

35. B. Chen and M. Bartlett. A one-step solid phase extraction method for bioanalysis of a phosphorothioate oligonucleotide and its 3' n-1 metabolite from rat plasma by UHPLC-MS/MS. *AAPS J.*, **2012**, 14, 772-780.

36. C. Brugidou, A. Rocher, E. Giraud, B. Lelong, B. Marin and M. Raimbault. A New High Performance Liquid Chromatographic Technique for Separation and Determination of Adenylic and Nicotinamide Nucleotides in Lactobacillus Plantarum. *Biotechnol. Tech.*, **1991**, 5, 475-478.

37. T. Zhou and C. A. Lucy. Hydrophilic interaction chromatography of nucleotides and their pathway intermediates on titania. *J. Chromatogr. A,* **2008**, 1187, 87-93.

38. G. Zhang, A. D. Walker, Z. Lin, X. Han, M. Blatnik, R. C. Steenwyk and E. A. Groeber. Strategies for quantitation of endogenous adenine nucleotides in human plasma using novel ion-pair hydrophilic interaction chromatography coupled with tandem mass spectrometry. *J. Chromatogr. A,* **2014**, 1325, 129-136.

39. Y. Pico, C. Blasco and G. Font. Environmental and food applications of LC-tandem mass spectrometry in pesticide-residue analysis: an overview. *Mass Spectrom. Rev.*, **2004**, 23, 45-85.

40. E. Dudley and L. Bond. Mass spectrometry analysis of nucleosides and nucleotides. *Mass Spectrom. Rev.*, **2014**, 33, 302-331.

41. E. Dodbiba, Z. S. Breitbach, E. Wanigasekara, T. Payagala, X. Zhang and D. W. Armstrong. Detection of nucleotides in positive-mode electrospray ionization mass spectrometry using multiply-charged cationic ion-pairing reagents. *Anal. Bioanal. Chem.*, **2010**, 398, 367-376.

42. J. Zhang, T. Raglione, Q. Wang, B. Kleintop, F. Tomasella and X. Liang. Regeneration of tetrabutylammonium ion-pairing reagent distribution in a gradient elution of reversed phase ion-pair chromatography. *J. Chromatogr. Sci.*, **2011**, 49, 825-831.

43. H. Liu, L. Lam, B. Chi, A. F. Kadjo and P. K. Dasgupta. Transient Ion-Pair Separations for Electrospray Mass Spectrometry. *Anal. Chem.*, **2016**, 88, 2059-2064.

44. B. Yu, Z. Yang, J. Li, S. Minakhina, M. Yang, R. W. Padgett, R. Steward and X. Chen. Methylation as a crucial step in plant microRNA biogenesis. *Science*, **2005**, 307, 932-935.

45. F. Juhling, M. Morl, R. K. Hartmann, M. Sprinzl, P. F. Stadler and J. Putz. tRNAdb 2009: compilation of tRNA sequences and tRNA genes. *Nucleic Acids Res.*, **2009**, 37, D159-D162.

46. C. W. Hu, H. H. Liu, Y. J. Li and M. R. Chao. Direct analysis of 5-methylcytosine and 5-methyl-2'-deoxycytidine in human urine by isotope dilution LC-MS/MS: correlations with N-methylated purines and oxidized DNA lesions. *Chem. Res. Toxicol.*, **2012**, 25, 462-470.

47. M. Hengesbach, M. Meusburger, F. Lyko and M. Helm. Use of DNAzymes for site-specific analysis of ribonucleotide modifications. *RNA*, **2008**, 14, 180-187.

48. A. J. Westermann, S. A. Gorski and J. Vogel. Dual RNA-seq of pathogen and host. *Nat. Rev. Microbiol.*, **2012**, 10, 618-630.

49. J. F. Perez and P. J. Reeds. A new stable isotope method enables the simultaneous measurement of nucleic acid and protein synthesis in vivo in mice. *J. Nutr.*, **1998**, 128, 1562-1569.

50. R. Deterding, G. Retsch-Bogart, L. Milgram, R. Gibson, C. Daines, P. L. Zeitlin, C. Milla, B. Marshall, L. Lavange, J. Engels, D. Mathews, J. Gorden, A. Schaberg, J. Williams, B. Ramsey and N. Cystic Fibrosis Foundation Therapeutics Development. Safety and tolerability of denufosol tetrasodium inhalation solution, a novel P2Y2 receptor agonist: results of a phase 1/phase 2 multicenter study in mild to moderate cystic fibrosis. *Pediatr. Pulm.*, **2005**, 39, 339-348.

51. B. S. Nielsen, S. Jorgensen, J. U. Fog, R. Sokilde, I. J. Christensen, U. Hansen, N. Brunner, A. Baker, S. Moller and H. J. Nielsen. High levels of microRNA-21 in the stroma of colorectal cancers predict short disease-free survival in stage II colon cancer patients. *Clin. Exp. Metastas.*, **2011**, 28, 27-38.

52. G. Schoch, G. Heller-Schoch, J. Muller, P. Clemens, A. Holtgrewe and M. Heddrich. Excretion of normal and modified RNA catabolites and creatinine in the urine as a function of nutrition in children. *Monatsschrift Kinderheilkunde : Organ der Deutschen Gesellschaft fur Kinderheilkunde*, **1983**, 131, 259-263.

53. T. Dawiskiba, S. Deja, A. Mulak, A. Zabek, E. Jawien, D. Pawelka, M. Banasik, A. Mastalerz-Migas, W. Balcerzak, K. Kaliszewski, J. Skora, P. Barc, K. Korta, K. Pormanczuk, P. Szyber, A. Litarski and P. Mlynarz. Serum and urine metabolomic fingerprinting in diagnostics of inflammatory bowel diseases. *World J. Gastroentero.*, **2014**, 20, 163-174.

54. A. Langerman, R. M. Patel, E. E. Cohen, E. A. Blair and K. M. Stenson. Airway management before chemoradiation for advanced head and neck cancer. *Head Neck*, **2012**, 34, 254-259.

55. R. Etzioni, N. Urban, S. Ramsey, M. McIntosh, S. Schwartz, B. Reid, J. Radich, G. Anderson and L. Hartwell. The case for early detection. *Nat. Rev. Cancer*, **2003**, 3, 243-252.

56. R. Kobayashi. A proteomics approach to find a new breast cancer-specific antigenic marker - Commentary. *Clin. Cancer Res.*, **2001**, 7, 3325-3327.

57. W. Y. Hsu, C. J. Chen, Y. C. Huang, F. J. Tsai, L. B. Jeng and C. C. Lai. Urinary nucleosides as biomarkers of breast, colon, lung, and gastric cancer in Taiwanese. *PLoS One*, **2013**, 8, e81701.

58. A. Seidel, S. Brunner, P. Seidel, G. I. Fritz and O. Herbarth. Modified nucleosides: an accurate tumour marker for clinical diagnosis of cancer, early detection and therapy control. *Br. J. Cancer*, **2006**, 94, 1726-1733.

59. C. Yi and T. Pan. Cellular dynamics of RNA modification. *Acc. Chem. Res.*, **2011**, 44, 1380-1388.

60. K. Itoh, S. Aida, S. Ishiwata, T. Yamaguchi, N. Ishida and M. Mizugaki. Immunochemical Detection of Urinary 5-Methyl-2'-Deoxycytidine as a Potential Biologic Marker for Leukemia. *Clin. Chim. Acta*, **1995**, 234, 37-45.

61. I. Darwish, S. Emara, H. Askal, N. El-Rabbat, K. Omura, K. Hirose, T. Akizawa and M. Yoshioka. Competitive immunoassay method for 5-methyl-2 '-deoxycytidine. *Anal. Chim. Acta*, **2000**, 413, 79-86.

62. T. Rasmuson and G. R. Bjork. Urinary excretion of pseudouridine and prognosis of patients with malignant lymphoma. *Acta. Oncol.*, **1995**, 34, 61-67.

63. A. J. Sasco, F. Rey, C. Reynaud, J. Y. Bobin, M. Clavel and A. Niveleau. Breast cancer prognostic significance of some modified urinary nucleosides. *Cancer Lett.*, **1996**, 108, 157-162.

64. S. H. Cho, M. H. Choi, W. Y. Lee and B. C. Chung. Evaluation of urinary nucleosides in breast cancer patients before and after tumor removal. *Clin. Biochem.*, **2009**, 42, 540-543.

65. W. Y. Hsu, W. D. Lin, Y. Tsai, C. T. Lin, H. C. Wang, L. B. Jeng, C. C. Lee, Y. C. Lin, C. C. Lai and F. J. Tsai. Analysis of urinary nucleosides as potential tumor markers in human breast cancer by high performance liquid chromatography/electrospray ionization tandem mass spectrometry. *Clin. Chim. Acta*, **2011**, 412, 1861-1866.

66. W. Struck, D. Siluk, A. Yumba-Mpanga, M. Markuszewski, R. Kaliszan and M. J. Markuszewski. Liquid chromatography tandem mass spectrometry study of urinary nucleosides as potential cancer markers. *J. Chromatogr. A*, **2013**, 1283, 122-131.

67. H. M. Woo, K. M. Kim, M. H. Choi, B. H. Jung, J. Lee, G. Kong, S. J. Nam, S. Kim, S. W. Bai and B. C. Chung. Mass spectrometry based metabolomic approaches in urinary biomarker study of women's cancers. *Clin. Chim. Acta*, **2009**, 400, 63-69.

68. A. Frickenschmidt, H. Frohlich, D. Bullinger, A. Zell, S. Laufer, C. H. Gleiter, H. Liebich and B. Kammerer. Metabonomics in cancer diagnosis: mass spectrometry-based profiling of urinary nucleosides from breast cancer patients. *Biomarkers*, **2008**, 13, 435-449.

69. C. Henneges, D. Bullinger, R. Fux, N. Friese, H. Seeger, H. Neubauer, S. Laufer, C. H. Gleiter, M. Schwab, A. Zell and B. Kammerer. Prediction of breast cancer by profiling of urinary RNA metabolites using Support Vector Machine-based feature selection. *BMC Cancer*, **2009**, 9, 104.

70. B. Feng, M. H. Zheng, Y. F. Zheng, A. G. Lu, J. W. Li, M. L. Wang, J. J. Ma, G. W. Xu, B. Y. Liu and Z. G. Zhu. Normal and modified urinary nucleosides represent novel biomarkers for colorectal cancer diagnosis and surgery monitoring. *J. Gastroenterol. Hepatol.*, **2005**, 20, 1913-1919.

71. Y. Qiu, G. Cai, M. Su, T. Chen, Y. Liu, Y. Xu, Y. Ni, A. Zhao, S. Cai, L. X. Xu and W. Jia. Urinary metabonomic study on colorectal cancer. *J. Proteome Res.*, **2010**, 9, 1627-1634.

72. M. Waszczuk-Jankowska, M. J. Markuszewski, M. Markuszewski and R. Kaliszan. Comparison of RP-HPLC columns used for determination of nucleoside metabolic patterns in urine of cancer patients. *Bioanalysis*, **2012**, 4, 1185-1194.

73. E. Szymanska, M. J. Markuszewski, M. Markuszewski and R. Kaliszan. Altered levels of nucleoside metabolite profiles in urogenital tract cancer measured by capillary electrophoresis. *J. Pharm. Biomed. Anal.*, **2010**, 53, 1305-1312.

74. L. B. Jeng, W. Y. Lo, W. Y. Hsu, W. D. Lin, C. T. Lin, C. C. Lai and F. J. Tsai. Analysis of urinary nucleosides as helper tumor markers in hepatocellular carcinoma diagnosis. *Rapid Commun. Mass Spectrom.*, **2009**, 23, 1543-1549.

75. J. Yang, G. Xu, Y. Zheng, H. Kong, C. Wang, X. Zhao and T. Pang. Strategy for metabonomics research based on high-performance liquid chromatography and liquid chromatography coupled with tandem mass spectrometry. *J. Chromatogr. A*, **2005**, 1084, 214-221.

76. E. Dudley, F. Lemiere, W. Van Dongen, J. I. Langridge, S. El-Sharkawi, D. E. Games, E. L. Esmans and R. P. Newton. Analysis of urinary nucleosides. III. Identification of 5'-deoxycytidine in urine of a patient with head and neck cancer. *Rapid Commun. Mass Spectrom.*, **2003**, 17, 1132-1136.

77. D. Bullinger, R. Fux, G. Nicholson, S. Plontke, C. Belka, S. Laufer, C. H. Gleiter and B. Kammerer. Identification of urinary modified nucleosides and ribosylated metabolites in humans via combined ESI-FTICR MS and ESI-IT MS analysis. *J. Am. Soc. Mass Spectrom.*, **2008**, 19, 1500-1513.

78. Y. X. Zhang. Artificial neural networks based on principal component analysis input selection for clinical pattern recognition analysis. *Talanta*, **2007**, 73, 68-75.

79. P. Tantipaiboonwong, S. Sinchaikul, S. Sriyam, S. Phutrakul and S. T. Chen. Different techniques for urinary protein analysis of normal and lung cancer patients. *Proteomics*, **2005**, 5, 1140-1149.

80. L. A. Agrofoglio, V. Bezy, P. Chaimbault, R. Delepee, B. Rhourri and P. Morin. Mass spectrometry based methods for analysis of nucleosides as antiviral drugs and potential tumor biomarkers. *Nucleosides Nucleotides Nucleic Acids*, **2007**, 26, 1523-1527.

81. Y. Bilbille, F. A. Vendeix, R. Guenther, A. Malkiewicz, X. Ariza, J. Vilarrasa and P. F. Agris. The structure of the human tRNALys3 anticodon bound to the HIV genome is stabilized by modified nucleosides and adjacent mismatch base pairs. *Nucleic Acids Res.*, **2009**, 37, 3342-3353.

82. C. Chantin, B. Bonin, R. Boulieu and C. Bory. Liquid-chromatographic study of purine metabolism abnormalities in purine nucleoside phosphorylase deficiency. *Clin. Chem.*, **1996**, 42, 326-328.

83. C. W. Gehrke, R. W. Zumwalt, R. A. McCune and K. C. Kuo. Quantitative high-performance liquid chromatography analysis of modified nucleosides in physiological fluids, tRNA, and DNA. *Recent results in cancer research. Fortschritte der Krebsforschung. Progres Dans Les Recherches Sur Le Cancer*, **1983**, 84, 344-359.

84. P. Seidel, A. Seidel and O. Herbarth. Multilayer perceptron tumour diagnosis based on chromatography analysis of urinary nucleosides. *Neural Netw.*, **2007**, 20, 646-651.

85. H. M. Liebich, C. Di Stefano, A. Wixforth and H. R. Schmid. Quantitation of urinary nucleosides by high-performance liquid chromatography. *J. Chromatogr. A*, **1997**, 763, 193-197.

86. F. Palmisano, T. Rotunno, M. La Sorsa, C. G. Zambonin and I. Abbate. Simultaneous determination of pseudouridine, neopterine and creatinine in urine by ion-pair high-performance liquid chromatography with in-series ultraviolet and fluorescence detection. *Analyst,* **1995**, 120, 2185-2189.

87. S. Studzinska and B. Buszewski. A new way to fast and high resolution determination of modified nucleosides. *J. Chromatogr. B Analyt. Technol. Biomed. Life Sci.*, **2012**, 887-888, 93-101.

88. J. I. Langridge, T. D. McClure, S. el-Shakawi, A. Fielding, K. H. Schram and R. P. Newton. Gas chromatography/mass spectrometric analysis of urinary nucleosides in cancer patients; potential of modified nucleosides as tumour markers. *Rapid Commun. Mass Spectrom.*, **1993**, 7, 427-434.

89. A. J. Teixeira, M. R. Ferreira, W. J. van Dijk, G. van de Werken and A. P. de Jong. Analysis of 8-hydroxy-2'-deoxyguanosine in rat urine and liver DNA by stable isotope dilution gas chromatography/mass spectrometry. *Anal. Biochem.*, **1995**, 226, 307-319.

90. M. Foksinski, D. Gackowski, R. Rozalski and R. Olinski. Cellular level of 8-oxo-2'-deoxyguanosine in DNA does not correlate with urinary excretion of the modified base/nucleoside. *Acta biochim. Pol.*, **2003**, 50, 549-553.

91. K. Roszkowski, D. Gackowski, R. Rozalski, T. Dziaman, A. Siomek, J. Guz, A. Szpila, M. Foksinski and R. Olinski. Small field radiotherapy of head and neck cancer patients is responsible for oxidatively damaged DNA/oxidative stress on the level of a whole organism. *Int. J. Cancer*, **2008**, 123, 1964-1967.
92. M. S. Cooke, R. Singh, G. K. Hall, V. Mistry, T. L. Duarte, P. B. Farmer and M. D. Evans. Evaluation of enzyme-linked immunosorbent assay and liquid chromatography-tandem mass spectrometry methodology for the analysis of 8-oxo-7,8-dihydro-2'-deoxyguanosine in saliva and urine. *Free Radic. Biol. Med.*, **2006**, 41, 1829-1836.
93. M. P. Marco, M. Nasiri, M. J. Kurth and B. D. Hammock. Enzyme-linked immunosorbent assay for the specific detection of the mercapturic acid metabolites of naphthalene. *Chem. Res. Toxicol.*, **1993**, 6, 284-293.
94. K. Itoh, T. Konno, T. Sasaki, S. Ishiwata, N. Ishida and M. Misugaki. Relationship of urinary pseudouridine and 1-methyladenosine to activity of leukemia and lymphoma. *Clin. Chim. Acta*, **1992**, 206, 181-189.
95. E. Michelini, P. Leskinen, M. Virta, M. Karp and A. Roda. A new recombinant cell-based bioluminescent assay for sensitive androgen-like compound detection. *Biosens. Bioelectron.*, **2005**, 20, 2261-2267.
96. H. M. Liebich, G. Xu, C. DiStefano, R. Lehmann, H. U. Haring, P. Lu and Y. Zhang. Analysis of normal and modified nucleosides in urine by capillary electrophoresis. *Chromatographia*, **1997**, 45, 396-401.

97. R. Zhao, G. Xu, B. Yue, H. M. Liebich and Y. Zhang. Artificial neural network classification based on capillary electrophoresis of urinary nucleosides for the clinical diagnosis of tumors. *J. Chromatogr. A,* **1998**, 828, 489-496.

98. J. H. Xiong, Y. F. Zheng, P. D. Zhang, X. Z. Shi, J. Yang, Y. K. Zhang and G. W. Xu. Application of the combination of capillary electrophoresis with wavelet neural network in the assisted clinical diagnosis of breast cancer. *Chem. J. Chin. Univ.-Chin.*, **2003**, 24, 803-807.

99. D. J. Weiss and C. E. Lunte. Detection of a urinary biomaker for oxidative DNA damage 8-hydroxydeoxyguanosine by capillary electrophoresis with electrochemical detection. *Electrophoresis*, **2000**, 21, 2080-2085.

100. T. Adam, P. Lochman and D. Friedecky. Screening method for inherited disorders of purine and pyrimidine metabolism by capillary electrophoresis with reversed electroosmotic flow. *J. Chromatogr. B Analyt. Technol. Biomed. Life Sci.*, **2002**, 767, 333-340.

101. W. Kang. Quantitative determination of uridine in rabbit plasma and urine by liquid chromatography coupled to a tandem mass spectrometry. *Biomed. Chromatogr.*, **2012**, 26, 541-544.

102. H. Y. Li, S. M. Wang, H. M. Liu, S. S. Bu, J. Li, D. Han, M. Z. Zhang and G. Y. Wu. Separation and identification of purine nucleosides in the urine of patients with malignant cancer by reverse phase liquid

chromatography/electrospray tandem mass spectrometry. *J. Mass. Spectrom.*, **2009**, 44, 641-651.

103. A. Van Dycke, A. Verstraete, K. Pil, R. Raedt, K. Vonck, D. Boison and P. Boon. Quantitative analysis of adenosine using liquid chromatography/atmospheric pressure chemical ionization-tandem mass spectrometry (LC/APCI-MS/MS). *J. Chromatogr. B Analyt. Technol. Biomed. Life Sci.*, **2010**, 878, 1493-1498.

104. A. H. Rageh and U. Pyell. Imidazolium-based ionic liquid-type surfactant as pseudostationary phase in micellar electrokinetic chromatography of highly hydrophilic urinary nucleosides. *J. Chromatogr. A*, **2013**, 1316, 135-146.

105. E. Dudley, R. Tuytten, A. Bond, F. Lemiere, A. G. Brenton, E. L. Esmans and R. P. Newton. Study of the mass spectrometric fragmentation of pseudouridine: comparison of fragmentation data obtained by matrix-assisted laser desorption/ionisation post-source decay, electrospray ion trap multistage mass spectrometry, and by a method utilising electrospray quadrupole time-of-flight tandem mass spectrometry and in-source fragmentation. *Rapid Commun. Mass Spectrom.*, **2005**, 19, 3075-3085.

106. D. G. Beach and W. Gabryelski. Nontarget analysis of urine by electrospray ionization-high field asymmetric waveform ion mobility-tandem mass spectrometry. *Anal. Chem.*, **2011**, 83, 9107-9113.

107. F. Teichert, S. Winkler, H. C. Keun, W. P. Steward, A. J. Gescher, P. B. Farmer and R. Singh. Evaluation of urinary ribonucleoside profiling for clinical biomarker discovery using constant neutral loss scanning liquid chromatography/tandem mass spectrometry. *Rapid Commun. Mass Spectrom.*, **2011**, 25, 2071-2082.

108. L. Novakova, T. Gottvald, H. Vlckova, F. Trejtnar, J. Mandikova and P. Solich. Highly sensitive fast determination of entecavir in rat urine by means of hydrophilic interaction chromatography-ultra-high-performance liquid chromatography-tandem mass spectrometry. *J. Chromatogr. A*, **2012**, 1259, 237-243.

109. E. Rodriguez-Gonzalo, D. Garcia-Gomez and R. Carabias-Martinez. Study of retention behaviour and mass spectrometry compatibility in zwitterionic hydrophilic interaction chromatography for the separation of modified nucleosides and nucleobases. *J. Chromatogr. A*, **2011**, 1218, 3994-4001.

110. E. Rodriguez-Gonzalo, D. Garcia-Gomez and R. Carabias-Martinez. Development and validation of a hydrophilic interaction chromatography-tandem mass spectrometry method with on-line polar extraction for the analysis of urinary nucleosides. Potential application in clinical diagnosis. *J. Chromatogr. A*, **2011**, 1218, 9055-9063.

111. Y. Sakaguchi, K. Miyauchi, B. I. Kang and T. Suzuki, Nucleoside Analysis by Hydrophilic Interaction Liquid Chromatography Coupled with Mass Spectrometry. *RNA Modification*, **2015**, 560, 19-28.

112. R. Tuytten, F. Lemiere, W. Van Dongen, E. Witters, E. L. Esmans, R. P. Newton and E. Dudley. Development of an on-line SPE-LC-ESI-MS method for urinary nucleosides: hyphenation of aprotic boronic acid chromatography with hydrophilic interaction LC-ESI-MS. *Anal. Chem.*, **2008**, 80, 1263-1271.

113. A. von Brocke, G. Nicholson and E. Bayer. Recent advances in capillary electrophoresis/electrospray-mass spectrometry. *Electrophoresis*, **2001**, 22, 1251-1266.

114. E. Rodriguez-Gonzalo, R. Hernandez-Prieto, D. Garcia-Gomez and R. Carabias-Martinez. Capillary electrophoresis-mass spectrometry for direct determination of urinary modified nucleosides. Evaluation of synthetic urine as a surrogate matrix for quantitative analysis. *J. Chromatogr. B Analyt. Technol. Biomed. Life Sci.*, **2013**, 942-943, 21-30.

115. E. Rodriguez-Gonzalo, R. Hernandez-Prieto, D. Garcia-Gomez and R. Carabias-Martinez. Development of a procedure for the isolation and enrichment of modified nucleosides and nucleobases from urine prior to their determination by capillary electrophoresis-mass spectrometry. *J. Pharm. Biomed. Anal.*, **2014**, 88, 489-496.

116. S. C. Nagel and J. J. Bromfield. Bisphenol a: a model endocrine disrupting chemical with a new potential mechanism of action. *Endocrinology*, **2013**, 154, 1962-1964.

117. F. Maqbool, S. Mostafalou, H. Bahadar and M. Abdollahi. Review of endocrine disorders associated with environmental toxicants and possible involved mechanisms. *Life Sci.*, **2016**, 145, 265-273.

118. C. S. Rosenfeld. Bisphenol A and phthalate endocrine disruption of parental and social behaviors. *Front. Neurosci.*, **2015**, 9, 57.

119. S. Pflieger-Bruss, H. C. Schuppe and W. B. Schill. The male reproductive system and its susceptibility to endocrine disrupting chemicals. *Andrologia*, **2004**, 36, 337-345.

120. X. Jie, W. Yang, Y. Jie, Q. Y. Fan, X. Y. Liu, L. Yan and H. J. Huang. Immune Effects of Nonylphenol on Offspring of Rats Exposed During Pregnancy. *Hum. Ecol. Risk Assess.*, **2010**, 16, 444-452.

121. S. Richard, S. Moslemi, H. Sipahutar, N. Benachour and G. E. Seralini. Differential effects of glyphosate and roundup on human placental cells and aromatase. *Environ. Health Persp.*, **2005**, 113, 716-720.

122. J. Peretz, L. Vrooman, W. A. Ricke, P. A. Hunt, S. Ehrlich, R. Hauser, V. Padmanabhan, H. S. Taylor, S. H. Swan, C. A. VandeVoort and J. A. Flaws. Bisphenol a and reproductive health: update of experimental and human evidence, 2007-2013. *Environ. Health Persp.*, **2014**, 122, 775-786.

123. C. M. Markey, P. R. Wadia, B. S. Rubin, C. Sonnenschein and A. M. Soto. Long-term effects of fetal exposure to low doses of the xenoestrogen bisphenol-A in the female mouse genital tract. *Biol. Reprod.*, **2005**, 72, 1344-1351.

124. H. M. Lam, S. M. Ho, J. Chen, M. Medvedovic and N. N. Tam. Bisphenol A Disrupts HNF4alpha-Regulated Gene Networks Linking to Prostate Preneoplasia and Immune Disruption in Noble Rats. *Endocrinology*, **2016**, 157, 207-219.

125. J. Jellyman, M. Ross and M. Desai. Sex-dependent metabolic abnormalities in maternal bisphenol a (BPA)-exposed offspring. *Am. J. Obstet. Gynecol.*, **2015**, 212, S100.

126. N. Chevalier, F. Brucker-Davis, N. Lahlou, P. Coquillard, M. Pugeat, P. Pacini, P. Panaia-Ferrari, K. Wagner-Mahler and P. Fenichel. A negative correlation between insulin-like peptide 3 and bisphenol A in human cord blood suggests an effect of endocrine disruptors on testicular descent during fetal development. *Hum. Reprod.*, **2015**, 30, 447-453.

127. S. Flint, T. Markle, S. Thompson and E. Wallace. Bisphenol A exposure, effects, and policy: a wildlife perspective. *J. Environ. Manage.*, **2012**, 104, 19-34.

128. Y. Gu, J. Yu, X. Hu and D. Yin. Characteristics of the alkylphenol and bisphenol A distributions in marine organisms and implications for human

health: A case study of the East China Sea. *Sci. Total. Environ.*, **2016**, 539, 460-469.

129. N. Ben-Jonathan and R. Steinmetz. Xenoestrogens: the emerging story of bisphenol a. *Trends Endocrinol. Metab.*, **1998**, 9, 124-128.

130. C. A. Richter, J. A. Taylor, R. L. Ruhlen, W. V. Welshons and F. S. Vom Saal. Estradiol and Bisphenol A stimulate androgen receptor and estrogen receptor gene expression in fetal mouse prostate mesenchyme cells. *Environ. Health Persp.*, **2007**, 115, 902-908.

131. W. Xi, C. K. Lee, W. S. Yeung, J. P. Giesy, M. H. Wong, X. Zhang, M. Hecker and C. K. Wong. Effect of perinatal and postnatal bisphenol A exposure to the regulatory circuits at the hypothalamus-pituitary-gonadal axis of CD-1 mice. *Reprod. Toxicol.*, **2011**, 31, 409-417.

132. C. L. Stowell, K. K. Barvian, P. C. Young, R. M. Bigsby, D. E. Verdugo, C. R. Bertozzi and T. S. Widlanski. A role for sulfation-desulfation in the uptake of bisphenol a into breast tumor cells. *Chem. Biol.*, **2006**, 13, 891-897.

133. D. S. Popa, P. Bolfa, B. Kiss, L. Vlase, R. Paltinean, A. Pop, C. Catoi, G. Crisan and F. Loghin. Influence of Genista tinctoria L. or methylparaben on subchronic toxicity of bisphenol A in rats. *Biomed. Environ. Sci.*, **2014**, 27, 85-96.

134. R. Steinmetz, N. G. Brown, D. L. Allen, R. M. Bigsby and N. Ben-Jonathan. The environmental estrogen bisphenol A stimulates prolactin release in vitro and in vivo. *Endocrinology*, **1997**, 138, 1780-1786.

135. A. Muhlhauser, M. Susiarjo, C. Rubio, J. Griswold, G. Gorence, T. Hassold and P. A. Hunt. Bisphenol A effects on the growing mouse oocyte are influenced by diet. *Biol. Reprod.*, **2009**, 80, 1066-1071.

136. O. Takahashi and S. Oishi. Testicular toxicity of dietarily or parenterally administered bisphenol A in rats and mice. *Food Chem. Toxicol.*, **2003**, 41, 1035-1044.

137. M. Garcia-Arevalo, P. Alonso-Magdalena, J. Rebelo Dos Santos, I. Quesada, E. M. Carneiro and A. Nadal. Exposure to bisphenol-A during pregnancy partially mimics the effects of a high-fat diet altering glucose homeostasis and gene expression in adult male mice. *PLoS One*, **2014**, 9, e100214.

138. S. Ali, G. Steinmetz, G. Montillet, M. H. Perrard, A. Loundou, P. Durand, M. R. Guichaoua and O. Prat. Exposure to low-dose bisphenol A impairs meiosis in the rat seminiferous tubule culture model: a physiotoxicogenomic approach. *PLoS One*, **2014**, 9, e106245.

139. Z. K. Hassan, M. A. Elobeid, P. Virk, S. A. Omer, M. ElAmin, M. H. Daghestani and E. M. AlOlayan. Bisphenol A induces hepatotoxicity through oxidative stress in rat model. *Oxid. Med. Cell. Longev.*, **2012**, 2012, 194829.

140. S. Yoshino, K. Yamaki, X. Li, T. Sai, R. Yanagisawa, H. Takano, S. Taneda, H. Hayashi and Y. Mori. Prenatal exposure to bisphenol A up-regulates immune responses, including T helper 1 and T helper 2 responses, in mice. *Immunology*, **2004**, 112, 489-495.

141. N. Ben-Jonathan, E. R. Hugo and T. D. Brandebourg. Effects of bisphenol A on adipokine release from human adipose tissue: Implications for the metabolic syndrome. *Mol. Cell. Endocrinol.*, **2009**, 304, 49-54.

142. L. N. Vandenberg, T. Colborn, T. B. Hayes, J. J. Heindel, D. R. Jacobs, Jr., D. H. Lee, T. Shioda, A. M. Soto, F. S. vom Saal, W. V. Welshons, R. T. Zoeller and J. P. Myers. Hormones and endocrine-disrupting chemicals: low-dose effects and nonmonotonic dose responses. *Endocr. Rev.*, **2012**, 33, 378-455.

143. R. R. Newbold, W. N. Jefferson and E. Padilla-Banks. Long-term adverse effects of neonatal exposure to bisphenol A on the murine female reproductive tract. *Reprod. Toxicol.*, **2007**, 24, 253-258.

144. F. S. vom Saal, P. S. Cooke, D. L. Buchanan, P. Palanza, K. A. Thayer, S. C. Nagel, S. Parmigiani and W. V. Welshons. A physiologically based approach to the study of bisphenol A and other estrogenic chemicals on the size of reproductive organs, daily sperm production, and behavior. *Toxicol. Ind. Health*, **1998**, 14, 239-260.

145. G. S. Prins, S. H. Ye, L. Birch, S. M. Ho and K. Kannan. Serum bisphenol A pharmacokinetics and prostate neoplastic responses following oral and

subcutaneous exposures in neonatal Sprague-Dawley rats. *Reprod. Toxicol.*, **2011**, 31, 1-9.

146. H. Nishizawa, M. Morita, M. Sugimoto, S. Imanishi and N. Manabe. Effects of in utero exposure to bisphenol A on mRNA expression of arylhydrocarbon and retinoid receptors in murine embryos. *J. Reprod. Dev.*, **2005**, 51, 315-324.

147. Z. Duan, L. Zhu, L. Zhu, Y. Kun and X. Zhu. Individual and joint toxic effects of pentachlorophenol and bisphenol A on the development of zebrafish (Danio rerio) embryo. *Ecotox. Environ. Safe.*, **2008**, 71, 774-780.

148. R. A. Keri, S. M. Ho, P. A. Hunt, K. E. Knudsen, A. M. Soto and G. S. Prins. An evaluation of evidence for the carcinogenic activity of bisphenol A. *Reprod. Toxicol.*, **2007**, 24, 240-252.

149. D. R. Ekman, D. M. Skelton, J. M. Davis, D. L. Villeneuve, J. E. Cavallin, A. Schroeder, K. M. Jensen, G. T. Ankley and T. W. Collette. Metabolite profiling of fish skin mucus: a novel approach for minimally-invasive environmental exposure monitoring and surveillance. *Environ. Sci. Technol.*, **2015**, 49, 3091-3100.

150. C. Ji, L. Wei, J. Zhao and H. Wu. Metabolomic analysis revealed that female mussel Mytilus galloprovincialis was sensitive to bisphenol A exposures. *Environ. Toxicol. Pharmacol.*, **2014**, 37, 844-849.

151. M. Chen, K. Zhou, X. Chen, S. Qiao, Y. Hu, B. Xu, B. Xu, X. Han, R. Tang, Z. Mao, C. Dong, D. Wu, Y. Wang, S. Wang, Z. Zhou, Y. Xia and X. Wang.

Metabolomic analysis reveals metabolic changes caused by bisphenol A in rats. *Toxicol. Sci.*, **2014**, 138, 256-267.

152. M. Chen, B. Xu, W. Ji, S. Qiao, N. Hu, Y. Hu, W. Wu, L. Qiu, R. Zhang, Y. Wang, S. Wang, Z. Zhou, Y. Xia and X. Wang. Bisphenol A alters n-6 fatty acid composition and decreases antioxidant enzyme levels in rat testes: a LC-QTOF-based metabolomics study. *PLoS One*, **2012**, 7, e44754.

153. J. R. Rochester. Bisphenol A and human health: a review of the literature. *Reprod. Toxicol.*, **2013**, 42, 132-155.

154. J. Zeng, H. Kuang, C. Hu, X. Shi, M. Yan, L. Xu, L. Wang, C. Xu and G. Xu. Effect of bisphenol A on rat metabolic profiling studied by using capillary electrophoresis time-of-flight mass spectrometry. *Environ. Sci. Technol.*, **2013**, 47, 7457-7465.

155. N. J. Cabaton, C. Canlet, P. R. Wadia, M. Tremblay-Franco, R. Gautier, J. Molina, C. Sonnenschein, J. P. Cravedi, B. S. Rubin, A. M. Soto and D. Zalko. Effects of low doses of bisphenol A on the metabolome of perinatally exposed CD-1 mice. *Environ. Health Persp.*, **2013**, 121, 586-593.

156. L. Canesi and E. Fabbri. Environmental Effects of BPA: Focus on Aquatic Species. *Dose-Response*, **2015**, 13, 1559325815598304.

157. X. Huo, D. Chen, Y. He, W. Zhu, W. Zhou and J. Zhang. Bisphenol-A and Female Infertility: A Possible Role of Gene-Environment Interactions. *Int. J. Environ. Res. Public Health*, **2015**, 12, 11101-11116.

158. M. Becker, T. Zweckmair, A. Forneck, T. Rosenau, A. Potthast and F. Liebner. Evaluation of different derivatisation approaches for gas chromatographic-mass spectrometric analysis of carbohydrates in complex matrices of biological and synthetic origin. *J. Chromatogr. A*, **2013**, 1281, 115-126.

159. X. R. Zhang and C. Q. Zhang. Nano n-Propylsulfonated Magnetic -Fe2O3 as an Efficient and Reusable Catalyst for the Synthesis O-Isopropylidene Derivatives of Carbohydrates. *J. Carbohydr. Chem.*, **2013**, 32, 249-258.

160. J. B. Behr. Synthesis and L-fucosidase inhibitory activity of a new series of cyclic sugar imines-in situ formation and assay of their saturated counterparts. *Tetrahedron Lett.*, **2009**, 50, 4498-4501.

161. Z. Zhu and J. K. Buolamwini. Constrained NBMPR analogue synthesis, pharmacophore mapping and 3D-QSAR modeling of equilibrative nucleoside transporter 1 (ENT1) inhibitory activity. *Bioorg. Med. Chem.*, **2008**, 16, 3848-3865.

162. N. Maezaki, N. Kojima, A. Sakamoto, H. Tominaga, C. Iwata, T. Tanaka, M. Monden, B. Damdinsuren and S. Nakamori. Total synthesis of the antitumor acetogenin mosin B: desymmetrization approach to the stereodivergent synthesis of threo/trans/erythro-type acetogenins. *Chem.-Eur. J.*, **2003**, 9, 389-399.

163. L. S. Jeong, D. K. Tosh, H. O. Kim, T. Wang, X. Hou, H. S. Yun, Y. Kwon, S. K. Lee, J. Choi and L. X. Zhao. First synthesis of 4'-selenonucleosides showing unusual Southern conformation. *Org. Lett.*, **2008**, 10, 209-212.

164. V. Cere, F. Peri, S. Pollicino, A. Ricci, F. J. Devlin, P. J. Stephens, F. Gasparrini, R. Rompietti and C. Villani. Synthesis, chromatographic separation, vibrational circular dichroism spectroscopy, and ab initio DFT studies of chiral thiepane tetraol derivatives. *J. Org. Chem.*, **2005**, 70, 664-669.

165. I. Karame, M. Alame, A. Kanj, G. N. Baydoun, H. Hazimeh, M. el Masri and L. Christ. Mild and efficient protection of diol and carbonyls as cyclic acetals catalysed by iron (III) chloride. *CR. Chim.*, **2011**, 14, 525-529.

166. F. A. Khan and C. N. Rao. An efficient synthesis of diquinane-based bis-gamma-lactones. *Tetrahedron Lett.*, **2006**, 47, 7567-7570.

167. J. M. Cheng, S. H. Chee, D. A. Knight, H. Acha-Orbea, I. F. Hermans, M. S. Timmer and B. L. Stocker. An improved synthesis of dansylated alpha-galactosylceramide and its use as a fluorescent probe for the monitoring of glycolipid uptake by cells. *Carbohydr. Res.*, **2011**, 346, 914-926.

168. M. R. Banks, A. J. Blake, J. I. G. Cadogan, I. M. Dawson, S. Gaur, I. Gosney, R. O. Gould, K. J. Grant and P. K. G. Hodgson. (5R)-7,8:9,10-Di-O-isopropylidene-2,6-dioxa-4-azaspiro[4,5]decan-3-one: a new chiral spirooxazolidin-2-one derived from D-(+)-galactose for use in asymmetric transformations. *J. Chem. Soc., Chem. Commun.*, **1993**, 14, 1146-1148.

169. C. C. Lin, M. D. Jan, S. S. Weng, C. C. Lin and C. T. Chen. O-Isopropylidenation of carbohydrates catalyzed by vanadyl triflate. *Carbohydr. Res.*, **2006**, 341, 1948-1953.

170. E. S. De Alvarenga, V. M. T. Carneiro, F. O. Silverio and W. A. Saliba. A high yield synthesis of 1,2 : 5,6-di-O-isopropylidene-D-mannitol. *J. Chil. Chem. Soc.*, **2006**, 51, 986-988.

171. T. S. Jin, S. L. Zhang, X. F. Wang, J. J. Guo and T. S. Li. An efficient and convenient method for preparation of 2,2-disubstituted and 2-monosubstituted 1,3-benzodioxoles from ketones and aldehydes with catechol catalysed by ZrO_2/SO_4^{2-}. *J. Chem. Res.-S*, **2001**, 7, 289-291.

172. V. A. Soloshonok and H. Ueki. Efficient and practical protection of the catechol residue of 3,4-dihydroxyphenylalanine (DOPA) derivative as acetonide. *Synthesis*, **2008**, 5, 693-695.

173. J. G. Wittmann, D. Heinrich, K. Gasow, A. Frey, U. Diederichsen and M. G. Rudolph. Structures of the human orotidine-5'-monophosphate decarboxylase support a covalent mechanism and provide a framework for drug design. *Structure*, **2008**, 16, 82-92.

174. A. M. Bello, E. Poduch, M. Fujihashi, M. Amani, Y. Li, I. Crandall, R. Hui, P. I. Lee, K. C. Kain, E. F. Pai and L. P. Kotra. A potent, covalent inhibitor of orotidine 5'-monophosphate decarboxylase with antimalarial activity. *J. Med. Chem.*, **2007**, 50, 915-921.

175. A. M. Bello, E. Poduch, M. Fujihashi, M. Amani, Y. Li, I. Crandall, R. Hui, P. I. Lee, K. C. Kain, E. F. Pai and L. P. Kotra. A potent, covalent inhibitor of orotidine 5 '-monophosphate decarboxylase with antimalarial activity. *J. Med. Chem.*, **2007**, 50, 915–921.

176. J. H. Cho, S. J. Coats and R. F. Schinazi. Efficient synthesis of exo-N-carbamoyl nucleosides: application to the synthesis of phosphoramidate prodrugs. *Org. Lett.*, **2012**, 14, 2488-2491.

177. J. L. Lukkarila, S. R. da Silva, M. Ali, V. M. Shahani, G. W. Xu, J. Berman, A. Roughton, S. Dhe-Paganon, A. D. Schimmer and P. T. Gunning. Identification of NAE Inhibitors Exhibiting Potent Activity in Leukemia Cells: Exploring the Structural Determinants of NAE Specificity. *ACS Med. Chem. Lett.*, **2011**, 2, 577-582.

178. V. G. Zaikin and J. M. Halket. Review: Derivatization in mass spectrometry--4. Formation of cyclic derivatives. *Eur. J. Mass Spectrom.*, **2004**, 10, 555-568.

179. D. M. Parkin, F. Bray, J. Ferlay and P. Pisani. Estimating the world cancer burden: Globocan 2000. *Int. J. Cancer.*, **2001**, 94, 153-156.

180. F. X. Bosch, J. Ribes, M. Diaz and R. Cleries. Primary liver cancer: worldwide incidence and trends. *Gastroenterology*, **2004**, 127, S5-S16.

181. J. P. Zhang, J. Yan, J. Xu, X. H. Pang, M. S. Chen, L. Li, C. Wu, S. P. Li and L. Zheng. Increased intratumoral IL-17-producing cells correlate with poor survival in hepatocellular carcinoma patients. *J. Hepatol.*, **2009**, 50, 980-989.

182. F. Trevisani, P. E. D'Intino, A. M. Morselli-Labate, G. Mazzella, E. Accogli, P. Caraceni, M. Domenicali, S. De Notariis, E. Roda and M. Bernardi. Serum alpha-fetoprotein for diagnosis of hepatocellular carcinoma in patients with chronic liver disease: influence of HBsAg and anti-HCV status. *J. Hepatol.*, **2001**, 34, 570-575.

183. C. W. Gehrke, K. C. Kuo, T. P. Waalkes and E. Borek. Patterns of urinary excretion of modified nucleosides. *Cancer Res.*, **1979**, 39, 1150-1153.

184. D. Bullinger, H. Frohlich, F. Klaus, H. Neubauer, A. Frickenschmidt, C. Henneges, A. Zell, S. Laufer, C. H. Gleiter, H. Liebich and B. Kammerer. Bioinformatical evaluation of modified nucleosides as biomedical markers in diagnosis of breast cancer. *Anal. Chim. Acta*, **2008**, 618, 29-34.

185. Y. Amuro, H. Nakaoka, S. Shimomura, M. Fujikura, T. Yamamoto, S. Tamura, T. Hada and K. Higashino. Serum Pseudouridine as a Biochemical Marker in Patients with Hepatocellular-Carcinoma. *Clin. Chim. Acta*, **1988**, 178, 151-158.

186. S. Tamura, Y. Amuro, T. Nakano, J. Fujii, Y. Moriwaki, T. Yamamoto, T. Hada and K. Higashino. Urinary excretion of pseudouridine in patients with hepatocellular carcinoma. *Cancer*, **1986**, 57, 1571-1575.

187. J. Yang, G. W. Xu, Y. F. Zheng, H. W. Kong, T. Pang, S. Lv and Q. Yang. Diagnosis of liver cancer using HPLC-based metabonomics avoiding false-positive result from hepatitis and hepatocirrhosis diseases. *J. Chromatogr. B Analyt. Technol. Biomed. Life Sci.*, **2004**, 813, 59-65.

188. H. Fan, S. P. Li, J. J. Xiang, C. M. Lai, F. Q. Yang, J. L. Gao and Y. T. Wang. Qualitative and quantitative determination of nucleosides, bases and their analogues in natural and cultured Cordyceps by pressurized liquid extraction and high performance liquid chromatography-electrospray ionization tandem mass spectrometry (HPLC-ESI-MS/MS). *Anal. Chim. Acta*, **2006**, 567, 218-228.

189. P. Liu, Y. Y. Li, H. M. Li, D. J. Wan and Y. J. Tang. Determination of the nucleosides and nucleobases in Tuber samples by dispersive solid-phase extraction combined with liquid chromatography-mass spectrometry. *Anal. Chim. Acta*, **2011**, 687, 159-167.

190. H. Y. Li, S. M. Wang, H. M. Liu, J. Li, D. Han, S. S. Bu and M. Z. Zhang. Analysis of modified nucleosides in the urine of patients with malignant cancer by liquid chromatography/electrospray ionization mass spectrometry. *Rapid Commun. Mass Spectrom.*, **2008**, 22, 3161-3171.

191. R. Tuytten, F. Lemiere, E. L. Esmans, W. A. Herrebout, B. J. van der Veken, B. U. Maes, E. Witters, R. P. Newton and E. Dudley. Role of nitrogen lewis basicity in boronate affinity chromatography of nucleosides. *Anal. Chem.*, **2007**, 79, 6662-6669.

192. H. Li, Y. Shan, L. Qiao, A. Dou, X. Shi and G. Xu. Facile synthesis of boronate-decorated polyethyleneimine-grafted hybrid magnetic nanoparticles

for the highly selective enrichment of modified nucleosides and ribosylated metabolites. *Anal. Chem.*, **2013**, 85, 11585-11592.

193. R. Ullmer, A. Plematl and A. Rizzi. Derivatization by 6-aminoquinolyl-N-hydroxysuccinimidyl carbamate for enhancing the ionization yield of small peptides and glycopeptides in matrix-assisted laser desorption/ionization and electrospray ionization mass spectrometry. *Rapid Commun. Mass Spectrom.* **2006**, 20, 1469-1479.

194. A. Bond, E. Dudley, F. Lemiere, R. Tuytten, S. El-Sharkawi, A. G. Brenton, E. L. Esmans and R. P. Newton. Analysis of urinary nucleosides. V. Identification of urinary pyrimidine nucleosides by liquid chromatography/electrospray mass spectrometry. *Rapid Commun. Mass Spectrom.*, **2006**, 20, 137-150.

195. B. Kammerer, A. Frickenschmidt, C. H. Gleiter, S. Laufer and H. Liebich. MALDI-TOF MS analysis of urinary nucleosides. *J. Am. Soc. Mass Spectrom.*, **2005**, 16, 940-947.

196. B. Kammerer, A. Frickenschmidt, C. E. Muller, S. Laufer, C. H. Gleiter and H. Liebich. Mass spectrometric identification of modified urinary nucleosides used as potential biomedical markers by LC-ITMS coupling. *Anal. Bioanal. Chem.*, **2005**, 382, 1017-1026.

197. F. S. Vom Saal, S. C. Nagel, B. L. Coe, B. M. Angle and J. A. Taylor. The estrogenic endocrine disrupting chemical bisphenol A (BPA) and obesity. *Mol. Cell. Endocrinol.*, **2012**, 354, 74-84.

198. S. Kitamura, T. Suzuki, S. Sanoh, R. Kohta, N. Jinno, K. Sugihara, S. Yoshihara, N. Fujimoto, H. Watanabe and S. Ohta. Comparative study of the endocrine-disrupting activity of bisphenol A and 19 related compounds. *Toxicol. Sci.*, **2005**, 84, 249-259.

199. R. Valentino, V. D'Esposito, F. Ariemma, I. Cimmino, F. Beguinot and P. Formisano. Bisphenol A environmental exposure and the detrimental effects on human metabolic health: is it necessary to revise the risk assessment in vulnerable population? *J. Endocrinol. Invest.*, **2016**, 39, 259-263.

200. M. E. Romano, G. M. Webster, A. M. Vuong, R. Thomas Zoeller, A. Chen, A. N. Hoofnagle, A. M. Calafat, M. R. Karagas, K. Yolton, B. P. Lanphear and J. M. Braun. Gestational urinary bisphenol A and maternal and newborn thyroid hormone concentrations: the HOME Study. *Environ. Res.*, **2015**, 138, 453-460.

201. L. Robinson and R. Miller. The Impact of Bisphenol A and Phthalates on Allergy, Asthma, and Immune Function: a Review of Latest Findings. *Curr. Environ. Health Rep.*, **2015**, 2, 379-387.

202. B. Castro, P. Sanchez, M. T. Miranda, J. M. Torres and E. Ortega. Identification of dopamine- and serotonin-related genes modulated by bisphenol A in the prefrontal cortex of male rats. *Chemosphere*, **2015**, 139, 235-239.

203. D. Franssen, A. Gerard, B. Hennuy, A. F. Donneau, J. P. Bourguignon and A. S. Parent. Delayed Neuroendocrine Sexual Maturation in Female Rats After a Very Low Dose of Bisphenol A Through Altered GABAergic

Neurotransmission and Opposing Effects of a High Dose. *Endocrinology*, **2016**, 157, 1740-1750.

204. I. Hussain, A. Bhan, K. I. Ansari, P. Deb, S. A. Bobzean, L. I. Perrotti and S. S. Mandal. Bisphenol-A induces expression of HOXC6, an estrogen-regulated homeobox-containing gene associated with breast cancer. *Biochim. Biophys. Acta*, **2015**, 1849, 697-708.

205. S. A. Ljunggren, M. Iggland, M. Ronn, L. Lind, P. M. Lind and H. Karlsson. Altered heart proteome in fructose-fed Fisher 344 rats exposed to bisphenol A. *Toxicology*, **2016**, 347-349, 6-16.

206. S. W. Jeong, S. M. Lee, S. S. Yum, T. Iguchi and Y. R. Seo. Genomic expression responses toward bisphenol-A toxicity in Daphnia magna in terms of reproductive activity. *Mol. Cell. Toxicol.*, **2013**, 9, 149-158.

207. D. Pfeifer, Y. M. Chung and M. C. Hu. Effects of Low-Dose Bisphenol A on DNA Damage and Proliferation of Breast Cells: The Role of c-Myc. *Environ. Health Persp.*, **2015**, 123, 1271-1279.

208. S. Li and C. E. Mason. The Pivotal Regulatory Landscape of RNA Modifications. *Annual Review of Genomics and Human Genetics*, 2014, 15, 127-150.

209. A. Seidel, P. Seidel, O. Manuwald and O. Herbarth. Modified nucleosides as biomarkers for early cancer diagnose in exposed populations. *Environ. Toxicol.*, **2015**, 30, 956-967.

210.M. Tanaka, S. Han, P. A. Kupfer, C. J. Leumann and W. E. Sonntag. An assay for RNA oxidation induced abasic sites using the Aldehyde Reactive Probe. *Free Radic. Res.*, **2011**, 45, 237-247.

211.C. L. Simms, B. H. Hudson, J. W. Mosior, A. S. Rangwala and H. S. Zaher. An active role for the ribosome in determining the fate of oxidized mRNA. *Cell Rep.*, **2014**, 9, 1256-1264.

212.J. Wu and Z. Li. Human polynucleotide phosphorylase reduces oxidative RNA damage and protects HeLa cell against oxidative stress. *Biochem. Biophys. Res. Commun.*, **2008**, 372, 288-292.

213.M. A. Lovell and W. R. Markesbery. Oxidatively modified RNA in mild cognitive impairment. *Neurobiol. Dis.*, **2008**, 29, 169-175.

214.D. Moravcova, J. Planeta, V. Kahle and M. Roth. Zwitterionic silica-based monolithic capillary columns for isocratic and gradient hydrophilic interaction liquid chromatography. *J. Chromatogr. A*, **2012**, 1270, 178-185.

215.X. Qiao, L. Zhang, N. Zhang, X. Wang, X. Qin, H. Yan and H. Liu. Imidazolium embedded C8 based stationary phase for simultaneous reversed-phase/hydrophilic interaction mixed-mode chromatography. *J. Chromatogr. A*, **2015**, 1400, 107-116.

216.H. Wang and S. V. Olesik. Development of a new separation media using ultra-thin glassy carbon film modified silica. *J. Chromatogr. A,* **2015**, 1379, 56-64.

217. C. D. Iverson, Y. Zhang and C. A. Lucy. Diazonium modification of porous graphitic carbon with catechol and amide groups for hydrophilic interaction and attenuated reversed phase liquid chromatography. *J. Chromatogr. A*, **2015**, 1422, 186-193.

218. X. Qiao, R. Li, W. Song, W. J. Miao, J. Liu, H. B. Chen, D. A. Guo and M. Ye. A targeted strategy to analyze untargeted mass spectral data: Rapid chemical profiling of Scutellaria baicalensis using ultra-high performance liquid chromatography coupled with hybrid quadrupole orbitrap mass spectrometry and key ion filtering. *J. Chromatogr. A*, **2016**, 1441, 83-95.

219. Y. Lin, R. Liu, F. Hu, R. Liu, T. Ruan and G. Jiang. Simultaneous qualitative and quantitative analysis of fluoroalkyl sulfonates in riverine water by liquid chromatography coupled with Orbitrap high resolution mass spectrometry. *J. Chromatogr. A*, **2016**, 1435, 66-74.

220. L. Sun, G. Zhu, S. Mou, Y. Zhao, M. M. Champion and N. J. Dovichi. Capillary zone electrophoresis-electrospray ionization-tandem mass spectrometry for quantitative parallel reaction monitoring of peptide abundance and single-shot proteomic analysis of a human cell line. *J. Chromatogr. A*, **2014**, 1359, 303-308.

221. Y. Li, J. Zhang, Y. Jin, L. Wang, W. Zhao, W. Zhang, L. Zhai, Y. Zhang, Y. Zhang and J. Zhou. Hybrid quadrupole-orbitrap mass spectrometry analysis with accurate-mass database and parallel reaction monitoring for high-

throughput screening and quantification of multi-xenobiotics in honey. *J. Chromatogr. A*, **2016**, 1429, 119-126.

222. Z. Radak and I. Boldogh. 8-Oxo-7,8-dihydroguanine: links to gene expression, aging, and defense against oxidative stress. *Free Radic. Biol. Med.*, **2010**, 49, 587-596.

223. J. Michalowicz, K. Mokra and A. Bak. Bisphenol A and its analogs induce morphological and biochemical alterations in human peripheral blood mononuclear cells (in vitro study). *Toxicol. in Vitro*, **2015**, 29, 1464-1472.

224. F. Xin, L. Jiang, X. Liu, C. Geng, W. Wang, L. Zhong, G. Yang and M. Chen. Bisphenol A induces oxidative stress-associated DNA damage in INS-1 cells. *Mutat. Res. Genet. Toxicol. Environ. Mutagen.*, **2014**, 769, 29-33.

225. W. Martinet, G. R. de Meyer, A. G. Herman and M. M. Kockx. Reactive oxygen species induce RNA damage in human atherosclerosis. *Eur. J. Clin. Invest.*, **2004**, 34, 323-327.

226. E. Gajewski, G. Rao, Z. Nackerdien and M. Dizdaroglu. Modification of DNA bases in mammalian chromatin by radiation-generated free radicals. *Biochemistry*, **1990**, 29, 7876-7882.

227. S. Dukan, A. Farewell, M. Ballesteros, F. Taddei, M. Radman and T. Nystrom. Protein oxidation in response to increased transcriptional or translational errors. *Proc. Natl. Acad. Sci. U. S. A.*, **2000**, 97, 5746-5749.

228.M. Aydogan, A. Korkmaz, N. Barlas and D. Kolankaya. The effect of vitamin C on bisphenol A, nonylphenol and octylphenol induced brain damages of male rats. *Toxicology*, **2008**, 249, 35-39.

229.Q. Wang, L. Wang, R. Han, L. Yang, Q. Zhou and X. Huang. Effects of bisphenol A on antioxidant system in soybean seedling roots. *Environ. Toxicol. Chem.*, **2015**, 34, 1127-1133.

230.P. A. Aas, M. Otterlei, P. O. Falnes, C. B. Vagbo, F. Skorpen, M. Akbari, O. Sundheim, M. Bjoras, G. Slupphaug, E. Seeberg and H. E. Krokan. Human and bacterial oxidative demethylases repair alkylation damage in both RNA and DNA. *Nature*, **2003**, 421, 859-863.

231.Q. Kong and C. L. Lin. Oxidative damage to RNA: mechanisms, consequences, and diseases. *Cell. Mol. Life Sci.*, **2010**, 67, 1817-1829.

232.Z. Li, S. Malla, B. Shin and J. M. Li. Battle against RNA oxidation: molecular mechanisms for reducing oxidized RNA to protect cells. *Wiley Interdiscip. Rev. RNA*, **2014**, 5, 335-346.

233.M. Li and Z. W. Cai. Simultaneous determination of aconitine, mesaconitine, hypaconitine, bulleyaconitine and lappaconitine in human urine by liquid chromatography-electrospray ionization-tandem mass spectrometry. *Anal. Methods*, **2013**, 5, 4034-4038.

234.S. Li, Y. Jin, Z. Tang, S. Lin, H. Liu, Y. Jiang and Z. Cai. A novel method of liquid chromatography-tandem mass spectrometry combined with chemical

derivatization for the determination of ribonucleosides in urine. *Anal. Chim. Acta*, **2015**, 864, 30-38.

235. S. Kitamura, T. Suzuki, S. Sanoh, R. Kohta, N. Jinno, K. Sugihara, S. Yoshihara, N. Fujimoto, H. Watanabe and S. Ohta. Comparative study of the endocrine-disrupting activity of bisphenol A and 19 related compounds. *Toxicol. Sci.*, **2005**, 84, 249-259.

236. C. Liao and K. Kannan. Widespread occurrence of bisphenol A in paper and paper products: implications for human exposure. *Environ. Sci. Technol.*, **2011**, 45, 9372-9379.

237. C. Y. Liao, F. Liu, Y. Guo, H. B. Moon, H. Nakata, Q. Wu and K. Kannan. Occurrence of Eight Bisphenol Analogues in Indoor Dust from the United States and Several Asian Countries: Implications for Human Exposure. *Environ. Sci. Technol.*, **2012**, 46, 9138-9145.

238. L. N. Vandenberg, T. Colborn, T. B. Hayes, J. J. Heindel, D. R. Jacobs, Jr., D.-H. Lee, T. Shioda, A. M. Soto, F. S. vom Saal, W. V. Welshons, R. T. Zoeller and J. P. Myers. Hormones and Endocrine-Disrupting Chemicals: Low-Dose Effects and Nonmonotonic Dose Responses. *Endocr. Rev.*, **2012**, 33, 378-455.

239. G. S. Prins, S.-H. Ye, L. Birch, S.-m. Ho and K. Kannan. Serum bisphenol A pharmacokinetics and prostate neoplastic responses following oral and subcutaneous exposures in neonatal Sprague-Dawley rats. *Reprod. Toxicol.*, **2011**, 31, 1-9.

240.H. Nishizawa, M. Morita, M. Sugimoto, S. Imanishi and N. Manabe. Effects of in utero exposure to bisphenol a on mRNA expression of arylhydrocarbon and retinoid receptors in murine embryos. *J. Reprod. Dev.*, **2005**, 51, 315-324.

241.R. A. Keri, S.-M. Ho, P. A. Hunt, K. E. Knudsen, A. M. Soto and G. S. Prins. An evaluation of evidence for the carcinogenic activity of bisphenol A. *Reprod. Toxicol.*, **2007**, 24, 240-252.

242.R. R. Newbold, W. N. Jefferson and E. Padilla-Banks. Long-term adverse effects of neonatal exposure to bisphenol A on the murine female reproductive tract. *Reprod. Toxicol.*, **2007**, 24, 253-258.

243.D. R. Ekman, D. M. Skelton, J. M. Davis, D. L. Villeneuve, J. E. Cavallin, A. Schroeder, K. M. Jensen, G. T. Ankley and T. W. Collette. Metabolite Profiling of Fish Skin Mucus: A Novel Approach for Minimally-Invasive Environmental Exposure Monitoring and Surveillance. *Environ. Sci. Technol.*, **2015**, 49, 3091-3100.

244.K. De Schutter and E. J. Van Damme. Protein-carbohydrate interactions as part of plant defense and animal immunity. *Molecules*, **2015**, 20, 9029-9053.

245.A. Seidel, P. Seidel, O. Manuwald and O. Herbarth. Modified nucleosides as biomarkers for early cancer diagnose in exposed populations. *Environ. Toxicol.*, **2015**, 30, 956-967.

246. M. Idzko, D. Ferrari, A. K. Riegel and H. K. Eltzschig. Extracellular nucleotide and nucleoside signaling in vascular and blood disease. *Blood*, **2014**, 124, 1029-1037.

247. D. Boison. Modulators of nucleoside metabolism in the therapy of brain diseases. *Curr. Top. Med. Chem.*, **2011**, 11, 1068-1086.

248. N. J. Cabaton, C. Canlet, P. R. Wadia, M. Tremblay-Franco, R. Gautier, J. Molina, C. Sonnenschein, J.-P. Cravedi, B. S. Rubin, A. M. Soto and D. Zalko. Effects of Low Doses of Bisphenol A on the Metabolome of Perinatally Exposed CD-1 Mice. *Environ. Health Persp.*, **2013**, 121, 586-593.

249. W. Xu, D. Chen, N. Wang, T. Zhang, R. Zhou, T. Huan, Y. Lu, X. Su, Q. Xie, L. Li and L. Li. Development of high-performance chemical isotope labeling LC-MS for profiling the human fecal metabolome. *Anal. Chem.*, **2015**, 87, 829-836.

250. K. Guo, F. Bamforth and L. A. Li. Qualitative Metabolome Analysis of Human Cerebrospinal Fluid by C-13-/C-12-Isotope Dansylation Labeling Combined with Liquid Chromatography Fourier Transform Ion Cyclotron Resonance Mass Spectrometry. *J. Am. Soc. Mass Spectrom.*, **2011**, 22, 339-347.

251. J. Leng, Q. Guan, T. Sun, H. Wang, J. Cui, Q. Liu, Z. Zhang, M. Zhang and Y. Guo. Direct infusion electrospray ionization-ion mobility-mass spectrometry for comparative profiling of fatty acids based on stable isotope labeling. *Anal. Chim. Acta*, **2015**, 887, 148-154.

252. Y. Q. Huang, Q. Y. Wang, J. Q. Liu, Y. H. Hao, B. F. Yuan and Y. Q. Feng. Isotope labelling--paired homologous double neutral loss scan-mass spectrometry for profiling of metabolites with a carboxyl group. *Analyst*, **2014**, 139, 3446-3454.

253. R. Zhou, C. L. Tseng, T. Huan and L. Li. IsoMS: automated processing of LC-MS data generated by a chemical isotope labeling metabolomics platform. *Anal. Chem.*, **2014**, 86, 4675-4679.

254. C. Bueschl, R. Krska, B. Kluger and R. Schuhmacher. Isotopic labeling-assisted metabolomics using LC-MS. *Anal. Bioanal. Chem.*, **2013**, 405, 27-33.

255. S. M. Martin, C. Delporte, A. Farrell, N. N. Iglesias, N. McLoughlin and J. Bones. Comparative analysis of monoclonal antibody N-glycosylation using stable isotope labelling and UPLC-fluorescence-MS. *Analyst*, **2015**, 140, 1442-1447.

256. Y. Q. Huang, J. Q. Liu, H. Y. Gong, J. Yang, Y. S. Li and Y. Q. Feng. Use of isotope mass probes for metabolic analysis of the jasmonate biosynthetic pathway. *Analyst*, **2011**, 136, 1515-1522.

257. M. E. D. C. Busto, M. Montes-Bayon, J. Bettmer and A. Sanz-Medel. Stable isotope labelling and FPLC-ICP-SFMS for the accurate determination of clinical iron status parameters in human serum. *Analyst*, **2008**, 133, 379-384.

258. T. Huan and L. Li. Quantitative Metabolome Analysis Based on Chromatographic Peak Reconstruction in Chemical Isotope Labeling Liquid Chromatography Mass Spectrometry. *Anal. Chem.*, **2015**, 87, 7011-7016.

259. L. Yu, P. Liu, Y. L. Wang, Q. W. Yu, B. F. Yuan and Y. Q. Feng. Profiling of aldehyde-containing compounds by stable isotope labelling-assisted mass spectrometry analysis. *Analyst*, **2015**, 140, 5276-5286.

260. R. Zhou, T. Huan and L. Li. Development of versatile isotopic labeling reagents for profiling the amine submetabolome by liquid chromatography-mass spectrometry. *Anal. Chim. Acta*, **2015**, 881, 107-116.

261. K. Guo, C. Ji and L. Li. Stable-isotope dimethylation labeling combined with LC-ESI MS for quantification of amine-containing metabolites in biological samples. *Anal. Chem.*, **2007**, 79, 8631-8638.

262. R. Tautenhahn, G. J. Patti, D. Rinehart and G. Siuzdak. XCMS Online: a web-based platform to process untargeted metabolomic data. *Anal. Chem.*, **2012**, 84, 5035-5039.

263. K. Kera, Y. Ogata, T. Ara, Y. Nagashima, N. Shimada, N. Sakurai, D. Shibata and H. Suzuki. ShiftedIonsFinder: A standalone Java tool for finding peaks with specified mass differences by comparing mass spectra of isotope-labeled and unlabeled data sets. *Plant Biotechnol.*, **2014**, 31, 269-274.

264. J. G. Xia, I. V. Sinelnikov, B. Han and D. S. Wishart. MetaboAnalyst 3.0-making metabolomics more meaningful. *Nucleic Acids Res.*, **2015**, 43, W251-W257.

265. A. Karnovsky, T. Weymouth, T. Hull, V. G. Tarcea, G. Scardoni, C. Laudanna, M. A. Sartor, K. A. Stringer, H. V. Jagadish, C. Burant, B. Athey and G. S. Omenn. Metscape 2 bioinformatics tool for the analysis and visualization of metabolomics and gene expression data. *Bioinformatics*, **2012**, 28, 373-380.

266. J. S. Park, B. J. Lee, K. S. Kang, J. H. Tai, J. J. Cho, M. H. Cho, T. Inoue and Y. S. Lee. Hormonal effects of several chemicals in recombinant yeast, MCF-7 cells and uterotrophic assays in mice. *J. Microbiol. Biotechnol.*, **2000**, 10, 293-299.

267. M. Ezechias, K. Svobodova and T. Cajthaml. Hormonal activities of new brominated flame retardants. *Chemosphere*, **2012**, 87, 820-824.

268. K. Ino, Y. Kitagawa, T. Watanabe, H. Shiku, M. Koide, T. Itayama, T. Yasukawa and T. Matsue. Detection of hormone active chemicals using genetically engineered yeast cells and microfluidic devices with interdigitated array electrodes. *Electrophoresis*, **2009**, 30, 3406-3412.

269. L. L. Li, Q. Q. Wang, Y. Zhang, Y. Z. Niu, X. J. Yao and H. X. Liu. The Molecular Mechanism of Bisphenol A (BPA) as an Endocrine Disruptor by Interacting with Nuclear Receptors: Insights from Molecular Dynamics (MD) Simulations. *PLoS One*, **2015**, 10, e0120330.

270. U. Eichenlaub-Ritter and F. Pacchierotti. Bisphenol A Effects on Mammalian Oogenesis and Epigenetic Integrity of Oocytes: A Case Study Exploring Risks of Endocrine Disrupting Chemicals. *Biomed Res. Int.*, **2015**, 2015, 698795.

271. E. S. Erden, S. Motor, I. Ustun, M. Demirkose, R. Yuksel, R. Okur, S. Oktar, Y. Yakar, S. Sungur and C. Gokce. Investigation of Bisphenol A as an endocrine disruptor, total thiol, malondialdehyde, and C-reactive protein levels in chronic obstructive pulmonary disease. *Eur. Rev. Med. Pharmacol. Sci.*, **2014**, 18, 3477-3483.

272. R. Liang, J. Zhou and J. Liu. Construction of a bacterial assay for estrogen detection based on an estrogen-sensitive intein. *Appl. Environ. Microbiol.*, **2011**, 77, 2488-2495.

273. J. Li, M. Ma and Z. Wang. A two-hybrid yeast assay to quantify the effects of xenobiotics on retinoid X receptor-mediated gene expression. *Toxicol. Lett.*, **2008**, 176, 198-206.

274. S. H. Cho, M. H. Choi, O. S. Kwon, W. Y. Lee and B. C. Chung. Metabolic significance of bisphenol A-induced oxidative stress in rat urine measured by liquid chromatography-mass spectrometry. *J. Appl. Toxicol.*, **2009**, 29, 110-117.

275. C. Bottcher, E. V. Roepenack-Lahaye, E. Willscher, D. Scheel and S. Clemens. Evaluation of matrix effects in metabolite profiling based on capillary liquid

chromatography electrospray ionization quadrupole time-of-flight mass spectrometry. *Anal. Chem.*, **2007**, 79, 1507-1513.

276. M. Mateos-Vivas, E. Rodriguez-Gonzalo, D. Garcia-Gomez and R. Carabias-Martinez. Hydrophilic interaction chromatography coupled to tandem mass spectrometry in the presence of hydrophilic ion-pairing reagents for the separation of nucleosides and nucleotide mono-, di- and triphosphates. *J. Chromatogr. A*, **2015**, 1414, 129-137.

277. M. P. Finnegan, H. Z. Zhang and J. F. Banfield. Phase stability and transformation in titania nanoparticles in aqueous solutions dominated by surface energy. *J. Phys. Chem. C*, **2007**, 111, 1962-1968.

278. J. Rappsilber, M. Mann and Y. Ishihama. Protocol for micro-purification, enrichment, pre-fractionation and storage of peptides for proteomics using StageTips. *Nat. Protoc.*, **2007**, 2, 1896-1906.

279. H. K. Kweon and K. Hakansson. Metal oxide-based enrichment combined with gas-phase ion-electron reactions for improved mass spectrometric characterization of protein phosphorylation. *J. Proteome Res.*, **2008**, 7, 749-755.

280. X. Sun, F. Ge, C. L. Xiao, X. F. Yin, R. Ge, L. H. Zhang and Q. Y. He. Phosphoproteomic analysis reveals the multiple roles of phosphorylation in pathogenic bacterium Streptococcus pneumoniae. *J. Proteome Res.*, **2010**, 9, 275-282.

281. Z. Cui, J. Hou, X. Chen, J. Li, Z. Xie, P. Xue, T. Cai, P. Wu, T. Xu and F. Yang. The profile of mitochondrial proteins and their phosphorylation signaling network in INS-1 beta cells. *J. Proteome Res.*, **2010**, 9, 2898-2908.

282. J. Ge, L. Zhao, L. R. Chen and Y. P. Shi. Titanium-Coated Silica Spheres Prepared by Self-Assembly Technique for Use as HPLC Packing. *J. Chromatogr. Sci.*, **2010**, 48, 29-34.

283. M. R. Larsen, T. E. Thingholm, O. N. Jensen, P. Roepstorff and T. J. Jorgensen. Highly selective enrichment of phosphorylated peptides from peptide mixtures using titanium dioxide microcolumns. *Mol. Cell. Proteomics*, **2005**, 4, 873-886.

284. J. G. Douglass, R. I. Patel, B. R. Yerxa, S. R. Shaver, P. S. Watson, K. Bednarski, R. Plourde, C. C. Redick, K. Brubaker, A. C. Jones and J. L. Boyer. Lipophilic modifications to dinucleoside polyphosphates and nucleotides that confer antagonist properties at the platelet P2Y12 receptor. *J. Med. Chem.*, **2008**, 51, 1007-1025.

285. H. Ko, R. L. Carter, L. Cosyn, R. Petrelli, S. de Castro, P. Besada, Y. Zhou, L. Cappellacci, P. Franchetti, M. Grifantini, S. Van Calenbergh, T. K. Harden and K. A. Jacobson. Synthesis and potency of novel uracil nucleotides and derivatives as P2Y2 and P2Y6 receptor agonists. *Bioorg. Med. Chem.*, **2008**, 16, 6319-6332.

286. S. K. Bhowmik and B. H. Jung. Analysis of plasma nucleotides in rat by micellar electrokinetic capillary chromatography/electrospray ionization mass spectrometry. *Rapid Commun. Mass Spectrom.*, **2012**, 26, 1426-1436.

CURRICULUM VITAE

Academic qualifications of the thesis author, Mr. LI Shangfu:

- Received the degree of Bachelor of Chemistry from Tsinghua University, July 2008.

- Received the degree of Master of Chemistry from Tsinghua University, July 2011.

September 2016